

Parametric Analysis of CO2 Laser for Quality of Weldox-700 Material

Vadhel Ajay Jethabhai
Department of Mechanical Engineering
Indus Institute of Technology and Engineering
Ahmedabad, Gujarat, India

Jignesh Patel
Department of Mechanical Engineering
Indus Institute of Technology and Engineering
Ahmedabad, Gujarat, India

Abstract: “Laser Cutting of weldox-700 materials is popular processes in manufacturing industries This research paper for primary study for evaluate the effect of the processing parameters (Laser Power, gas pressure, pulse frequency and Cutting speed) under the quality of the cut for weldox-700 materials. Then the experiment was done by 6mm thick weldox-700 material plates. In this experiment focused on establish relation of different parameters on Cutting quality, which is decided by the Surface Roughness and Kerf Width.

Keywords: Weldox-700, Cutting Speed, Cutting Quality, Laser Power, Taguchi method, Surface Roughness, Kerf Width

1. INTRODUCTION :

Laser Cutting machine definition describes itself “Laser machine is a device which is used to generate & amplifies light. Laser stands for Light Amplification by Stimulated Emission of Radiation. Laser machine is an electrical-optical device that produces coherent radiation. Simply put, a Laser is a device that creates and amplifies a narrow, intense beam of coherent light” [1].In the industries the high accuracy of Cutting, higher production rate, good Cutting quality this all thing proves that co2 Laser machine is good choice for industrial application. There are many parameters are affected like Laser Power, Cutting speed, gas pressure, pulse frequency, thickness of material plates, focus length then after measure Surface Roughness and Kerf Widths References[2] give detailed descriptions of the Laser machine and the mechanism of Laser Cutting of materials an Fig. 1shows Schematic illustration for the process of co2 Laser Cutting of metals. In this research paper Cutting of hardest material Weldox-700 is selected which is used in earth moving machine parts. Weldox-700 has hardness of 700 HBW; it has also very good weld ability and good hardness. So it is used in dumper bodies, mining equipment, water tanks, concreter crusher and over head cranes [3].

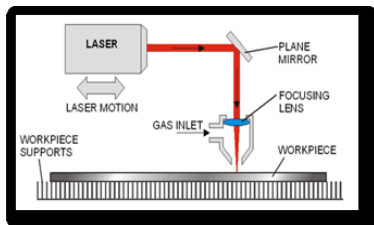


Figure 1: Schematic illustration for the process of CO2 Laser Cutting of metals

2. EXPERIMENTAL PROCEDURE AND OPERATION PARAMETERS :

2.1 Material :

The base material used in this study was weldox-700 sheet 6 mm thick, whose chemical composition listed in Table 1. This weldox-700[3].

C	Si	Mn	P	S	Mo	Cu
0.20	0.60	1.60	0.020	0.010	0.70	0.30

Table 1: chemical composition of weldox-700

2.2 Taguchi method based experiment :

These experiments were performed with a 3.2 kW CO2, To prevent the instability and damage caused by back reflections, the cavity is isolated by using a beam bender mirror with a multilayer coating that absorbs the back reflected Laser beam. The Laser beam was focused using a 127mm focal length lens except for the tests conducted to detect the influence of this parameter. In CW mode, when the Laser source delivers a constant Power, the experiments were performed varying one factor at a time. The ranges of Cutting parameter are summarized in Table 2. A commercial Cutting head incorporating a conical converging coaxial nozzle with a 1.5 mm exit diameter was employed to supply the assist gas in a coaxial manner with the Laser beam. In the tests conducted to reveal the influence of the nozzle exit on the quality of the cuts, nozzles with an exit diameter of 1.5 mm were also used. The distance from the lower part of the nozzle to the plate was fixed at 1.5mm except for the tests conducted to reveal the influence of this parameter. Compressed air, nitrogen and oxygen at various pressures were used as assist gases. Based on

experience for similar materials, oxygen and nitrogen are the most recommended gases for the experimentation [4].

Most of the tests were performed using argon as assist gas except from the test performed to investigate the influence of the gas nature. In order to compare the results, the experiments were performed on unidirectional straight line Cutting. On the other hand, the experiments conducted in pulsed mode were performed by means of one-factor-at-a-time experiments in a first stage. The ranges of Cutting parameters are summarized in Table 2 Furthermore; a full factorial design (FFD) approach was also performed to efficiently screen out the key variables significantly affecting on the response variables.

Symbol	Factor	Unit	Level 1	Level 2	Level 3
A	Power	Watt	1100	1200	1300
B	Pressure	Bar	0.3	0.4	0.5
C	Speed	Mm/m in	300	400	500

Table 2: control factor & theirs level used in experiment

2.3 Surface Roughness Measurement :

The Surface Roughness for all trial runs is measured with Profilometer named as sj-201P. After the measuring number of samples through Surface Roughness tester (SJ -201P) In which we have measured L1, L2, L3 sample lengths and considered their average value in terms of length in mm. in figure we have described measuring Surface Roughness of the sample and in table shown results of Surface Roughness test according to experiment.

2.4 Specification of Mitutoyo surface tester SJ-201P[5] :

- Measurement range : 350µm
- Tip radius : 5µm
- Measuring force : 4mN(Mega Newton)
- Radius of skid curvature : 40mm
- Detector drive range: 21mm
- Traversing speed:1) Measurement: 0.25 to 0.5 mm/s
2) Return: 0.8 mm/s
- AC Power supply 100V, 120V, 230V

Table 3: Specification of surface tester SJ-201P

Trail No	A	B	C	D
1	1	1	1	1
2	1	1	2	2
3	1	1	3	3
4	1	2	1	2
5	1	2	2	3
6	1	2	3	1
7	1	3	1	3
8	1	3	2	1
9	1	3	3	2
10	2	1	1	2
11	2	1	2	3
12	2	1	3	1
13	2	2	1	3
14	2	2	2	1
15	2	2	3	2
16	2	3	1	1
17	2	3	2	2
18	2	3	3	3
19	3	1	1	3
15	3	1	2	1
21	3	1	3	2
22	3	2	1	1
23	3	2	2	2
24	3	2	3	3
20	3	3	1	2
26	3	3	2	3
27	3	3	3	1

Table 4: Lay out using L27



Figure 2: Surface Roughness Testing



Figure 3: Avg of Surface Roughness of plate 1 and sub part 2

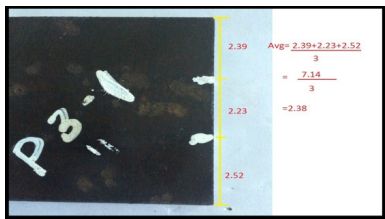


Figure 4: Avg of Surface Roughness of plate 3 and sub part 1

Table 5: Results of Surface Roughness obtained by experiment

Trail No	Power(Watt)	Pressure (bar)	Cutting Speed (mm/min)	Pulse frequency (Hz)	Roughness (micron)
1	1100	0.3	300	15	2.03
2	1100	0.3	400	20	1.09
3	1100	0.3	500	25	1.96
4	1100	0.4	300	20	2.73
5	1100	0.4	400	25	1.75
6	1100	0.4	500	15	2.88
7	1100	0.5	300	25	3.38
8	1100	0.5	400	15	2.96
9	1100	0.5	500	20	3.69
10	1200	0.3	300	20	1.82
11	1200	0.3	400	25	2.51
12	1200	0.3	500	15	2.68
13	1200	0.4	300	25	2.59
14	1200	0.4	400	15	2.72
15	1200	0.4	500	20	3.04
16	1200	0.5	300	15	2.48
17	1200	0.5	400	20	3.08
18	1200	0.5	500	25	3.46
19	1300	0.3	300	25	2.38
20	1300	0.3	400	15	2.14
21	1300	0.3	500	20	1.93
22	1300	0.4	300	15	2.47
23	1300	0.4	400	20	2.57
24	1300	0.4	500	25	3.25
25	1300	0.5	300	20	2.65
26	1300	0.5	400	25	3.98
27	1300	0.5	500	15	3.59

2.5 Kerf Width Measurement :

The Kerf Width measurement was done by equipment using by digital camera and image tool programs. In which first digital camera was used to take the photographs of top bottom cut kerf of test piece, after that the photographs were transmitted in computer then after uploaded in image tool software for used to measure length along kerf gap[6].

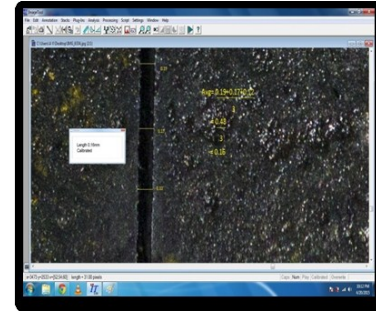


Figure 5: Kerf Width Analysis for plate no1 cut no7 by Image tool 3.0

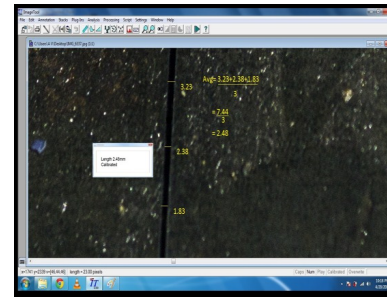


Figure 6: Kerf Width Analysis for plate no3 cut no9 by Image tool 3.0

Table 6: Results of Kerf Width obtained by experiment

Trail No	Power(Watt)	Pressure (bar)	Cutting Speed (mm/min)	Pulse frequency (Hz)	Kerfs Width (mm)
1	1100	0.3	300	15	0.40
2	1100	0.3	400	20	0.22
3	1100	0.3	500	25	0.28
4	1100	0.4	300	20	0.19
5	1100	0.4	400	25	0.87
6	1100	0.4	500	15	0.33
7	1100	0.5	300	25	0.16
8	1100	0.5	400	15	1.89
9	1100	0.5	500	20	0.37
10	1200	0.3	300	20	0.82
11	1200	0.3	400	25	0.56
12	1200	0.3	500	15	0.93
13	1200	0.4	300	25	0.54
14	1200	0.4	400	15	0.78
15	1200	0.4	500	20	0.48
16	1200	0.5	300	15	0.90
17	1200	0.5	400	20	1.29
18	1200	0.5	500	25	0.37
19	1300	0.3	300	25	1.13
20	1300	0.3	400	15	0.51
21	1300	0.3	500	20	1.86
22	1300	0.4	300	15	1.29
23	1300	0.4	400	20	0.49
24	1300	0.4	500	25	2.28
25	1300	0.5	300	20	1.47
26	1300	0.5	400	25	1.26
27	1300	0.5	500	15	2.48

3. DISCUSSION AND CONCLUSION :

3.1 Discussion about Surface Roughness:

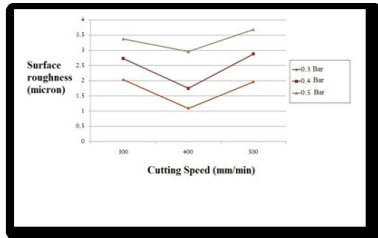


Figure 7: Graph of Cutting speed Vs Roughness with Laser Power 1100 watt

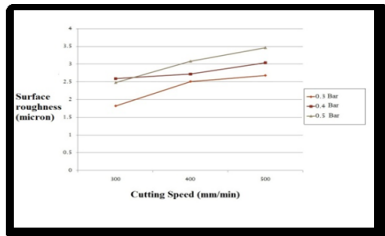


Figure 8: Graph of Cutting speed Vs Roughness with Laser Power 1200 watt

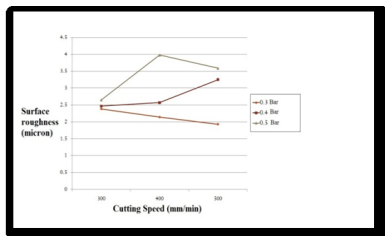


Figure 9: Graph of Cutting speed Vs Roughness with Laser Power 1300 watt

3.2 Conclusion of Surface Roughness:

After studied the performance the of CO2 Laser Cutting of weldox- 700 for 6mm thickness with oxygen assistant gas cut by CO2 Laser Cutting machine made by Trumpf Laser Technology. After the experiment the cut quality was defined by focusing on Surface Roughness.

When the Laser Power is minimum like 1100watt, Cutting speed is medium and the gas pressure is medium we get best Surface Roughness like **1.09micron**.

But when the Laser Power and Cutting speed are increased we get rough Surface Roughness and we seen it in 1200watt Cutting speed and 1300watt Laser Power graphs, and when the Laser Power is maximum like 1300watt get maximum Surface Roughness up to **3.98micron**.

Sr. No	Laser Power (watt)	Pressure (bar)	Cutting Speed (mm/min)	Pulse frequency (Hz)	Surface Roughness (micron)
1	1100	0.3	400	20	1.09
2	1300	0.5	400	25	3.98

3.3 Discussion about Kerf Width:

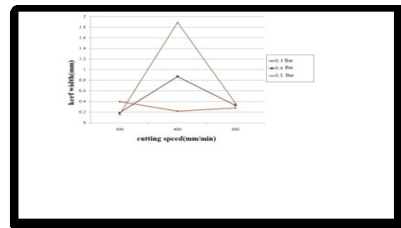


Figure 10: Graph of Cutting speed Vs Kerf Width with Laser Power 1100 watt

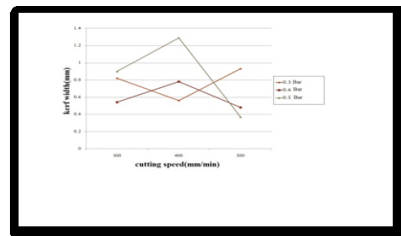


Figure 11: Graph of Cutting speed Vs Kerf Width with Laser Power 1200 watt

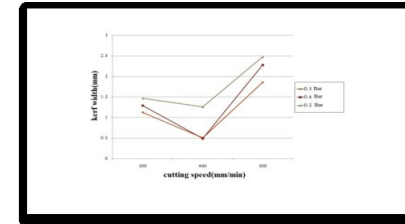


Figure 12: Graph of Cutting speed Vs Kerf Width with Laser Power 1300 watt

3.4 Conclusion of Kerf Width :

After studied the performance the of CO2 Laser Cutting of weldox- 700 for 6mm thickness with oxygen assistant gas cut by CO2 Laser Cutting machine made by Trumpf Laser Technology. After the experiment the cut quality was defined by focusing on Surface Roughness

In which when the Laser Power is Minimum like 1100watt and the Cutting speed is minimum 300 and gas pressure is medium 0.5 we get Minimum Kerf Width like **0.16mm**.

When the speed and Power are increased the Kerf Width is increased. When the Power is highest 1300watt and Cutting speed is highest 500 Kerf Widths is increased up to **2.48mm**.

Sr. No	Laser Power (watt)	Pressure (bar)	Cutting Speed (mm/min)	Pulse frequency (Hz)	Kerf Width (mm)
1	1100	0.5	300	25	0.16
2	1300	0.5	500	15	2.48

4. References:

- <http://en.wikipedia.org/wiki/Laser>
- George Chryssolouris, "Laser Machining", New, Springer-Verlag, 1991;
- www.weldox.com
- <http://support.minitab.com/en-us/minitab/17/topic-library/modeling-statistics/doe/taguchi-designs/taguchi-designs/>
- https://www.atecorp.com/ATECorp/media/pdfs/data-sheets/Mitutoyo-SJ-201P_Datasheet.pdf
- <http://compdent.uthscsa.edu/dig/itdesc.html>

- Gould, R. Gordon (1959). "The LASER, Light Amplification by Stimulated Emission of Radiation". In Franken, P.A. and Sands, R.H. (Eds.), The Ann Arbor Conference on Optical Pumping, the University of Michigan, 15 June through 18 June 1959. p. 128.OCLC 02460155.
- Chu, Steven; Townes, Charles (2003). "Arthur Schawlow". In Edward P. Lazar (ed.), Biographical Memoirs. vol. 83. National Academy of Sciences. p. 202. ISBN 0-309-08699-X
- Nolen,jim;Derek verno."The carbon Dioxide Laser". Davidson Physics. Retried 17 Aug 2014
- https://www.idc-online.com/technical_references/pdfs/mechanical_engineering/Parametric%20investigation
- Achievements in Materials and manufacturing Engineering 54/1 (2012) 128-134
- Jia Deli, You Bo (2010) - "An intelligent control strategy for plasma arc Cutting technology" Harbin University of Science and Technology, Harbin 150080, China
- Jiayou Wang &Zhengyu Zhu &Conghui He &Feng Yang (2010) - "Effect of dual swirling plasma arc Cutting parameters on kerf characteristics" Int J Mater Form (2011) 4:39-43
- <http://www.revt.n.ro/pdf4-Radovanovic>
- https://www.idc-online.com/technical_references/pdfs/mechanical_engineering/Parametric%20investigation.pdf
- <http://www.tribology.fink.rs/journals/2012/2012-4/7.pdf>
- <http://www.ijsea.com/archive/volume2/issue6/IJSEA02061003.html>
- http://www.ijetae.com/files/Volume3Issue4/IJETAE_0413_35.pdf
- K.A. Ghany, M. Newishy, Cutting of 1.2 mm thick austenitic stainless steel sheet using pulsed and CW Nd YAG Laser, Journal of Material Processing Technology 168 (2005) 438-447
- S.-L. Chen, The effects of high-pressure assistant-gas flow on high Power CO2 Laser Cutting, Journal of Material Processing Technology 88 (1999) 57-66
- N. Raja ram, J.S. Ahmad, S.H. Cheraghi, —CO2 Laser cut quality of 4130 steell, International Journal of Machine Tools and Manufacture 43 (2003) 351-358.

- F. Caiazza, F. Curcio, G. Daurelio, F. Memola Capece Minutolo, —Laser Cutting of different polymeric plastics
- M. Zaied, E. Bayraktar, D. Katundi, M. Boujelbene, I. Miraoui, —Effect of Laser Cutting parameters on surface quality of low carbon steel (S235), Journal of
- N. Rajendran, M.B. Pate, The effect of Laser beam velocity on cut quality and surface temperature, American Society of Mechanical Engineers, Heat Transfer Division 104 (1988) 121-127
- Schuoeker, D. (1998). Handbook of the Euro Laser Academy.
- S. Crouch and Thomas Savery, The Miner's Friend: Or an Engine to Raise Water by Fire, 1827, Page 12-16

- [27] Phillip J. Ross, Taguchi Techniques For Quality Engineering, Tata McGraw Hill, 2nd Edition, 2012 Page 91-179
- [28] Avani Kumar Dubey, and Vinod Yadava. Optimization of kerf quality during pulsed Laser Cutting of aluminium alloy sheet. Journal of materials processing technology, pages 412–418, 2008.
- [29] A.Riveiro et al. The Role of the Assist Gas Nature in Laser Cutting of Aluminum Alloys. Physics Procedia, pages 548–554, 2011.
- [30] Arindam Ghosal, and Alakesh Manna. Response surface method based optimization of ytterbium fiber Laser parameter during machining of Al/AL2O3-MMC. Optics and Laser Technology, pages 67–76, 2013.
- [31] <http://www.annualreviews.org/doi/abs/10.1146/annurev.pc.34.100183.003013>
- [32] http://www.rp-photonics.com/solid_state_Lasers.html
- [33] http://www.rp-photonics.com/fiber_Lasers.html
- [34] http://www.rp-photonics.com/semiconductor_Lasers.html
- [35] <http://www.colby.edu/chemistry/PChem/lab/DyeLaser.pdf>
- [36] http://www.rp-photonics.com/free_electron_Lasers.html
- [37] <http://www2.isye.gatech.edu/~roshan/publications/Taguchi.pdf>
- [38] <http://www2.kuas.edu.tw/prof/shihtao/qms/Powerpoint/fooster%20text/Ch07S-new.ppt>

Pitch Variations amongst Mild and Moderate Mentally Impaired Person

Kamakshi
Department of Software Engineering
ITM University
Gurgaon, India

Sumanlata Gautam
Department of Computer Science Engineering
ITM University
Gurgaon, India

Abstract: Speech is an expression of thoughts which is performed by interacting with people. As every technique in this world it has its own drawbacks, which includes inability to understand the sound or perceive it either from listener end or disruptive atypical speech generation at the speaker end.

In life we encounter number of people who are mentally unstable. In addition to the issues faced in performing basic work like confident walking public behavior and presentation, they may also suffer heavily with the speech stigma. While they speak they often sound like noise and are not understandable. Mental retardation is a relative term. Its meaning depends on the requisites of a society. A society of well grown and groomed people demands presence of intelligence and intellectualism, they search for person's social behavior to decide if a person is mentally impaired or not. This study is an attempt to find the differences and observe the pattern of pitch variation in 2 main categories of Mental retardation i.e. Mild mental retardation and moderate mental retardation.

Keywords: speech; mental retardation; spectrum analysis; pitch variation;

1. INTRODUCTION

For years there has been a setback in the field of Speech processing. There have been very few concerned researches going on to analyze and betterment of speech produced by mental patient. Researches are now more focused on to understand the root cause and brain damage which causes Speech impairment along with mental illness.

Our day to day routine, our work life, personal expressions and gratitude, needs and necessities all revolves around how we communicate it to others, and the answer lies as through interactions and speech. This requirement has made Speech as most powerful tool human have to influence and share their plans for any task.

Discussing a bit about speech production, it is created by the vibes which are created by collision of air pushed from lungs to the glottal muscles situated in our glottis or say mouth through the vocal cord.

Here we will not discuss about people who may have injured glottis or vocal cords but those people in the society which we come across who are not able to communicate efficiently due to multiple mental reasons which affects their lives. Major reasons include incapability to form a meaningful sentence or providing intone to words with special meaning, issues with speaking in an understandable format and accent or crooked pitch produced by them. In general if we talk about a normal growing person without mental illness, for adults, average pitch fluctuates through 85 Hz – 155 Hz (male) and 165 Hz – 255 Hz (female).[1] Likewise, pitch for child remains till 500 Hz.

2. MILD AND MODERATE MENTAL RETARDATION

Determining the percentage or measures of a person's retardation is not possible, as it varies with all the physical, mental, social, emotional and natural conditions. For instance, a person might be understandable to someone which would present him less retard however the same person may not be understandable to other person, so he will be considered highly retard by the other person. Surveys have given an estimate that 85 % of mental [2] patients are least severely retarded, or can be categorized into mild group. Carving and understanding the facts and truth of the mentally impairment people, it is found that population categorized under mild MR have an IQ scores amid fifty to seventy-five. They can live with self-sufficiency and independently, with the support provided by community.

Whereas the remaining 10% of population [3] which is suffering an ailment of severe mental problem is categorized as moderately retarded. They are usually suspected to obtain an IQ score which may be in middle of thirty five – fifty five. Possibly they are often found to be able to carry out only selfcare tasks with moderate supervision.

They typically acquire communication skills in childhood and they are able to live and perform daily routine tasks with totally supervised environment such as group home to stay in league with community. A moderately retarded person finds it more difficult to explain his thoughts than a Mild retarded person.

It becomes difficult for a mentally impaired person to maintain good rate of speech and ends up with [4] a slow rate odd articulation of sentences spoken. Prosodic features in their speech tends to be monotonous. The major obstruction in their expressiveness is the inability to learn remember and

determine apt and specific words to present a meaningful thought, which also results into syntactical mistakes as well. This discussion is in precedence to the various types and classifications of speech disorders which a person (typically developing or mentally retarded person) may have.

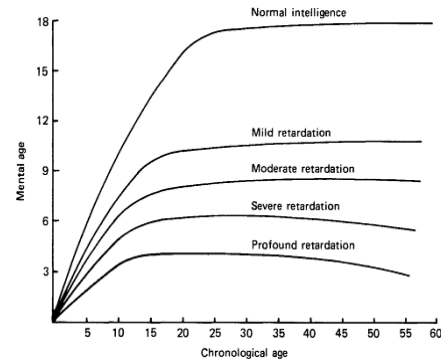


Figure 1. Mental age growth curves corresponding to normal intelligence & to the 4 levels of retardation

From ages it has been misinterpreted that Mental Retardation is same as Autism. [5] There is huge amount of dissimilarity between both of them. The sufferers of mental impendence, dearth the ability to perform routine tasks. Their intellectual, intelligence and behavioral capabilities are below the standards to live an independent life.

Autistic people are fully capable of performing all tasks and live an independent lifestyle however they pose problem in speaking.

Other than the disorders developed from childhood we may come across with another phenomenon i.e. Aphasia. In this, once the language is developed, [6] person may still fall into loss of language disorder. Predominantly adults are majorly sufferers of this language disorder. Aphasia may develop brusquely to anyone without prior disorders. Strokes are one of the key reason for Aphasia disease. Aphasia can be categorized as fluent and non-fluent.

The first Category of Fluent Aphasia speakers would not wobble or speak indifferently but they unknowingly face problems of low speech content and meaningless sentences. They are mostly unable to repeat the words and follow visual cues.

The non-fluent category of Aphasia is of higher concerns. It relates to a person's ability to utter words. One takes many pauses [7] and lots of time to utter words. Though their comprehension is surprisingly good but their omission of words makes it really hard to understand.

To reach to the depth of this knowledge area, and searching for new aspects with high precision, accuracy and sensitivity, multiple activities are performed like conducting discussions, research and experimenting and analytic groups are formed.

3. CAUSE

Low IQ scores and limitations in adaptive skills are hallmarks of mental retardation. Aggression, which sometimes leads them to hurt themselves and also such mood disorders are sometimes associated with the disability. The severity of the symptoms and the age at which they first appear depends on the cause of disorder of impairment. MR Children at mild levels reach to the developmental marks suggestively delayed. If the root of impairment is [8] chromosomal or other genetic disorders, it is often apparent from infancy. Injuries and illness from childhood are prime reasons why one may suddenly acquire speech disorder. Once easy the skills of learning and adapting suddenly becomes challenging or impossible to master. Mental retardation causes remain unknown and mystery in around 35% cases.

The slums and poverty stricken population of children is most affected with the mental illness. As it is hard for them to find healthy living conditions and support from society, moreover malnutrition and lack of medical attention they are totally ignored with any symptoms or taken care if they develop retardation.

4. EXPERIMENT

Comparative study has been performed to observe the pitch variation in Moderate mentally retarded group and Mild mentally retarded group. Aim is to compare possible differences between them.

There variety of methods and tools for speech processing for the estimation of pitch and analyzing the spectrum. We have conducted our research using PRAAT tool and analyzed speech of each and every sample using the same tool. The samples were converted to Mono file for better results.

4.1 Participants

Speakers were enlisted from a mental retardation school located in Rohtak. A total of 12 samples were recorded. 6 sample each of Mild MR and Moderate MR. We had taken all the necessary permissions from school and parents of the children and the session was conducted in the supervision of their parents and people taking care of them.

Table 1. Database of MR speakers

Group name	No of samples
Mild MR	6
Moderate MR	6
Total samples	12

4.2 Procedure

A meditation room with silent and minimal noise was arranged for the purpose of best recordings. Preferably fans and air conditioners were also switched off. Sony Professional recorder was used to record speech samples at 16 bit PCM and 44 kHz sampling rate. We found many people suffering from different categories of MR: mild MR, moderate MR, severe MR, and profound MR. But we have in-cooperated mild and moderate MR people to participate in the experiment.

5. RESULTS

5.1 Spectrum and Pitch Analysis

We have analyzed all the samples to calculate the pitch of audios. Figure2 displays the spectrum analysis of mild and moderate MR speakers. In part (A) if we look at the waveform of Mild MR there is fluency of speaking words. Whereas in part (B) the waveform is quite different, there is a lot of pauses between the words also the speaker is taking time in speaking them.

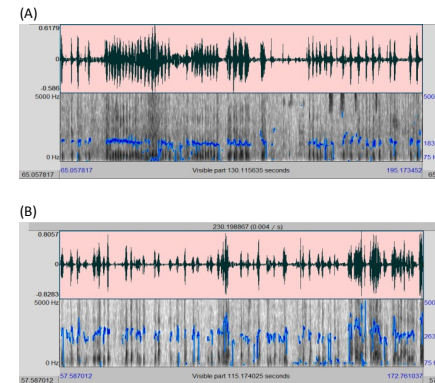


Figure2. Spectrum analysis of MR speakers (A) mild MR (B) moderate MR

The Pitch of mild MR person is comparably adjacent to those who are not having any impairment during the person's development. On the other hand the Pitch of moderate MR is very high in comparison to Mild MR.

5.2 Pitch variation

Values of pitch of all MR participants have been calculated using tool Praat. There is pattern observed in Mild and Moderate MR.

5.2.1. Mild MR

In mild MR the pitch of speaker is ranging from 120-180 approximately

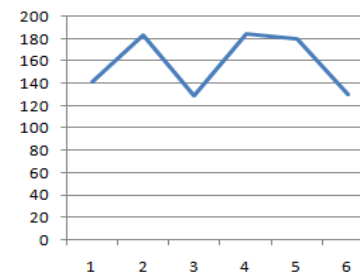


Figure 3. Pitch variation in adults suffering from mild MR

5.2.2. Moderate MR

In moderate MR the pitch variation is seen from 210 -270 approximately which is quite in comparison with mild MR.

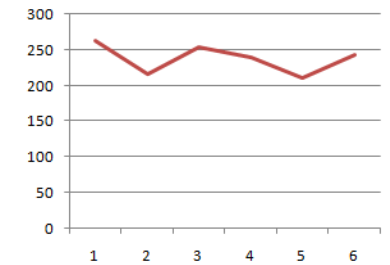


Figure 4. Pitch variation in adults suffering from moderate MR

5.2.3. Comparison between Mild and Moderate MR

Above figure shows the comparison of pitch rate for both the groups of Mild and Moderate mentally retarded Adults. We found that the pitch of adults with Moderate MR is higher than that of Mild MR

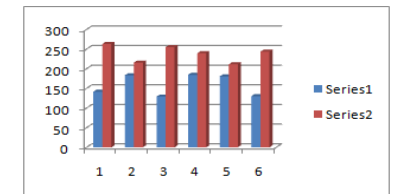


Figure 5. Comparison between Mild & Moderate MR (series1: mild MR, series 2: moderate MR)

Table 2. : Mean pitch of adults for both groups

Group	Average pitch (Hz)
Mild MR	158.4
Moderate MR	237.9

Results reveal that there is major difference mean pitch of mild MR and moderate MR. Mean pitch of Mild MR is low than that of moderate MR

6. TREATMENT AND PREVENTION

Musical therapies, extracurricular activities and social programs can help a lot in [9] treating people suffering from neurological-disorders.

The level of training depends on the degree of retardation. Mild MR can often acquire the skills needed to live independently. Moderate to profoundly retarded individuals usually require supervised community living.

Family support is very important in curing and helping mental retardation. A warm, supportive and homely environment is essential to help them.

7. FUTURE WORK

In Future the Speech of persons suffering from neurological disorder must be focused with nature of pitch variation and real cause behind the disorder. On the basis of pitch values we have attempted to present speech analysis and pitch variation but other than that fields regarding, intonation, time duration and rate of speech are key areas which still needs great focus.

8. ACKNOWLEDGMENTS

Thanking with deep gratitude to all the participants of the recording procedure I would like to extend my cordial respect to all the people who have evidenced their care to me by supporting and supervising all through my project.

My extreme respects to my guide Sumanlata Gautam for her constant and critical reviews which encouraged me to execute this paper. The in-depth insight of the system demonstrated by her helped me throughout this paper.

Lastly thanks to the schools for showing a new aspect of children with special abilities and providing permissions for conducting the research.

9. REFERENCES

[1] M. Benzeguiba, R. De Mori, O. Deroo, S. Dupon, T. Erbes, D. Jouviet, L. Fissore, P. Laface, A. Mertins, C. Ri s, R. Rose, V. Tyagi, C. Wel lekens, L. L. 1993. "Automatic Speech Recognition and Speech Variability: a Review"

[2] PC Gupta, Anjali Mathur, "Predicting the Class of a Mentally Disabled Patient to Check the level of Mental Retardation by using Feed Forward Back Propagation Neural Network", International Journal of Computer Applications, Volume 41, March 2012

[3] X. Wu and Y. Yan. "Speaker adaptation using constrained Transformation", IEEE Trans. on Speech and Audio Processing, 12(2):168-174, March 2004.

[4] Buschmann A, Jooss B, Rupp A, et al: "Children with developmental language delay at 24 months of age: results of a diagnostic work-up", Tavel, P. 2007 Modeling and Simulation Design. AK Peters Ltd.

[5] N. Evelyn Thayamani, Dr M. Parimala Fathima, Dr S. Mohan, Volume 2, Issue 6, June 2013, "Articulation and Reflection in Learning Process", Global Research Analysis (GRA)

[6] Elizabeth Bates, Elizabeth Bates, Brian MacWhinney, Cross Linguistic Research in Aphasia. Brain and Language, 41, 123-148, 1991.

[7] Dorothy Charles, Christopher Olm, John Powers, Sharon Ash, David J Irwin, Corey T McMillan, Katya Rascovsky, Murray Grossman, "Grammatical comprehension deficits in non-fluent/grammatical primary progressive aphasia", J Neurol Neurosurg Psychiatry, Sept 2013

[8] Birgitta Winnepeninckx, Liesbeth Rooms and R. Frank Kooy, "MENTAL RETARDATION: A REVIEW OF THE GENETIC CAUSES" The British Journal of Developmental Disabilities, Vol. 49, Part 1, JANUARY 2003

[9] "Speech Disorders - Children", The New York Times, May 2015.

Parametric Analysis of EN8 (AISI 1040) Alloy steel on Plasma Arc Cutting

Parthkumar M. Patel
Department of Mechanical Engineering
Indus Institute of Technology and Engineering (IITE)
Ahmedabad, India

Jaypalsinh Rana
Department of Mechanical Engineering
Indus Institute of Technology and Engineering (IITE)
Ahmedabad, India

Abstract: There are many cutting process available in the market. But, the plasma arc cutting process is one of the most effective process for the cutting of the material. In this research paper, study about the effect of selected plasma cutting parameters such as air pressure, current flow rate, cutting speed and arc gap etc. used and cutting of EN8 (AISI 1040) material. The experiment was done on the 8mm thick plate. In this experiment, the main focus on select the best parameter combination for cutting using material removal rate (MRR), surface roughness (SR) and kerf width (KW).

Keywords: EN8 (AISI 1040), Air pressure, Cutting speed, Arc gap, MRR, SR, KW, Taguchi design.

1. INTRODUCTION

Plasma is bright radiating light energy and hot radiating thermal energy. Plasma is treated as the 4th aggregate state of matter. Some examples of plasma are stars, static electricity, lightning, neon lights, fluorescent bulbs and plasma televisions. Plasma arc cutting is a thermal non-traditional cutting process. Plasma arc cutting process operates on direct current, straight polarity having electrode negative with a constricted transferred arc as shown in Figure 1. [1]

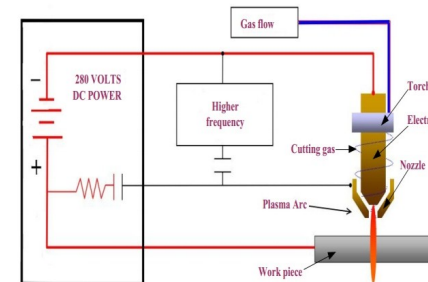


Figure 1: Schematic diagram of plasma arc cutting process

In industries. Plasma arc cutting process is most preferable for better accuracy of cutting, high production rate and good quality of cutting. There are many parameters affected on the cutting process of any material such as Air pressure, cutting pressure, selection of primary and secondary cutting gas, current flow rate, cutting speed and arc gap etc. in this research, using these plasma parameter measure the material removal rate (MRR), surface roughness (SR) and kerf width (KW). Reference [1] gives the detail information about plasma cutting process of material an Fig. 1 shows schematic diagram of plasma cutting process. In this research, medium strength steel EN8 (AISI 1040) selected which is suitable for shafts, stressed pins, studs, keys, general purpose axles and gears etc. [2]

2. EXPERIMENTAL PROCEDURE AND PARAMETERS

2.1 Material:

In this study, the EN8 (AISI 1040) medium strength steel of 8mm thick material selected whose chemical composition listed in table 1.

Fe	C	Mn	Si	S	P
94.30-96.50	0.36-0.44	0.60-1.00	0.10-0.40	>0.050	>0.050

Table 1: Chemical composition of EN8 (AISI 1040)

2.2 Taguchi method based experiments:

These experiments were performed with a 35 N/cm² (3.5 bar) of cutting gas pressure, to remove the instability and damage created by the high pressure of the cutting. In this research, the specified selected parameter were used with specified range of cutting process. Table 2 which shows the selected parameter for the cutting process of EN8 material. In this process, the list of fixed parameter shown in Table 3. The full factorial method was used to generate the L16 array and best combination of cutting parameter affecting on the response parameter. The L16 orthogonal array table created using taguchi full factorial method shown in table 4. [5] [6]

Parameter	Sign	Level 1	Level 2	Level 3	Level 4
Air Pressure (N/cm ²)	A	30	40	45	55
Current flow rate (Amp.)	B	50	70	90	110
Cutting speed (mm/min)	C	550	650	750	850
Arc gap (mm)	D	3	4	5	5.5

Table 2: Input parameter for cutting process

Fixed parameter	Set value
Material	EN8 (AISI 1040)
Cutting pressure	35N/cm ² (3.5 bar)
Cutting gas	O ₂
Shielding gas	Air

Table 3: Fixed parameter for cutting process

2.3 Material Removal Rate (MRR):

The material removal rate, MRR, can be defined as the volume of material removed divided by the machining time. Material Removal Rate (MRR) is defined by:

$$MRR = \frac{WRW}{T} \text{ [gm/min]}$$

Where,

WRW: Work piece Removal Weight (gm)

T: cutting time (min)

2.4 Surface Roughness measurement:

The surface roughness for all the cutting pieces measured using the profilometer or surface tester named as SJ-201P. Fig. 2 shows the measuring process of surface roughness. [4]

2.5 Specification of Mitutoyo surface tester SJ-201P:

Measurement range	350µm
Tip radius	5µm
Measuring force	4mN (0.4gf)
Detector drive range	21mm

Traversing speed	Measurement:- 0.25mm/sec, 0.5mm/sec
	Return:- 0.8mm/sec
Bottom configuration	V way
AC power supply	100V, 120V, 230V

Table 4: Specification of surface tester SJ-201P

2.6 Kerf Width (KW):

The kerf width of the cutting pieces was measured using the vernier caliper. Fig. 3 and 4 shows the measuring process of kerf width.

Exp. No	Air pressure (N/cm ²)	Current flow rate (A)	Cutting speed (mm/min)	Arc gap (mm)
1	30	50	550	3
2	30	70	650	4
3	30	90	750	5
4	30	110	850	5.5
5	40	50	650	5
6	40	70	550	5.5
7	40	90	850	3
8	40	110	750	4
9	45	50	750	5.5
10	45	70	850	5
11	45	90	550	4
12	45	110	650	3
13	55	50	850	4
14	55	70	750	3
15	55	90	650	5.5
16	55	110	550	5

Table 5: L16 orthogonal array for experimental setup



Figure 2: Measuring of surface roughness



Figure 3: cutting piece measured by outer jaw of vernier caliper

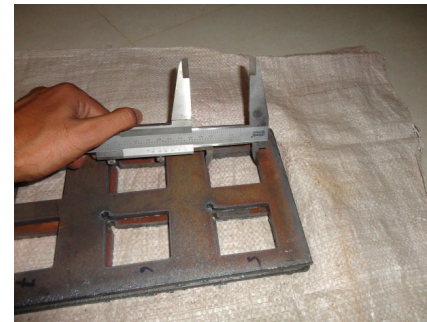


Figure 4: Hole measured by outer jaw of vernier caliper

Exp. no	Air pressure	Current flow rate	Cutting Speed	Arc gap	MRR (gm/min)	SR (µm)	KW (mm)
1	30	50	550	3	132.526	2.89	3.48
2	30	70	650	4	119.402	2.55	4.01
3	30	90	750	5	105.461	2.33	3.25
4	30	110	850	5.5	199.095	2.17	3.31
5	40	50	650	5	103.004	2.72	2.5
6	40	70	550	5.5	125.412	2.47	2.54
7	40	90	850	3	112.994	2.27	3.26
8	40	110	750	4	110.403	3.08	3.23
9	45	50	750	5.5	118.143	2.26	2.93
10	45	70	850	5	138.309	1.89	3.07
11	45	90	550	4	135.593	2.49	3.14
12	45	110	650	3	129.292	3.18	3.09
13	55	50	850	4	104.683	1.84	2.94
14	55	70	750	3	117.839	2.33	3.09
15	55	90	650	5.5	123.188	2.46	3.25
16	55	110	550	5	131.687	3.23	3.13

Table 6: Results obtain from the experiment

3. DISCUSSION AND CONCLUSION

3.1 Discussion about MRR:

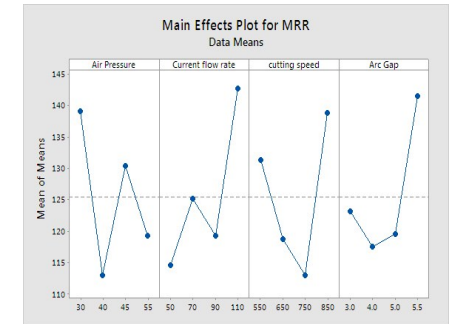


Figure 5: Main effect graph for MRR

In this research, the larger amount of MRR was most effective for the process. Fig. 5 shows that the higher MRR will meet at

air pressure 30 N/cm², current flow rate 110 A, cutting speed 850 mm/min and arc gap 5.5 mm. The graph generate by the use of MINITAB 17 statistical software for MRR.

It has been conclude that the optimum combination of each process parameter for higher MRR is meeting at high cutting speed [C4], low air pressure [A1], high current flow rate [B4] and high arc gap [D4].

Exp. no	Air pressure	Current flow rate	Cutting speed	Arc gap	MRR
1	30	110	850	5.5	199.095
2	40	50	650	5	103.004

3.2 Discussion about SR:



Figure 6: Main effect for SR

In this research, the smaller amount of SR value was effective for the experiment. Fig. 6 shows that the higher MRR will meet at air pressure 45 N/cm², current flow rate 70 A, cutting speed 850 mm/min and arc gap 5.5 mm. The graph generate by the use of MINITAB 17 statistical software for MRR.

It has been conclude that the optimum combination of each process parameter for higher MRR is meeting at high cutting speed [C4], higher medium air pressure [A3], lower medium current flow rate [B2] and high arc gap [D4].

Exp. no	Air pressure	Current flow rate	Cutting speed	Arc gap	SR
1	50	110	550	5	3.23
2	55	50	850	4	1.84

3.3 Discussion about KW:

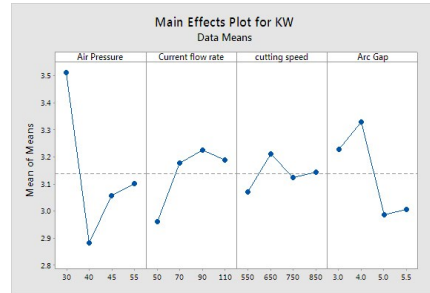


Figure 7: Main effect for KW

In this research, the smaller amount of KW value was effective for the experiment. Fig. 7 shows that the higher MRR will meet at air pressure 40 N/cm², current flow rate 50 A, cutting speed 550 mm/min and arc gap 5 mm. The graph generate by the use of MINITAB 17 statistical software for MRR.

It has been conclude that the optimum combination of each process parameter for higher MRR is meeting at low cutting speed [C1], lower medium air pressure [A2], low current flow rate [B1] and higher medium arc gap [D3].

Exp. no	Air pressure	Current flow rate	Cutting speed	Arc gap	SR
1	30	70	650	4	4.01
2	40	50	650	5	2.50

4. REFERENCES

- [1]Facts about plasma technology and plasma cutting, https://boc.com.au/boc_sp/au/downloads/gas_brochures/BOC_217076_FactsAboutPlasmaTechnology_FA%20low%20res.pdf
- [2] http://en.wikipedia.org/wiki/Plasma_cutting
- [3]www.hypertherm.com
- [4]https://www.atecorp.com/ATECorp/media/pdfs/datasheets/Mitutoyo-SJ-201P_Datasheet.pdf
- [5]<http://support.minitab.com/enus/minitab/17/topiclibrar/modeling-statistics/doe/taguchidesigns/taguchidesigns/>
- [6] http://nutek-us.com/DOE_Topic_Overviews35Pg.pdf
- [7]https://controls.engin.umich.edu/wiki/images/0/0b/Lecture_25.pdf
- [8]Gullu A., Atici U., "Investigation of the effects of plasma arc parameters on the structure variation of AISI 304 and St 52 steels" Materials and Design 27, 2006, pp. 1157-1162
- [9]Chen J., Li Y., Cox R., "Taguchi-based six sigma approach to optimize plasma cutting process: an industrial case study" international journal advance manufacturing Technology, 2009, pp. 760-769
- [10]Wang J., Zhu Z., He C., Yang F., "Effect of dual swirling plasma arc cutting parameters on kerf characteristics", international journal material form 4:, 2011, pp. 39-43
- [11]Samardzic I., Stoic A., Klaric S., Pavic J., "possibilities of cost effective plasma cutting application" 4th DAAAM International Conference on Advanced Technologies for Developing Countries, 2005, pp. 307-312
- [12]E. Gariboldi, B. Previtali (2004) - "High tolerance plasma arc cutting of commercially pure titanium"
- [13]Asiabanpour Bahram (2009) Optimizing the automated plasma cutting process by design of experiments. Int. J. Rapid Manufacturing, Vol. 1, No. 1, 2009.
- [14]Conrads H and Sachmidt M, Plasma generation and plasma source, plasma source sci. Technol 9, 2000, pp. 441-454
- [15]Colombo V., Concetti A., Ghedini E., Rotundo F., Sanibondi P., Dallavalle S., "Advances in plasma arc cutting technology the experimental part of an integrated approach", plasma chemistry and plasma processing, vol.32, No. 3, 2011, pp. 411-426
- [16]R. Bini, B.M. Colosimo, A.E. Kutlu, M. Monno (2007) - "Experimental study of the features of the kerf generated by a 200A high tolerance plasma arc cutting system" Department of Mechanical Engineering, Politecnico di Milano, Via Bonardi 9, 20133 Milano, Italy.
- [17]w.j.xu, j.c.fang, y.s. lu (2002) - "study on ceramic cutting of plasma arc" School of Mechanical Engineering, Dalian University of Technology Dalian 116023, PR China. journal of materials processing technology 129 (2002) 152-156
- [18]Ejik C., Fostervoll H., Sallom Z. K., Akselsen O. M., "plasma welding of NITI to NITI, stainless steel and hastelloy c276" ASM Materials Solutions Conference, Pittsburgh Pennsylvania, USA, 13-15 October 2003

A K-Means based Model towards Ebola Virus Prorogation Prediction

Baohua LIU
Department of Computer
Science, Shandong University
of Science and Technology,
Qingdao 266590, China

Xudong Wang
Department of Information
System, Shanghai University,
Shanghai 201800, China

Qi Gao
Department of Mathematics,
Shandong Normal University,
Jinan 250002 China.

Cong LIU
Department of Computer
Science, Shandong University
of Science and Technology,
Qingdao 266590, China

Abstract: Ebola hemorrhagic fever is a disease caused by one of five different Ebola viruses. Four of the strains can cause severe illness in humans and animals. Humans can be infected by other humans if they come in contact with body fluids from an infected person or contaminated objects from infected persons. Humans can also be exposed to the virus, for example, by butchering infected animals. Deadly human Ebola outbreaks have been confirmed in the following countries: Democratic Republic of the Congo (DRC), Gabon, South Sudan, Ivory Coast, Uganda, and Republic of the Congo (ROC), Guinea and Liberia. In this sense, it is of vital importance to analysis the history data and predicts its propagation. More specifically, a model based k-means algorithm to determine the optimal locations of virus delivery is constructed and tested Using Mab-lab programming. By experiment, we find that our model can work well and lead to a relatively accurate prediction, which can help the government forecast the epidemic spread more efficiently.

Keywords: Date Mining; K-Means Technique; Algorithm Complexity; Ebola Infect Prediction; Mat-lab Simulate

1. INTRODUCTION

Ebola also known Ebola virus, which is a very rare virus in southern Sudan in 1976 and Izard Ebola River discovery of its existence, hence the name^[1]. According to the World Health Organization's message, since December 2013, the outbreak of the Ebola virus outbreak in West Africa continued, in Guinea, Sierra Leone and Liberia infected at least 567 people, including 350 deaths^[2]. The disease has a high risk of death, killing between 25 and 90 percent of those infected with an average of about 50 percent and has caused immense sorrow especially for the African people^[3]. If there is no effective drug control measures and the epidemic will continue to spread it, and spread to the whole world.

Based on the data from World Health Organization, Ebola virus does not spread through the air, and no evidence has proved that the virus undergo the variation. Mode of transmission of Ebola virus is close direct contact with body fluids of patients, including the patient's blood, excrement, vomit which serve the strongest infection. Virus can also be found in saliva and tears.

We build a model to simulate the spreading of the disease, a model based k-means algorithm to determine the optimal locations of delivery. By the experiment, we find our model can work well, they can help government forecast the epidemic spread, and can save a lot of resource.

2. FORECASTING OF EBOLA CRISIS

Ebola outbreak in Guinea after a steady period of time and, more recently was "looked up" trend. 2014, ravaged West African country of Guinea, Liberia, Sierra Leone, the Ebola virus spreading at an alarming rate. By February 6, 2015^[4], the World Health Organization had reported 22,525 confirmed, probable and suspected cases in West Africa, with 2988 in

Guinea, 8745 in Liberia and 10792 in Sierra Leone. What is worth, it has caused 9004 deaths.

Ebola outbreak in Guinea after a steady period of time and, more recently was "looked up" trend. We care about the few infected person can infect assigned to the crowd, with the passage of time, whether the disease will spread, causing many people are infected. It cannot wait to predict the ratio of Ebola virus spreads.

As it is shown in table 1, we have found some data from the site of WHO (World Health Organization). By these data, we can discover the trend of Ebola virus spreads.

Table 1. number of infection in Guinea, Liberia, Sierra Leone

	Guinea	Liberia	Sierra Leone
2014-11-24		2753	
2014-11-25	1892		5595
2014-11-28	1921	2801	5831
2014-11-29		2805	
2014-11-30	1929		5978
2014-12-1			6039
2014-12-2	1949	2824	6201
2014-12-3	1956	2830	
2014-12-6	2035		6317
2014-12-7	2051	2869	6375
2014-12-9	2081	2946	6457
2014-12-10	2096		6497
2014-12-13	2115		6638
2014-12-14	2127	3021	6702
2014-12-16	2164		
2014-12-17			6856
2014-12-18		3085	

2014-12-20	2259	3085	6975
2014-12-21	2284		7017
2014-12-24	2342	3108	7160
2014-12-27	2384		7326
2014-12-28	2397	3110	7354
2014-12-31	2435	3116	7476
2015-1-2		3118	
2015-1-3	2465	3118	7570
2015-1-4	2471		7602
2015-1-5	2477		
2015-1-6		3123	7759
2015-1-7	2493	3123	
2015-1-10	2508		7766
2015-1-11	2514	3127	7786
2015-1-12	2522	3127	7802
2015-1-13	2525		7825
2015-1-15		3131	
2015-1-17	2539		7883
2015-1-18	2539	3135	7903
2015-1-19	2542		7909
2015-1-20	2545	3136	7921
2015-1-24	2559		7963
2015-1-25	2569	3138	7968
2015-1-26	2571	3138	7977
2015-1-27	2575		7989
2015-1-28		3138	
2015-1-31	2593	3143	8042
2015-2-1	2608	3143	8059
2015-2-2	2621		8063
2015-2-3	2628		8084

2.1 Ebola virus infection forecast model without drug

To make it easier to understand the model, we first list the symbols used in the following table.

Table 2. Symbols used in the model

$i(t)$	the number of infected individuals in the t day
$s(t)$	the number of susceptible individuals in the t day
N	total people in the country
k	infection coefficient

Assumption

(1) $s(t)$ represents the number of susceptible people in the t day, and $i(t)$ represents the number of infection people in the t day.

(2) Each day it increase $k0$ infection, and $k=0$ can be calculated by the following equation: $K0=k*s(t)$.

(3) People will not die in the country, that is to say, $s(t)+i(t)=N$.

By the three assumptions, we can obtain the following differential equation[7-9]:

$$(1)$$

Solve the differential equation, we achieve

$$(2)$$

Figure 1 shows the trend of $i(t)$ with the increasing of t .

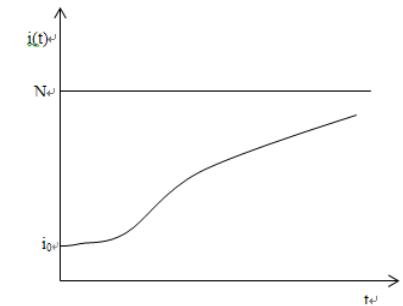


Figure 1. Change of the infected people

We can see from the chart, the number of infection people is increasing with t, the speed is very quick at the start time, but when there are a lot of people infected, the speed is become low. When $t \rightarrow \infty$, $i(t) \rightarrow N$.

According to the model, and combine with the data in table 1, we obtain the infection trend in Sierra Leone by matlab^[5], it is showed in Figure 2.

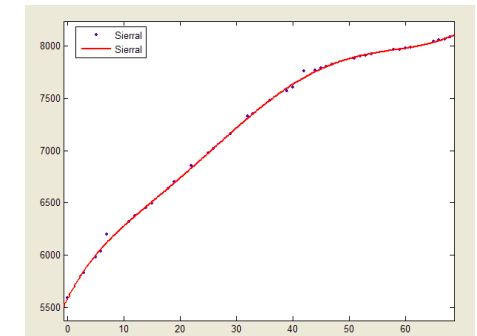


Figure 2. Trend of number of infected people in Sierra Leone

We select November 25, 2014 as the first day, use matlab plot the chart, it can be seen from the chart that the infection ratio is decline. We predict the future infection number by the model, list them in table 3.

Table 3 Number of the infected in the next five days

time	2-4	2-5	2-6	2-7	2-8
number	8089	8116	8146	8180	8219

2.2 The SIR model

Assume the world medical association has developed a new medication that can stop Ebola and cure patients whose disease is not advanced, the model above can not meet the situation, so we build the following model. As the first step in the modeling process, we identify the independent and dependent variables. The independent variable is time t, measured in days.

To make it easier to understand the model, we first list the symbols used in the following table.

Table 4. Symbols used in the model

$S(t)$	the number of susceptible individuals
$I(t)$	the number of infected individuals
$R(t)$	the number of recovered individuals
N	the total population in the country
$s(t)=S(t)/N$	the susceptible fraction of the population
$i(t)=I(t)/N$	the infected fraction of the population
$r(t)=R(t)/N$	the recovered fraction of the population
b	the number of people infected contact
k	recover ratio

Assumption

(1) No one is added to the susceptible group, since we are ignoring births and immigration. The only way an individual leaves the susceptible group is by becoming infected. We assume that the time-rate of change of $S(t)$, the number of susceptibles, depends on the number already susceptible, the number of individuals already infected, and the amount of contact between susceptible and infected. In particular, suppose that each infected individual has a fixed number b of contacts per day that are sufficient to spread the disease. Not all these contacts are with susceptible individuals. If we assume a homogeneous mixing of the population, the fraction of these contacts that are with susceptible is $s(t)$. Thus, on average, each infected individual generates $b s(t)$ new infected individuals per day. With a large susceptible population and a relatively small infected population, we can ignore tricky counting situations such as a single susceptible encountering more than one infected in a given day.

(2) We also assume that a fixed fraction k of the infected group will recover during any given day. For example, if the average duration of infection is three days, then, on average, one-third of the currently infected population recovers each day. (Strictly speaking, what we mean by "infected" is really "infectious," that is, capable of spreading the disease to a susceptible person. A "recovered" person can still feel miserable, and might even die later from pneumonia.)

It may seem more natural to work with population counts, but some of our calculations will be simpler if we use the fractions instead. We complete our model by giving each differential equation an initial condition. Our complete model is:

$$(3)$$

We don't know values for the parameters b and k yet, but we can estimate them according to the data. We can use matlab to solve the differential equation and use it to plot the chart.

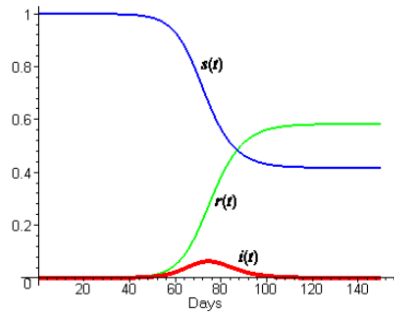


Figure 3. Change of ratios of infected, susceptible and removed people

From the chart, we can see before drugs play a part, the number of infection is increasing with time, achieve a peak value, then the number of infection will decrease by zero. After treatment, the number of susceptible plus the number of recover and death is the number of people in the country.

3. DETERMINING THE LOCATIONS OF DELIVERY

For a simpler demonstration of our model, we take the country of Sierra Leone to be the scope of consideration. The official site of the WHO provided two maps showing respectively the situation of transmission of the disease and the information regarding the currently opened Ebola treatment centers. For a more informative view, we combined the two maps:

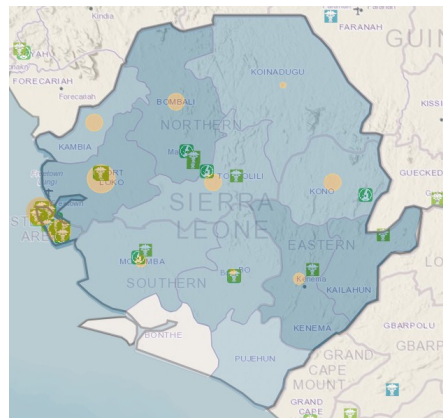


Figure 4. Transmission of Ebola in Sierra Leone

Symbols like this reveal that the locations of the currently functioning Ebola treatment centers. And the coloring of the regions reflects how heavily it has been hit by the disease in the long term. The heavier the color, the larger is the number of accumulated cases of infection. Finally the orange circles show how well the spreading of the disease has been contained in

those particular regions. Larger circles mean that more cases of infection have been confirmed over the last 21 days.

We suppose that multiple locations of initial deliveries rather than only one location of initial delivery will later result in easier and quicker distribution of the medication. In this particular case, we assume that initial deliveries will be made to three locations within the country.

In order to determine the locations for greater efficiency, we consider the locations of the Ebola treatment centers. We try to divide the treatment centers into three groups in such a way that treatment centers within the same group are geographically relatively closer to each other while the geographical distances are relatively larger between treatment centers that belong to different groups. We then determine one location of delivery within each of the three groups. For the purpose of the grouping of the treatment centers, we adopt the k-means clustering algorithm^[6].

First of all, we establish a certain rectangular coordinate system on the map and determine accordingly the coordinates of each of the Ebola treatment centers as shown in the figure below:

In the west-most part of the country where there are quite a number of treatment centers located very near to each other, we pick only one of them to be considered in the clustering process.

The geographical distances as the crow flies between any two of the Ebola treatment centers are listed in the matrix below:

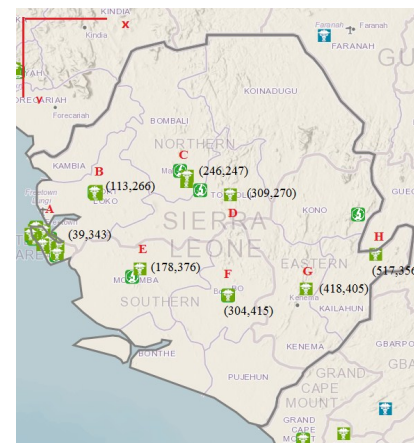


Figure 5. Geographical locations of ETCs in Sierra Leone

Table 5. Distances between ETCs

	A	B	C	D	E	F	G	H
A	0	106.794	228.178	279.694	142.864	274.607	384.038	478.177
B	106.794	0	134.35	196.041	127.769	242.244	335.181	413.903
C	228.178	134.35	0	67.0671	145.825	177.73	233.555	292.099
D	279.694	196.041	67.0671	0	168.514	145.086	173.511	225.078

E	142.864	127.769	145.825	168.514	0	131.898	241.746	339.589
F	274.607	242.244	177.73	145.086	131.898	0	114.438	221.02
G	384.038	335.181	233.555	173.511	241.746	114.438	0	110.463
H	478.177	413.903	292.099	225.078	339.589	221.02	110.463	0

Algorithm:

First we choose three of the initial centers of the three clusters denoted as: Cluster_i (i=1, 2, 3).

We then consider the distances between each of the rest of the treatment centers and each of the three treatment centers chosen as the center of the clusters $D_{p,ci}$.

Where p is any one of the rest of the treatment centers and c_i is any of the centers of the clusters, namely, at this particular moment, the treatment centers chosen as the initial centers of the clusters.

If for a given p , $\min\{D_{p,ci}\}=D_{p,cj}$, then p belongs to the j th cluster.

In the next iteration we first compute the new centers of Cluster_i (i = 1,2,3) as the means of p_i , where p_i is the treatment centers already assigned to Cluster_i:

$$(4)$$

Where n_i is the number of treatment centers in Cluster_i, x_{ij} is the x coordinate of the j th treatment center in Cluster_i and y_{ij} is the y coordinate of the j th treatment center in Cluster_i.

We compute again $\min\{D_{p,ci}\}$ for every i and determine once more time which cluster each treatment center belongs to in light of the new c_i for each Cluster_i.

We repeat this process until not a single one treatment center transmits from one cluster to another within an iteration.

At this time we take the clusters as the final result.

Solution:

First we take $A = (39,343)$, $C = (246, 247)$, $H = (517, 356)$ as the initial centers for each of the three clusters, see in figure 7.

And we apply the algorithm to the map, achieve the result shown in figure 8.

The result of the second iteration is exactly the same as the first. And the final result is depicted in the following figure 9.

Then we take the centers of each of the clusters as the initial delivery locations: $c_1 = (110, 328)$, $c_2 = (286, 311)$, $c_3 = (468, 380)$.

After the initial deliveries are made, medication should be then transmitted to the Ebola treatment centers within the corresponding cluster where they can be stored, organized and utilized for the treatment of the Ebola disease.



Figure 7. The initial centers of the clusters

4. CONCLUSION

When modeling the propagation of the disease, we not only adopt a fitting algorithm based on the relevant data obtained from the WHO official website, but we also discuss the incorporation of the SIR model which takes into account the dynamics of an infectious disease itself.

To help plan out the delivery of the medication, we not only consider the transmission of the disease but we also take into account the locations of the Ebola treatment centers currently established. This adds to the practicality of our model.

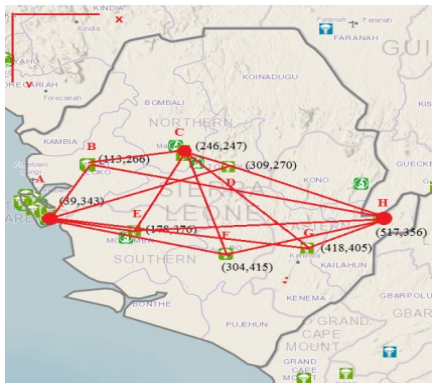


Figure 8. The crow-fly distances of ETCs

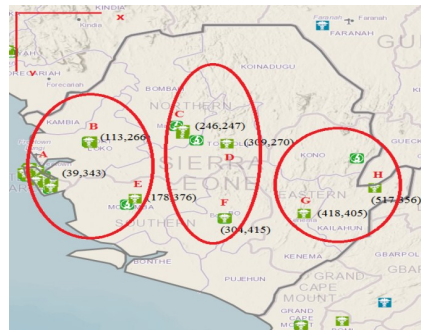


Figure 9 Result of the clustering algorithm

5. ACKNOWLEDGMENTS

This work was supported in part by the Graduate Innovation Foundation Project of Shan-dong University of Science and Technology (YC140106). Also, we would like to thank those anonymous reviewers for their constructive comments to help us improve the paper.

6. REFERENCES

- [1] L. Zhang, H. Wang. Forty years of the war against Ebola. Zhejiang Univ-Sci B 2014; 15(9): 761-765.
- [2] "Ebola virus disease Fact sheet No. 103". World Health Organization, September 2014.
- [3] Birmingham, K and Cooney, S. Ebola: small, but real progress (news feature). Nature Med 2002;8:313.
- [4] <http://apps.who.int/gho/data/view.ebola-sitrep.ebola-summary-20150206?lang=en>
- [5] Zhuo Jinwu. Matlab in the application of mathematical modeling. Beijing university of aeronautics and astronautics. 2011.
- [6] Jiawei Han. Data Mining. China Machine Press. 2013.

Modified Page Rank Model in Investigation of Criminal Gang

Ting LU
Research Center for Cloud Computing
North China University of Technology,
Beijing 100043, China

Qi Gao
Department of Mathematics,
Shandong Normal University,
Jinan 250002 China.

Xudong Wang
Department of Information System,
Shanghai University,
Shanghai 201800,China

Cong LIU
Department of Computer Science, Shandong
University of Science and Technology,
Qingdao 266590, China

Abstract: In this paper, we consider a criminal investigation on the collective guilt of part members in a working group. Assuming that the statistics we used are reliable, we present the Page Rank Model based on mutual information. First, we use the average mutual information between non-suspicious topics and the suspicious topics to score the topics by degree of suspicion. Second, we build the correlation matrix based on the degree of suspicion and acquire the corresponding Markov state transition matrix. Then, we set the original value for all members of the working group based on the degree of suspicion. At the last, we calculate the suspected degree of each member in the working group. In the small 10-people case, we build the improved Page Rank model. By calculating the statistics of this case, we acquire a table which indicates the ranking of the suspected degree. In contrast with the results given in this issue, we find these two results basically match each other, indicating the model we have built is feasible. In the current case, firstly, we obtain a ranking list on 15 topics in order of suspicion via Page Rank Model based on mutual information. Secondly, we acquire the stable point of Markov state transition matrix using the Markov chain. Then, we build the connection matrix based on the degree of suspicion and acquire the corresponding Markov state transition matrix. Last, we calculate the degree of 83 candidates. From the result, we can see that those suspicious are on the top of the ranking list while those innocent people are at the bottom of the list, representing that the model we have built is feasible. When suspicious topics and conspirators changed, a relatively good result can also be obtained by this model. In the current case, we have the evidence to believe that Dolores and Jerome, who are the senior managers, have significant suspicion. It is recommended that future attention should be paid to them. The Page Rank Model, based on mutual information, takes full account of the information flow in message distribution network. This model can not only deal with the statistics used in conspiracy, but also be applied to detect the infected cells in a biological network. Finally, we present the advantages and disadvantages of this model and the direction of improvements.

Keywords: Page Rank ;Markov Chain; Criminal Gangs; Biological Model; Algorithm; Markov Chain

1. INTRODUCTION

1.1 Background

With the advent of the information age, information technology development has brought new challenges and opportunities to the public security work. Because of its superiority, people are paying close attention to how to integrate and reuse to the public security data resources and how to achieve comprehensive application of global data, the automatic association of all kinds of information as well as the automatic mining function of a variety of cues, which will provide integrated applications in the information handling. Using the semantic network analysis and the relevant models plays a major role in improving the efficiency and accuracy of detection.

1.2 What is "Crime Gangs"?

Crime Gangs is a crime form, referring to the two or more persons jointly committing one or more crimes. Intelligence information (such as the collection of the relevant people's conversations in this given case) is the technical basis of the intelligence analysis. The implementation of criminal intelligence analysis is based on intelligence gathering, mining and establishing crime patterns, analyzing and judging criminal clues as well as a variety of relationships. Building an efficient model to analyze the relevant information will surely provide

some useful clues for the detection of cases and the judgment of criminal suspects.

1.3 The Mission of Our Team

In this paper, we would like to introduce the theory of information analysis to solve the problems, which is described as follows: In the previous case, it is our team's duty to identify the guilty parties among the 10 candidates. Similarly, the other problem is to solve a relatively larger case, where there are about 83 candidates.

The analysis and process of these problems are divided into three steps. Firstly, we use the method of mutual information to score all the topics mentioned. Secondly, we can acquire the correlation matrix by calculating the score of the associated topics among the candidates. Thirdly, by solving the Markov Transfer Matrix, we get the stable point of Markov Transfer Matrix, which is the final index of 83 candidates. By analyzing this index, the 83 degree of suspicion can be determined.

2. PROBLEM ANALYSIS

2.1 Topics' Suspicious Degree Analysis

First, we analyze the suspicious degree of talks between each other, using the mutual information and entropy in information theory, defined as $M(A,B) = I(A) + I(B) - I(A,B)$, to obtain the

scores of the 12 undetermined topics and the scores of suspicious ones (Obviously, the scores of the suspicious are supposed to be higher than the others). Further illustration is put in models.

2.2 The Transmission of Suspicious Information in the Working Group Analysis

The work group is divided into five parts, namely, the confirmed suspects, the people with some suspicion, the undetermined people and the innocent (listed by the degree of suspicion). Because we refer to Google's PageRank algorithm, we need to obtain the correlation matrix of this group of people first. Then we can use this algorithm to get the Markov Transfer Matrix and later get the stable points using the nature of Markov. The acquisition of the correlation matrix is based on the message topics among the 83 people. We can use g_{ij} to represent the total scores of all the topics, thus getting an 83*83 correlation matrix.

2.3 The Initial Vector Distribution of the Working Group Analysis

To solve the Markov stable point, we need to use the initial vector distribution. We define the scores of the suspicious as α (The total number of this group of people is n); the scores of the innocent is 0; the scores of the undecided is β (The total number of this group of people is m). They satisfy the equation $n\alpha + m\beta = 1$, and then we can decide the values of α and β through the search of α with step size of 0.1

3. BASIC ASSUMPTIONS OF OUR MODEL

- 3.1. All data is true and reliable.
- 3.2. There is valid evidence to prove the people who are suspicious.
- 3.3. There is valid evidence to prove the people who are innocent.
- 3.4. The suspicious topics have higher degree of doubt than that of the undetermined ones.
- 3.5. An objective and subjective attitude is kept in the process of handling the cases.
- 3.6. These topics give a valid summary of the messages.

4. MODEL AND SOLUTION

Our whole model is divided into 3 parts, including 3.1, 3.2 and 3.3. In the 3.4 part, we use the whole model to analyze a simple example. And in 3.5 and 3.6, we solve the real problem presented in question 1, and its changed version in question 2.

4.1 Mutual Information Algorithm

Let me put a simple example to better illustrate this algorithm. "What a good weather today! I would like to go fishing." A says to B. The words, such as "today", "weather", "good", "I", "fishing" involved in this conversation, can be seen as key words, and we can use a_1, a_2, \dots to represent them. When B says to A: "Yeah, really good weather! I will go climbing." Also, the words such as "weather", "hiking", "good", "I", can be extracted as key words and we can use b_1, b_2, \dots to represent them. Here, we list the relationship between the words of these two people.

Table 1: the language relationship table

	today	good	fishing	weather	I	0	0
A	1	1	1	1	1	0	0
B				weather	I	good	climbing

	0	0	0	1	1	1	1
--	---	---	---	---	---	---	---

Notes: "1" in the second row and second column of the table represents the key word "today" said by A, but "0" in the fourth row and second column represents that B didn't say the key word "1" indicates the value of mentioned topic in the chat, "0" indicates the value of topic which is not mentioned in the table.

We can use the formula of mutual information $M(X,Y) = I(X) + I(Y) - I(X,Y)$ to get the value of the mutual information, defined as $M(X,Y)$, where $I(X)$ represents the entropy from A, $I(Y)$ represents the entropy from B.

$$I(X) = -P_0 \log P_0 - P_1 \log P_1 \quad (4.1-1)$$

$$I(Y) = -P_0 \log P_0 - P_1 \log P_1 \quad (4.1-2)$$

$$I(X,Y) = -P_{10} \log P_{10} - P_{11} \log P_{11} - P_{01} \log P_{01} \quad (4.1-3)$$

P_0 and P_1 denoting the probability of 0 and 1 respectively; P_{10} , P_{11} and P_{01} denoting the probability of (1, 0), (1, 1) and (0, 1) respectively.

4.2 Markov Chain Model

In order to get the Markov state transition matrix, we first need to get the 83*83 Markov correlation matrix (rows represent the person's words, columns represent the words that others said to him /her). According to each topic, sum up the weight of the words involved in the conversation between one person and the others so as to get the total weight of one person, in the same way, we can come to the other people's weight, thus getting an 83*83 Markov correlation matrix.

Although we use Google's Page Rank model, some people are not the information receivers in the case, so it is unavoidable that the sum of a few columns in the association matrix is 0. Taking this into account, when computing the Markov Transfer Matrix, we do some special handling on the correlation matrix to make the sum of all the columns of the correlation matrix non-zero.

Define the Markov Transfer Matrix as $A = (a_{ij})$, then

$$c_j = \sum_i g'_{ij} \quad (4.2-1)$$

$$r_i = \sum_j g_{ij} \quad (4.2-2)$$

C_j represents the sum of columns in matrix $G(g_{ij})$, r_i represents the sum of rows in matrix $G(g_{ij})$, g_{ij} represents the elements in the correlation matrix $G(g_{ij})$.

The formula used to solve the elements in transfer matrix A is

$$a_{ij} = \frac{(1-d)}{n} + d * \frac{g'_{ij}}{c_j} \quad (4.2-3)$$

d is a model parameter, we choose to define $d = 0.85$ based on experience. a_{ij} represents the summed scores of the message topics involved in the conversation from person j to person i . From the basic nature of the Markov chain, there is a stationary distribution in the regular Markov chain $x = (x_1, x_2, \dots)$, then we can get the sorting in accordance with the conspiracy possibility.

4.3 Improved Page Rank Model

As we have known, there are 7 conspirators among the 83 people in the second case and each person's scores can be defined as $P(i), i = 1, 2, \dots$. And the scores of each innocent person can be defined as $P(j), j = 1, 2, \dots, 8$. The model is as follows:

$$\max M(\lambda, s) = \sum_{i=1}^7 P(i) - \sum_{j=1}^8 P(j) \quad (4.3-1)$$

s.t.

$$Ax = x \quad (4.3-2)$$

$$\sum_{i=1}^n x_i = 1 \quad (4.3-3)$$

The objective function indicates the maximum probability gap between the known conspirators and the innocent (All the conspirators are put in the upper part of the list, and all innocence in the lower part of the list, leaving the undecided people located in the middle of the list). We use k to express the maximum of mutual information in the 12 topics. λ represents the steps from the upper bound to 20. Through the debugging and analysis, we find that when λ is given a value of 0.5, the results will be much more in line with the subject requirements. S is the initial vector distribution, the percentage of each conspirator is 0.1, and the percentage of each innocent person equals to 0, so the undetermined equally allocate the remaining percentage. We define that s ranges from 0.5 to 0.9 is distributed in steps of 0.1, and we can get an initial vector distribution on the subject on the whole.

4.4 Solution of The 10-people Case

In practice, we conducted some exploratory analysis on the previous case, and get 4 ranking list of the probability of all the people when defining $k=1, 10, 12, 15, 17, 20$, respectively. Through comparative analysis, we find that when $k=17$, the ranking we get will be more in line with the true outcome of the case than other values, that is, people like Inez don't get off, people like Carol are not falsely accused, and people like Bob do not have the opportunity to get reduced sentences. When $k=17$, we can obtain a ranking list of suspicious degree, listed as follows:

Table 2: The Sorting Table of the degree of Suspicious (k=17)

Ranking	Number	Name
1	7	George
2	2	Bob
3	9	Inez
4	4	Dave
5	5	Ellen
6	1	Anne
7	8	Harry
8	10	Jaye
9	3	Carol
10	6	Fred

Conclusion Analysis:

(1)George and Dave are the given co-conspirators, ranking fourth in the list. Meanwhile, Bob ranks second, illustrating he is one of the co-conspirators, so he cannot get off. Inez ranks third, meaning that we can also catch him.
(2)Jaye and Anne are both ranked relatively rearward, which is in accordance with the given information. And based on Carol ranking No.9, we can basically determine her innocence. Overall, the solution derived from our models can meet the actual requirements and have some promotional value.
From the previous analysis, we know that the 10-people case is a microcosm of the current case, and the results of small case subject has been given to us, so understanding and solving the smaller case can be seen as a test of our models, which may help us to modify them.

4.5 The Solution of the Current case for Problem 1

When conducting an exploratory analysis on the current case, we used the same way as the first one to analyze. We found that

when $k=17$ or $k=20$, we can get two basically the same probability rankings of all the people, much more in line with the requirements listed in the subject.

First, we can obtain the ranking list of the 15 topics using the Mutual Information Method.

Table 3: Score Ranking List of 15 Topics

Number	Score
1	0.883016
2	0.857865
3	0.898072
4	0.87294
5	0.872976
6	0.857882
1	1
8	0.888021
9	0.883014
10	0.893037
11	1
12	0.888021
13	1
14	0.888034
15	0.883008

Notes: The numbers of suspicious topics are 7, 11, 13. The suspicious degree ranking of the suspected, innocent and the senior managers based on $k=17$.

Table4: The Sorting Table Based on the Suspicious Degree of the Conspirators, Non-conspirators and Senior Managers (K=17)

Ranking	Name	Number
1	Yao	68
2	Alex	22
4	Paul	44
6	Harvey	50
7	Dolores	11
8	Ulf	55
17	Jerome	17
19	Jean	19
27	Paige	3
28	Elsie	38
31	Darlene	49
46	Chris	1
57	Tran	65
58	Ellin	69
60	Gretchen	5

Notes: The senior managers are Dolores, Jerome and Gretchen.
Conclusion Analysis:

- (1) By analyzing the result, we can find that two senior managers, namely Dolores and Jerome are both conspirators.
- (2) The already known conspirators are shown in the forefront of the ranking list, we can basically draw that they are the conspirators.
- (3) The already known non-conspirators are all at the rear of the ranking list, except for Paige who ranks 27, the others can be determined to be innocent. Although there are a few minor differences, this result has been very much in line with the actual situation, which means the feasibility and stability of the model is very well.

4.6 The Solution of the Current Case for Problem 2

As to the second requirement, we can also use the Improved Page Rank Model to analyze data. First obtain a modified ranking list of the 15 topics, listed as follows:

Table 5: Score Ranking List of the 15 Modified Topics

number	score
1	1
2	1.177737
3	1.20412
4	1.193429
5	1.172717
6	1.167063
7	1
8	1.199102
9	1.193429
10	1.20412
11	1
12	1.20412
13	1
14	1.173339
15	1.193429

Then we can get the ranking list about the suspicion degree of the suspected, the innocent and the senior managers.

Table 6: The Sorting Table Based on the Suspicious Degree of the Conspirators, Non-conspirators and Senior Managers

Number	Name
1	Yao
2	Alex
4	Paul
6	Harvey
7	Dolores
8	Ulf
17	Jerome
19	Jean

27	Paige
28	Elsie
30	Darlene
45	Chris
57	Ellin
58	Tran
60	Gretchen

Notes: The senior managers are Dolores, Jerome and Gretchen, the 7 suspected people are Yao, Alex, Paul, Harvey, Ulf, Elsie.

Conclusion Analysis

The newly added conspirator Chris does not make much difference in results compared with the ones in the first requirement. According to analysis, this may be due to Chris's inactive involvement in the conversation, so even if he is one of the conspirators, his influence on others is very weak, resulting in the basically similar results.

4.7 The Solution of the Current Case for Problem 3

In this section, we introduce the conception of Semantic network and apply the theory of Similarity to the calculation of topic scores.

As we have obtained the original messages, which is a much bigger corpus than that we used in the first two questions, so we can apply the similarity analyze into our model. To describe it in detail:

First: Calculate the similarities of among the 3 suspected messages(A) and the 12 unsuspected messages (B),

A includes A1, A2, A3, B includes,

$$Sim(A_i, B_j) = \frac{\alpha}{d + \alpha} \quad (4.7-1)$$

d : the distance between the two corpus.

α : an changeable parameter.(usually between 0 and 1)

Second: give the index rank of B1, B2, ..., B12

$$B_j = \sum_{i=1}^{12} Sim(A_i, B_j), (i = 1, 2, 3) \quad (4.7-2)$$

Third: set the value of A1, A2, A3.

$$A_i = Max(B_j), (i = 1, 2, 3; j = 1 \dots 12) \quad (4.7-3)$$

So far, we successfully obtain the rank of the 15 messages, comparing with the rank based on the index of mutual information; this model theoretically provides a more credible result.

5. ADVANTAGES AND

DISADVANTAGES

5.1 Advantages:

We introduced the concept of mutual information when computing topics, and build the relationship between the suspicious topics and the undetermined ones.

5.2 Disadvantages:

- As it is mentioned in requirement 3 that due to the limitation of the message traffic, we can just roughly determine the doubt degree of the topics by semantic network analysis.

- Though the computing of the mutual information, we can just determine the values of the 12 undetermined topics, however, the values of the 3 higher suspected ones are artificially assigned.

- Without much experience for reference in the model, the accuracy of the results may be undermined.

6. PROMOTION OF THE MODEL

Through the analysis, we found that our model is considerable promotional, such as being used as a method to find the infected or diseased cells in a biological network. Briefly speaking, if we can get the meaningful characteristics from all the cells can calculate the mutual information between these characteristics. Later, we can try to obtain the mutual information between the undetermined cells and the infected ones so as to get the probability ranking list of the undetermined. Though the detecting process, we may use the Improved Search-based Page Rank Model and the Markov Transfer Matrix to simplify our operation as well as increase the validity of our research.

We have introduced the mutual information theory in analyzing this problem in the first two parts, with a relatively satisfactory result. As far as we know, semantic network analysis which is a widely used in artificial intelligence and computational linguistics. It provides a structure and process for reasoning about knowledge or language. And another useful computational linguistics capability in natural language processing is text analysis.

7. CONCLUSION

In this paper, we introduce the model of improved Page Rank algorithm based on mutual information and successfully solved the case problems. The consequences are listed as follows: In the previous case, George and Dave are the given co-conspirators. Bob and Inez are proved other co-conspirators. Carol is innocent. Overall, the solution derived from our models can meet the actual requirements and have some promotional value. Then in the next case, by analyzing the result, we can find that two senior managers, namely Dolores and Jerome are both conspirators. This will help the investigation of the cases. The other version of the second case, the newly added suspect Chris does not make much difference in results compared with the ones in the first requirement. According to analysis, this may be due to Chris's inactive involvement in the conversation, so even if he is one of the conspirators, his influence on others is very weak, resulting in the basically similar results.

All in all, as we only use the topics which are derived from original messages in mutual information analysis, so our result will be more valid if we have a larger corpus. That is to say, we can introduce semantic network and use similarity-computing to acquire a more precise result, in that way, our judgment will be more reasonable.

8. ACKNOWLEDGMENTS

This work was supported in part by the Graduate Innovation Foundation Project of Shan-dong University of Science and Technology (YC140106). Also, we would like to thank those anonymous reviewers for their constructive comments to help us improve the paper.

9. REFERENCES

- [1]Haveliwala, T. (1999) Efficient Computation of PageRank. Technical Report. Stanford.
- [2]Battiti, R.(1994)Using mutual information for selecting features in supervised neural net learning.
- [3]Terry. (1999) The Page Rank Citation Ranking: Bringing Order to the Web. Technical Report. Stanford InfoLab.
- [4]Jackendoff, Ray S.(1972) Semantic Interpretation in Generative Grammar.
- [5]Xing, W., Ghorbani A. (2004) Weighted Page Rank algorithm, Communication Networks and Services Research. Proceedings.

- [6]Catherine Benincasa (2006) Page Rank Algorithm.
- [7]John F. Sowa (1991) Principles of Semantic Networks. Alexander Kraskov, Harald Stogbauer, and Peter Grassberger (2004) Estimating mutual information.

Model Based Test Case Prioritization for Cost Reduction using Genetic Algorithm

Neha Sharma
CSE/IT Dept,
ITM University

Ms Sujata
CSE/IT Dept,
ITM University

Abstract: Real time implementation of the software system requires being more versatile. In the maintenance phase, the modified system under regression testing must assure that the existing system remains defect free. Test case prioritization technique of regression testing includes code as well as model based methods of prioritizing the test cases. System model based test case prioritization can detect the severe faults early as compare to the code based test case prioritization. Model based prioritization techniques based on requirements in a cost effective manner has not been taken for study so far. Model based testing used to test the functionality of the software system based on requirement. An effective model based approach is defined for prioritizing test cases and to generate the effective test sequence. The test cases are rescheduled based on requirement analysis and user view analysis. With the use of weighted approach the overall cost is estimated to test the functionality of the model elements. Here, the genetic approach has been applied to generate efficient test path. The regression cost in terms of effort has been reduced under model based prioritization approach.

Keywords: regression testing; test case prioritization; model based test case prioritization; genetic algorithm

1. INTRODUCTION

Software testing is a process used to find out the correctness, completeness, and quality of developed system. Simply, it is an activity to check whether the actual results match the expected outcome and to ensure that the system is defect free. Software testing throughout maintenance phase is the most difficult task for software engineers. They depend on reusability of test suite in regression testing that incurs the cost which is a major concern. We can improve the testing efficiency by focusing the test cases which likely to contain most severe faults. In the maintenance phase of the software life cycle model, the updated system can increase lots of error in the existing system. Regression testing test case prioritization gives highly efficient result as compared to all other available techniques of regression testing. Test case prioritization technique can fulfill the major goal of testing [7]. Executing the most efficient test case earlier may have less risk of fetching the error in the modified system. There are number of approaches to perform regression testing [6]. In which genetic algorithm has been defined for finding the global optimal solution related to any problem concern [11] [14].

Test case prioritization regression method is categories into two: code based test case prioritization and model based test case prioritization. Code based technique focuses on testing the code of the system under the specified criteria such as statement coverage, branch coverage and functional coverage. Whereas the model based prioritization method concern about the functionality of the model elements [2]. The model based regression testing may be used with the information of the solely code or without the knowledge of the code. There are some modeling language which focuses on the finite state of the model and the use case modeling language.

2. TEST CASE PRIORITIZATION PROBLEM

Test cases in the test suites are reschedule which will further prioritize using an algorithm. Before dealing with prioritization algorithms the problem associated with test case prioritization requires understanding which is defined as follows [6][7]:

Given: T is test suites, PT refers to a number of ways they are chosen, where f is a function whose value depends on permutation of these T to some real number.

Problem: We have to find T' such that T' ∈ PT For all T, (T' ∈ PT) where (T' = T) and f(T') >= f(T).

3. TEST CASE PRIORITIZATION METHOD

In terms of cost, time and efforts test case prioritization estimated as an efficient regression testing approach. It is used to reorder the test cases without having reducing or selecting any of the test cases from existing test suite. Test case prioritization further categories in two approaches [7]: General test case prioritization and Version based test case prioritization

To know general test case prioritization, consider a program P has test suite T with prioritized suite T' which is calculated without having familiar with modified program P'. It gives more successful prioritized suite than the original one. General test case prioritization approach focuses on the

existing test suites without having any knowledge of updated version.

Within version specific test case prioritization, knowledge of modified program P' must require for prioritizing T test suite. It reschedules the available test cases with higher efficiency over the original order of the test cases. The version specific test case prioritization technique knows about the modified version of the system. Version specific prioritization may be more effective for modified program P' as compare to general test case prioritization, which is less effective in a successive release version [7]. Both the test case prioritization approach can work on the modified version of the system but in case of modified version test case prioritization it is necessary to have modification information. It uses the modified information for reordering the test cases. These approaches give more competent order of test suite for detecting the severe faults early.

3.1 Code based test case prioritization

The code based method focuses on the source code of the system to prioritize the test cases in a suite. While considering the code coverage criteria there are number of techniques such as statements, branches and functional coverage test case prioritization.

These techniques use the information from the earlier execution. Some of the test case prioritization techniques are no prioritization, random prioritization, optimal prioritization, total statement coverage, additional statement coverage, simple branch coverage, additional branch coverage, total functional coverage and additional functional coverage. Additional coverage techniques outperformed the total coverage technique of prioritization [7]. These techniques can detect the severe fault earlier and they are also improving the reliability of the modified system. For measuring the efficiency of the techniques average faults per minute is calculated using APFD metric. There is some other method of test case prioritization that focuses on historical based information such as earlier test cost, fault severity information, number of test case requirement in the earlier testing, number of faults detected etc. [13]

3.2 Model based test case prioritization.

In model based test case prioritization software system testing has been performed. System model has been used for selecting and generating the test cases for the updated model. It focuses on the testing of a modified model. Model based approach is generally divided into two: first method is appropriate for the modified model and changes occur in the source code. Second method of model based test case prioritization doesn't deal with the changes in the modified model whereas its major concern is only to the change source code. In the second method, modified elements in the given model have been identified. And, based on that collecting information and execution information the test cases are prioritized for retesting the whole system[1][2]. After updating the system, the modified system must be tested to check the faults whether existing or not. It focuses on the requirement and the design of the complete system [3]. The model based testing can achieve the objectives of test case prioritization early in comparable to the code based test case prioritization. In this approach test cases are generated

earlier so, the effectiveness of the test suite is known earlier. It can decrease the cost in terms of time and efforts and also improve the quality of the overall system [9]. The design phase of the software development needs more concentration. The model based approach focuses on the modeling of the system which has been used for state based system like an embedded system. It is used to get about the system behavior by considering some modeling languages such as specification description language (SDL), use case modeling language (UML), state charts, extended finite state machine, control flow structures and component integration graphs. EFSM (extended finite state machine) system model has been used to give the actual state and the transition between the states [1][3][4][11]. Whenever the action has been triggered the transition is shown using edges in the system model. It helps in developing the system design as well as in prioritizing the tests cases. The major goal of model based approach is to find the most severe fault during the implementation of the system. It is easy to test the model as test the actual system. The post processing of the test suite can be reducing if the prioritization of test cases has been done at the time of test case generation [8][12].

4. RELATED WORK

Requirement based modeling technique of test case prioritization can detect the severe faults earlier. It can fetch the faults in the earlier stage while gathering requirements[10]. When the cost related to each of the requirement has been known earlier in the testing approach then the cost of the complete system could be maintain in the next version of the software [11]. By testing the functional specification of the model, efficiency of a system can be improved. The requirements are weighted based on the factors for detecting the severe faults. The value given to the factor based on the people involved in the system development [5]. So it may possible that the resultant obtained differ based on the model which is considered. The historical based information such as the time taken by the test case; number of test cases run in the earlier testing, code coverage information, impact of the earlier testing etc can give highly efficient prioritization sequence of test sequence [14]. The model to be tested based on the state and the events corresponding to the each of the state of the system. The state can be known based on the event occur such as if state, when state; attribute state, system state and the output state[12].

Requirements which are of major concern for the tester, developer and the customer will be gathered first. The user view analysis has been performed so that the most important requirement tests earlier. After gathering requirements model using has been created using specification description language.

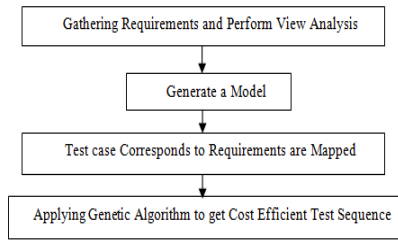


Figure 1. Procedure for Model Based TCP

The model created focuses on the state and transition between the several activities of mobile video communication system. By using genetic based approach test sequence has been generated. The work has been done in a user friendly environment so as to reduce the cost of the system.

5. EMPIRICAL STUDY

The model based test case prioritization method of regression testing firstly gathered the requirements based on the module. Requirement associated with the specific module will be mapped to the test cases [12]. Earlier testing of the requirement assures the higher efficient system at the end. Requirements are the basic building block of the system which has been assigned by the developer and the customer. If the requirements are tested then it will give higher assurance of customer satisfaction of the system. But it is very difficult while the requirements are changing or flexible. The cost is the major issue of concern in the regression testing. The test case prioritization approach of testing is highly efficient over the other approaches of regression testing.

Figure 2. Shows the states while video communication has been made via mobile. Each of the state has the transitions and there are about 57 test cases used to test the transition among all the state in a sample model. The TCP prioritize the test case without of selecting or minimizing of the test case from the test sequences. We have software system based on which the modules are define with its specific estimated time. We can define the estimated time based on which the tester, developer and user prioritize the test case. The prioritize value has been assign within a range of 1 to 5.

The test case having higher importance to the individual assign prioritize value (pv) as 5. User permission, identification, type of data communicated, location of video, session of video played, memory space, speed of uploading and downloading, server response while fetching a video has been tested. The user of the system has been explained in the below a state-transition diagram. The user of the system

must authenticate with the server before uploading or search for any video.

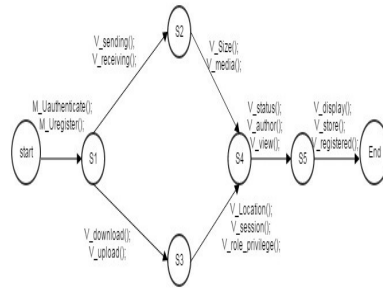


Figure 2. A Sample Model of Mobile Video Communication System

The developer's cost for the development point of view is initially higher. But as execution of test cases increase the cost is decreasing. For the tester, initial cost is less and it is increasing as the execution of test cases increases. Similarly, as per user perspective the test cost is decreasing. After implementing genetic algorithm using MATLAB with having mutation probability 0.8 and crossover probability 1.0 the test sequence has been generated. The cost for the developer, tester and customer has been defined in the figure 3, 4, 5.

The figure 5 shows that the actual cost of the test cases is high in earlier execution where the cost is reducing as on moving down in the bar. Hence it has been shown that the cost is improving.

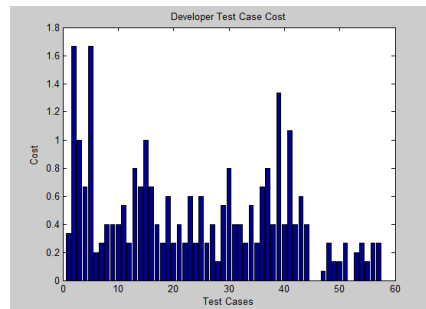


Figure 3. Developer Test Case Cost

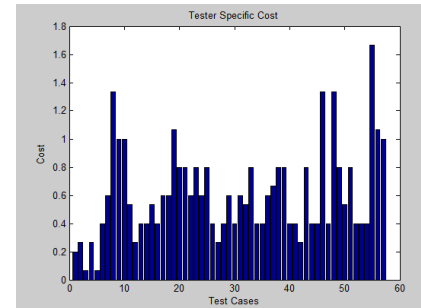


Figure 4. Tester Test Case Cost

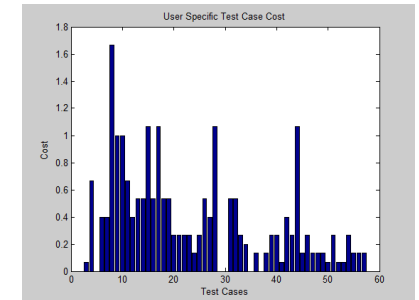


Figure 5. User Specific Test Case Cost

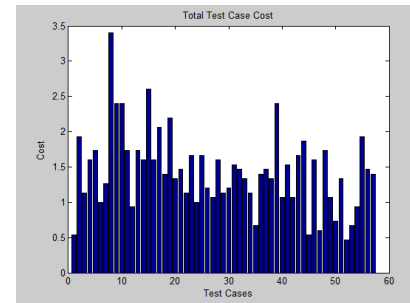


Figure 6. Total Test Case Cost

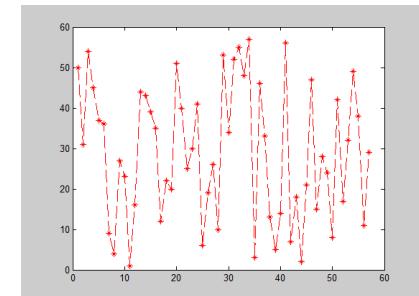


Figure 7. Sample of Test Case Pattern

The cost has been calculated based on the priority of the test cases assign by the developer, tester and the customer. The fitness function used is the summation of the cost of an individual member.

$$Developer = \frac{\sum_{i=1}^N Dev(i) * ViewDev(i)}{Maxvalue} \quad (1)$$

$$Customer = \frac{\sum_{i=1}^N Cust(i) * ViewCust(i)}{Maxvalue} \quad (2)$$

$$Tester = \frac{\sum_{i=1}^N Testr(i) * ViewTestr(i)}{Maxvalue} \quad (3)$$

$$fitness\ Cost = Developer + Customer + Tester \quad (4)$$

Where N is the total number of test cases and i is an individual test case

The overall cost is calculated by taking the summation of the all the above individual cost for the developer, customer and tester.

The cost obtained through from the equation 4. has been leveled using fuzzy logic. Fuzzy logic has defines for optimizing the cost and generate the best optimal sequence.

The figure 7 gives the path of execution of sample test cases which will gives lesser cost in terms of effort as compare to the random execution of test case. Here x-axis and y-axis gives the coordinate point of execution of the test case applying on the model. The result shows that the cost has been reduced while applying our genetic approach as compare to the random order of execution of test cases.

6. CONCLUSION AND FUTURE WORK

The Requirement model based test case prioritization can reduce the cost of the software. Considering the mobile video communication system, the authors has proposed the model based genetic algorithm for reducing the cost of the test case prioritization. The fitness function in genetic algorithm has been calculated by assigning prioritize value to each test case by the developer, tester and the user. The test case efficiency is based on the importance of the particular test case based on any of the module of the system. Genetic algorithm gives the best optimal set which is applicable throughout the system. With the use of our proposed approach the time of execution of the test case is reduce by generating the efficient prioritize test sequence. The most efficient test suite has been obtained by using fuzzy range. It provides the most versatile system so that if any changes found can easily be track and immediately changes has been checked for the failure. The algorithm defined use to reduce the cost based on efficiency of the test case for the particular module. The model based test case prioritization approach has not been used under hybrid approach of the regression testing. The hybrid approach focuses on the combination of either test cases selection and test case prioritization or test case reduction and test case prioritization techniques of regression testing. The fault detecting ability as well as the reliability of the system will be consider for covering more than one objective of regression testing.

7. REFERENCES

- [1]Bogdan Korel, George Koutsogiannakis, Luay H. Tahat (2008) "Application of System Models in Regression Test Suite Prioritization" IEEE,.
- [2]Bogdan Korel, George Koutsogiannakis (2009.)"Experimental Comparison of Code-Based and Model-Based Test Prioritization" IEEE DOI 10.1109/ICSTW.
- [3]Chris Nitin Adonis Petrus, M.S. Razou, M. Rajeev, M. Karthigesan (2013) "Model-Based Test Case Minimization and Prioritization for Improved Early Fault Detection Capability" ISSN: 2278-3075, Volume-2, Issue-5, April 2013
- [4]Daniel Di Nardo, Nadia Alshahwan, Lionel Briand, Yvan Labiche (2013) "Coverage-Based Test Case Prioritisation: An Industrial Case Study" IEEE 2013
- [5]Dr. Krishnamoorthi Ramasamy, Member IEEE and S. A. Sahaya Arul Mary. S.A (2008) "Incorporating Varying Requirement Priorities and Cost in test Case Prioritization for New and Regression Testing" International Conference on Computing , Communication And Networking(ICCN) IEEE 2008
- [6]G.Duggal, B.Suri, (2008) "Understanding Regression Testing Techniques", COIT, 2008, India
- [7] G. Rothermel, R.H. Untch, C. Chu, and M.J.Harold, (2001)"Prioritizing Test Cases for Regression Testing," IEEE Trans. Software Eng., vol. 27, no. 10, pp. 929-948, Oct. 2001.
- [8]Md. Junaid Arafeen and Hyunsook Do (2013) "Test Case Prioritization Using Requirements-Based Clustering" ICST-2013
- [9]Sebastian Elbaum, Gregg Rothermel, satya Kenduri, Alexy G. Malishensky (2004) " Selecting a Cost Effective Test Case Prioritization Technique" April 20, 2004
- [10]Sujata, Mohit Kumar, Dr. Varun Kumar (2010) "Requirment based test case prioritization using Genetic Algorithm" IJCST Vol. 1, Iss ue 2, December 2010
- [11]Wang Jun, Zhuang Yan, Jianyun Chen : (2011) "Test Case Prioritization Technique based on Genetic Algorithm" 2011 International Conference on Internet Computing and Information Services
- [12]Yasmine Ibrahim Salem, Riham Hassan (2011)"Requirement-Based Test Case Generation and Prioritization" IEEE 2011
- [13]Yu-Chi Huangc, Kuan-Li Penga, Chin-Yu Huang(2012)" A history-based cost-cognizant test case prioritization technique in regression testing " Science Direct. The Journal of Systems and Software 85 (2012) 626–637
- [14]Zheng Li, Mark Harman, and Robert M. Hierons (2007) " Search Algorithms for Regression Test Case Prioritization " IEEE Trans.Software Eng., vol. 33, no. 4, april 2007

Behavior of Circular Glass Fiber Reinforced Polymer Tubes Under Axial Compression

Yazhini A
Mepco Schlenk Engineering College
Sivakasi – 626 005,
Tamilnadu, India

Ramesh Babu C
Mepco Schlenk Engineering College
Sivakasi – 626 005
Tamilnadu, India

Abstract: This project involves an evaluation of behaviour of circular GFRP tubes under axial compression. Circular tube columns having different length and cross sections resulting in the range of combinations of global and sectional slenderness, were tested under axial load. From this study, the compressive strength, ultimate load and failure modes were determined. After experimental investigation on evaluation of behavior of GFRP tubes, numerical investigation process is started, using ANSYS. Finite element models of the circular tubes will be generated and analyzed using SHELL elements. In this process orthotropic properties has been defined to align the material direction of the composite lay-up and stacking sequence. The experimental results were compared with the analytical results. It includes the parametric study of L/D and D/t ratio of various dimensions and orientation in finite element model. It gives the best orientation angle for the compressive behavior of GFRP tubes

Keywords: Circular Glass Fiber Reinforced Polymer (GFRP), Compressive, shell, Fiber orientation

1. INTRODUCTION

1.1 Fiber Reinforced Polymer

In recent years, fiber reinforced polymer (FRP) have been used as an alternative for traditional materials. It have found increasingly wide applications in civil engineering, both in the new construction and in retro fit of existing structures. Fiber Reinforced Polymer composites possess several advantages over steel, due to high strength-to-weight ratio and good corrosion resistance. For the retrofit of structures, Fiber reinforced polymer has been used as an externally bonded reinforcement has become very popular in recent years. [1] In reinforced concrete column retrofit, FRP is primarily used as an external jacket to provide confinement to the concrete core. Confinement also enhances the compressive load capacity of a concrete filled FRP tube column, and reduces the required column cross-section compared to that of a conventional RC column [3]. In the last 20 years, various authors have addressed the performance and strength of pultruded GFRP members subject to concentric compression. Daniel C.T. Cardoso [5] derived the compressive strength equation for square GFRP tubes. The buckling behavior and interaction between crushing local and global buckling was observed. Jeffrey Richard Mitchell [8] have studied optimal partial concrete filling of frp and effect of d/t ratios for different laminates. The relationship between optimal partial concrete filling of frp and d/t ratio observed was linear.

1.2 Types of fibers

The classification of FRP composites is based on the types of fibers used as the reinforcement. There are three types of fibers dominating civil engineering industry: Glass, carbon and aramid fibers. Among these fibers Glass fibers plays a predominant role.

1.3 Glass Fiber Reinforced polymer

Glass fibers are a processed form of glass, which is composed of a number of oxides (mostly silica oxide), together with other raw materials (such as limestone, fluorspar, boric acid, clay). They are manufactured by drawing those melted oxides into filaments ranging from 3 mm to 24 mm. There are five forms of glass fibres used as the reinforcement of the matrix material: chopped fibres, chopped

strands, chopped strandmats, woven fabrics, and surface tissue.

Glass fiber reinforced polymer (GFRP) have gained acceptance among civil engineers due to their advantages over traditional construction materials: high strength to weight ratio and superior corrosion resistance, for instance. Additionally, large scale pultrusion of GFRP has contributed to reducing manufacturing costs, making these products competitive. Significant efforts are underway worldwide to develop standard provisions for the design of GFRP structural members. [2].

1.4 Member and section classification

Columns are conventionally classified as being short, intermediate or long based on their relative column slenderness ratio. Depending upon slenderness ratio the column generally fail by either local or global buckling.

2. EXPERIMENTAL PROGRAM

GFRP hollow tubes of various cross sections having different lengths and diameter were tested. 12 specimens were taken from 4 different batches of GFRP tubes. After arrangement on compressive testing machine the GFRP tubes were applied axial load. Axially compressive tests were processed to obtain material properties and compressive strength.

Table1. Specimen Specification

Diameter mm	No of specimen	Length mm	Thickness mm	D/t ratio	L/D ratio
320	3	579	5	64	1.8
325	3	653	7.5	43.3	2
164	3	338	3	54.6	3
310	3	1200	5	62	3.8



Figure 1 Tubes of various cross Section



Figure 2 Tubes Of Same Diameter 320 mm

2.1 Experimental Set-Up

2.1.2 Short GFRP tube

In the compressive testing machine the hollow circular GFRP tubes were fixed by using base plates. Axial load is applied at the top of the plate and the load is transformed in the form of udl to the tube. On reaching the particular load, the tube crushed at the bottom producing a longitudinal crack with a large sound. The critical load at which the tube is crushed is obtained and the tube with an increased thickness has obtained more load value. The stress strain values are noted.



Figure 3. Experimental set-up for short tube

2.1.3 Long GFRP tube

The tube with the increased length is tested in the column testing frame. The bottom is fixed and at the top the axial load is applied in the form of udl through the base plates. The load is applied from the loading jack. The demec gauges are used to obtain the strain values. The experimental set up is shown in the figure 4.



Figure 4. Experimental set-up for Long tube

2.1.3 Crushed GFRP tube



Figure 5. Crushed at the bottom

On applying the load, the GFRP tube buckle with a longitudinal crack at the bottom. The original length has been changed. The deformed length is taken. The load vs displacement, stress vs strain curves have been obtained. The average load value is taken for the circular GFRP tubes. For the specimen 1,2,3 the obtained load value is 312 kN, 336 kN, 124 kN, 105.6 kN.

3. FINITE ELEMENT ANALYSIS

3.1 Application of ANSYS – FEA

Numerical methods provide a general device to study arbitrary geometries and loading conditions. Among them Finite Element Analysis has been broadly used in which it requires more set of data to obtain precise results. Structural analysis is one of the application of Finite Element Model. Two Different types of structural analysis are used.

- Static Analysis
- Buckling Analysis

3.2 Overview of analysis

This method is used to find the buckling load at which the structure becomes unstable. It includes the following steps.

- Erect the model
- Establish the static solution
- Attain the eigen value buckling solution
- Develop the solution
- Analyse the results

3.3 Elements used in ansys

In Ansys different types of elements are used depending on the problem nature and the type of analysis to be performed. Here shell elements have been used. For layered elements and different orientation shell 281 element is used. It is a 8-node structural solid element designed to model layered thick shells. For this key options, under storage of layer data all layers + middle data should be entered. For this orientation we should specify the following conditions.

- Individual layer properties should be defined.
- Define the number of layers.
- State the material properties.
- Assign layer orientation angle and thickness.
- Analyse the model.

3.4 Material properties

For GFRP tubes the following properties are used

Table 2 .Material Properties

Properties of GFRP	
Ex ,GPa	40.2
Ey ,GPa	6.2
Ez ,GPa	40
μ_{xy}	0.2
μ_{xz}	0.2
μ_{yz}	0.2
Gxy,GPa	3.0
Gxz,GPa	2.3
Gyz,GPa	1.51
Density , Kg/m ³	1910

4 .RESULTS AND DISCUSSION

For gfrp tube of external diameter 320mm and thickness 5mm, the buckling load is obtained by using shell 41 membrane element by eigen buckling method.

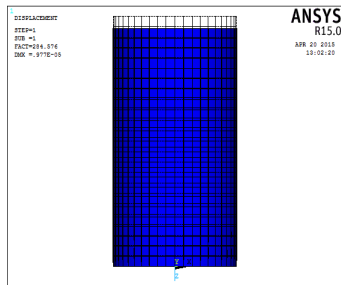


Figure 6 . Deformed + Un deformed for Diameter 320mm

Similarly for the GFRP tube of external diameter 310mm and an internal diameter of 300mm with a thickness of 5mm is analysed in Ansys by Eigen value buckling method and the buckling load is obtained

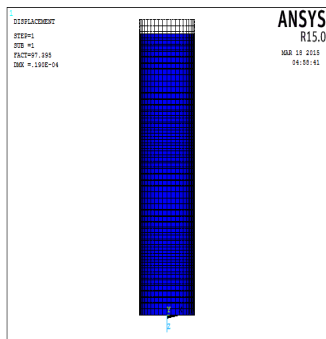


Figure 7. Deformed + Un deformed for diameter 310 mm

Table 3. Load calculation

S.No	Diameter mm	Length mm	Thickness mm	Load value kN
1	320	579	5	284.57
2	325	653	7.5	353.65
3	164	338	3	137
4	310	1200	5	97.3

Table 4 comparison between Load Values

Diameter mm	Experimental kN	Analytical kN
320	312	284.57
325	336	353.65
164	124	137
310	105.6	97.3

The results obtained from the experimental and analytical studies are distinct values.

4.1 Parametric study

This includes the parametric study of D/t ratio and L/D ratio.

i)Five specimen of constant D/t ratio and length is varied. The Diameter and thickness of the specimen is kept constant and the length is increased.

From the analysis it is found that the load gets decreased for the increase in length.

Table 5. Load value for varying L/D ratio

Sl. no	Length (mm)	Diameter (mm)	Thickness (mm)	D/t ratio	Load kN
1	1200	152	2.65	57.3	185
2	1500	152	2.65	57.3	118
3	1800	152	2.65	57.3	82.2
4	2100	152	2.65	57.3	60
5	2400	152	2.65	57.3	46.27

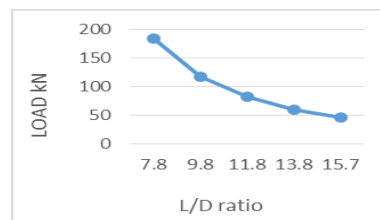


Figure 8. Load vs L/D ratio

ii) Five specimens with an external diameter 152 mm and the length 3600 mm of various thickness is analysed in numerical method. Orthotropic properties were used. The Diameter and length of the specimen (L/D) is kept constant and the

thickness is varied. From the analysis it is found that the load gets increased for the increase in thickness.

Table 6 .Load value for varying D/t ratio

Sl. no	Length (mm)	Diameter (mm)	Thickness (mm)	L/D ratio	Load kN
1	3600	152	4.65	23.6	36.0
2	3600	152	6.65	23.6	51.6
3	3600	152	8.65	23.6	67.4
4	3600	152	10.65	23.6	82.66
5	3600	152	12.65	23.6	103.1

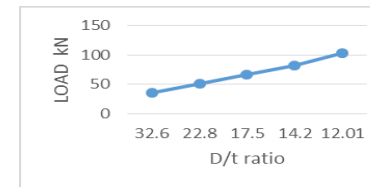


Figure 9. Load vs D/t ratio

4.2 Stacking sequence

The stacking sequence plays a crucial role in compressive strength of the GFRP tube. In this the stacking sequence for 14, 19, 25 layers are processed. The stacking sequence for 19 layers is shown in fig.

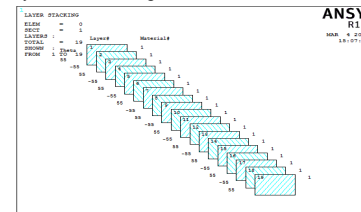
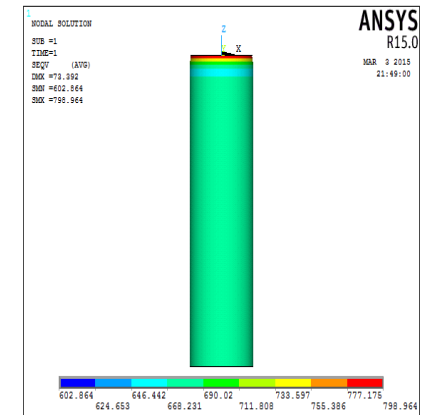


Figure 10. Stacking Sequence for 19 layers

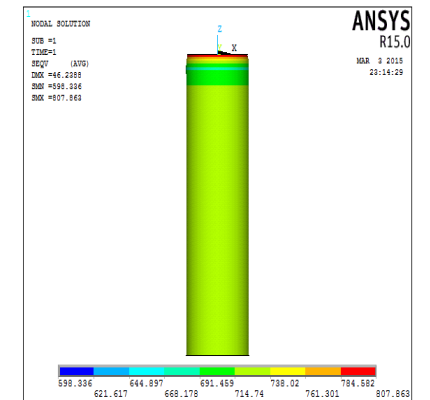
Angle ply laminates which is having plies of same material and thickness is oriented only in + θ and - θ are used. Example for angle ply laminate is [19/-19/19/-19]

4.3 Stresses and deformation of gfrp tube of 14 layers

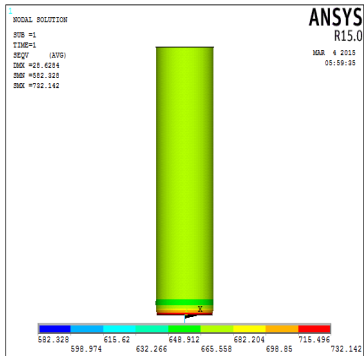
In ANSYS the GFRP tube oriented with the angle of 45°, 55°, 65°, 75°, 85° is analysed using shell 281 element. The stresses and deformations are observed. The angle at which the maximum stress occur is the best angle for the fiber orientation. It gives more strength.



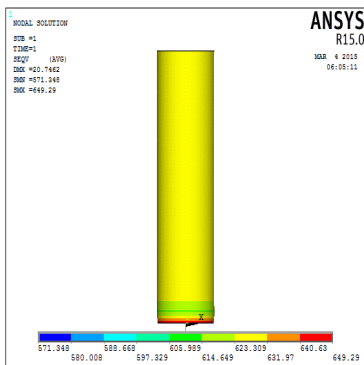
a) 45° orientation



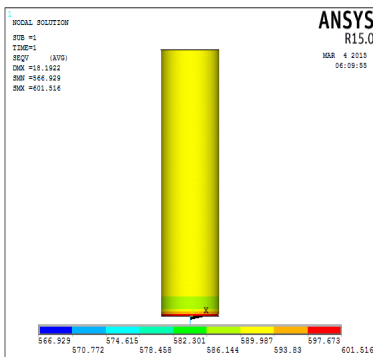
b) 55° orientation



c) 65° orientation



d) 75° orientation



e) 85° orientation

Table 7. Stress And Deformation For 14 layers

Orientation(θ°)	45°	55°	65°	75°	85°
Deformation (mm)	73.3	46.2	28.62	20.74	18.19
Stress N/mm^2	798.3	807.8	732.1	649.29	601.5

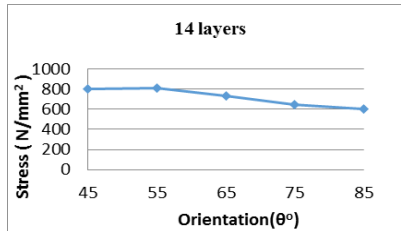
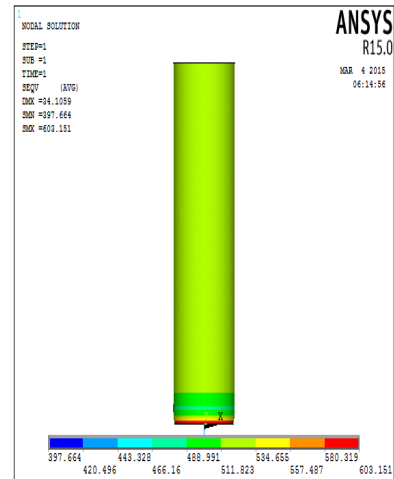
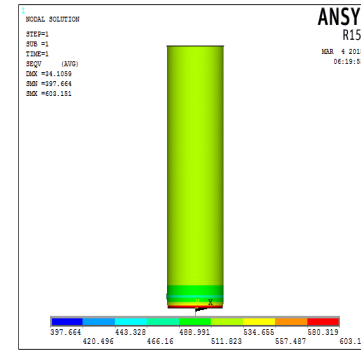


Figure 11. Stress vs orientation (14 layers)

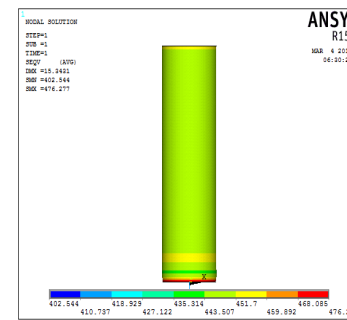
4.4 Stresses and deformation of GFRP tube of 19 layers



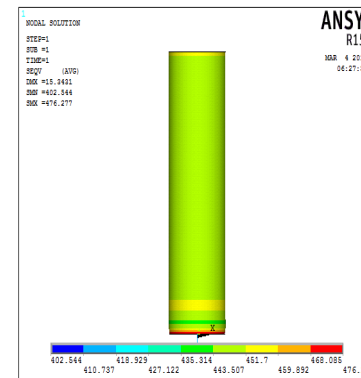
a) 45° orientation



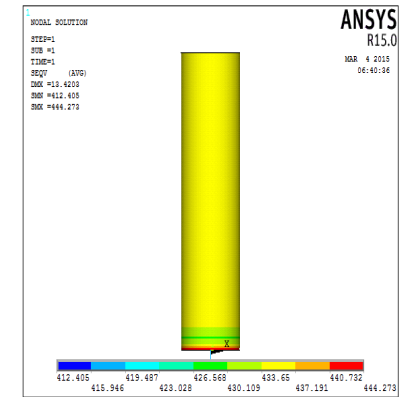
b) 55° orientation



c) 65° orientation



d) 75° orientation



e) 85° orientation

Table 8. Stress And Deformation For 19 Layers

Orientation (θ°)	45°	55°	65°	75°	85°
Deformation mm	34	34.1	15.34	15.3	13.42
Stress N/mm^2	603	603.1	476.2	476	444.2

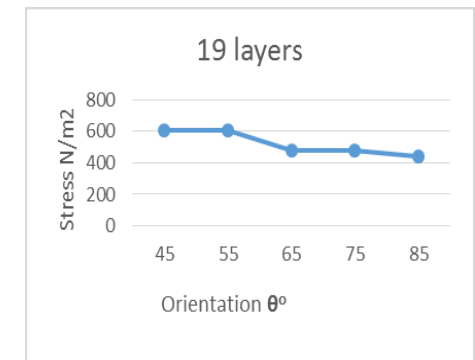


Figure 12 . Stress vs orientation (19 layers)

4.5 Stresses and deformation of GFRP tube of 25 layers

Similarly the stresses and deformation of GFRP tube of 25 layers are obtained using ANSYS.

Table 9 . Stress And Deformation For 25 layers

Orientation(θ°)	45°	55°	65°	75°	85°
Deformation mm	41.0	25.9	16.05	11.75	10.19
Stress N/mm ²	479	481	423.9	378.8	340.06

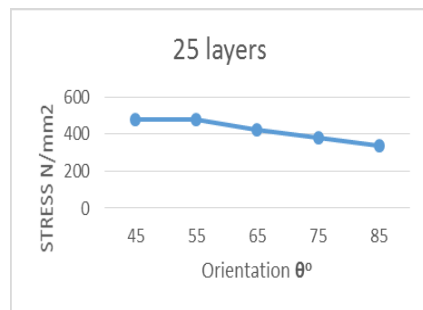


Figure 13. Stress vs orientation (25 layers)

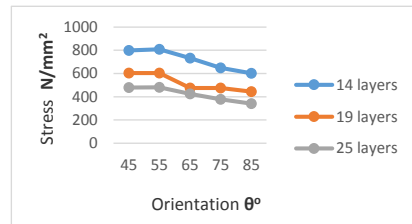


Figure 14. Stress vs orientation (All layers)

5. CONCLUSION AND REMARKS

The finite element analyses and experiment works were carried out to examine the compressive behavior of GFRP tubes under axial load. The static and buckling behavior of GFRP tubes were processed. Experimental results were compared with the FEM results. From the experimental work the load obtained is 312 kN, 336 kN, 124 kN, 105.6 kN and for the analytical work the load obtained is 284.57 kN, 353.65 kN, 137 kN, 97.3 kN. The results obtained are similar.

From the parametric study, it is found that the load gets decreased from 185 kN, 118 kN, 82.2 kN, 60 kN, 46.2 kN by

increasing the length from 1200 mm, 1500 mm, 1800 mm, 1800 mm, 2100 mm, 2400 mm and D/t is kept constant as 57.4 mm.

By keeping the slenderness ratio as 23.6 constant and by increasing the thickness 4.65 mm, 6.65 mm, 8.65 mm, 10.65 mm, 12.65 mm, the load gets increased from 36 kN, 51.6 kN, 67.4 kN, 82.6 kN, 103.1 kN. Increasing the shell thickness, increases the buckling resistance of GFRP tubes. The compressive strength also gets increased.

The stacking sequence of layer and orientation of fibers plays an important role in compressive strength of GFRP tubes. The orientation of fibers in GFRP tubes in 14, 19, 25 layer of stacking sequence have been studied. The orientation of fibers in 45°, 55°, 65°, 75°, 85° have been considered. In the case of variation of stresses with respect to fiber angle, the angle 55° gives the maximum stress value which proves the best orientation angle for GFRP tubes. Hence for this angle the compressive strength is more compared to other angle of orientation fibers.

7. REFERENCES

- [1] J.G. Teng a, T. Yu a, Y.L. Wong a, S.L. Dong b, "Hybrid FRP-concrete-steel tubular columns: Concept and behavior" Construction and Building Materials 21 (2007) 846-854
- [2] N. Silvestre "Buckling behaviour of elliptical cylindrical shells and tubes under Compression" International Journal of Solids and Structures 45 (2008) 4427-4447
- [3] Kian Karimi , Michael J. Tait, Wael W. El-Dakhkhni "Analytical modeling and axial load design of a novel FRP-encased steel-concrete composite column for various slenderness ratios" Engineering Structures 46 (2013) 526-534
- [4] N. Silvestre" Generalised beam theory to analyse the buckling behaviour of circular cylindrical shells and tubes" Thin-Walled Structures 45 (2007) 185-198
- [5] Daniel C.T. Cardoso a,b,c, Kent A. Harries a, Eduardo de M. Batista b" Compressive strength equation for GFRP square tube columns" Composites: Part B 59 (2014) 1-11
- [6] Butje Alfonsius Louk Faggi, Togay Ozbakkaloglu, "Compressive behavior of aramid FRP-HSC-steel double-skin tubular Columns" Construction and Building Materials 48 (2013) 554-565
- [7] Kent A. Harries a, Andrew J. Peck a, Elizabeth J. Abraham b, "Enhancing stability of structural steel sections using FRP" Thin-Walled Structures 47 (2009) 1092-1101
- [8] Jeffrey Richard Mitchell "Experimental And Numerical Investigations Into Optimal Partial Concrete Filling Of Frp And Steel Tubular Poles" Queen's University Kingston, Ontario, Canada September, 2008
- [9] Jianzhuang Xiao, Joan Tresserras, Vivian W.Y. Tam, "GFRP-tube confined RAC under axial and eccentric loading with and without expansive agent" Construction and Building Materials 73 (2014) 575-585

Accelerated Corrosion Fatigue Crack Growth Studies on IS 2062 Gr. E 300 Steel

S. Kelita
Department of Civil Engineering, Mepco Schlenk Engineering College,
Sivakasi – 626005

G. Raghava
Chief scientist
CSIR - Structural Engineering Research Centre,
Council of Scientific and Industrial Research
CSIR Campus, Taramani
Chennai - 600 113

S. Vishnuvardhan
Scientist
CSIR - Structural Engineering Research Centre,
Council of Scientific and Industrial Research
CSIR Campus, Taramani
Chennai - 600 113

C. Ramesh Babu
Assistant professor
Department of Civil Engineering, Mepco Schlenk Engineering College,
Sivakasi – 626 005

Abstract: Corrosion fatigue crack growth experiment was conducted on ESE(T) (Eccentrically-loaded Single Edge notch Tension) specimen made of IS 2062 steel in salt water environment. The specimen was placed in a transparent chamber made of perspex sheet containing 3.5% NaCl solution which acted as corrosion environment. The corrosion process was accelerated by applying constant direct current of 0.2 A which was supplied by means of a regulated power supply. The test was conducted using a ± 250 kN capacity computer controlled servo-hydraulic fatigue rated Universal Testing Machine. The maximum and minimum load values were 15 kN and 1.5 kN. The test frequency was 0.375 Hz and the stress ratio was 0.1. Number of cycles to crack initiation was determined. Crack growth data were recorded at regular intervals. Crack growth curves were plotted and material constants C and m were found. Analytical studies were carried out and the results were compared with experimental results. Details of the analytical and experimental studies and the results are presented in this paper.

Keywords: Fatigue crack growth, corrosion fatigue, IS 2062 Gr. E 300 steel, ESE(T) specimen, fatigue damage

1. INTRODUCTION

Some of the civil engineering, aerospace industry and infrastructure related structures are exposed to corrosion environment and subjected to repetitive operational loads, e.g., bridges, offshore structures, aircraft, power plant piping components. Corrosion is one of the most significant phenomena which happens for the alloys or metals used as implants in the body. Fatigue can affect the product as a whole or can cause defects in the components of the product. The coupled effects of fatigue and corrosion are more detrimental than either acting separately [1]. The maintenance, repair, and life expectancy of damaged engineering structures and machine components, issues caused by corrosion fatigue are of particular concern to both researchers and engineers. The corrosion fatigue crack growth (CFCG) rate is of great interest for the rational life prediction and the safety assessment of engineering structures. Corrosion environment significantly decreases the fatigue strength and life. In general, the test environments are found to influence significantly the fatigue and corrosion fatigue behavior of material, especially at low frequencies. At a low frequency, much more time is available for a corrosion mechanism than fatigue at a high frequency. The tests were carried out at a low frequency, generally lower than 1 Hz. Corrosive environment can cause higher crack growth rates than in dry air. In the fatigue mode of failure, crack will form, propagate and eventually rupture will occur. So there are three stages in fatigue life: i) Crack initiation, ii) Crack propagation, iii) Failure.

Raghava et al. [2] conducted fatigue crack growth studies on ESE(T) specimens made of IS 2062 Gr. E 300 steel in air and 3.5% NaCl aqueous environment. The corrosion fatigue crack growth studies were carried out at different levels of corrosion current by applying constant direct current. The test frequency was maintained in the range of 0.25 Hz to 0.75 Hz. The stress ratio was 0.1. Significant increase in crack growth rate was observed with the increase of corrosion

current. At test frequencies of 1 Hz and above, not much difference was observed in the results of fatigue crack growth studies in inert and corrosion environments. Chinniah et al. [3] observed the corrosion fatigue crack growth behavior of a Ni-Cr-Mn steel in 3.5% NaCl saturated solution using C(T) specimens. Fatigue crack growth rate was higher and threshold stress intensities were lower in aqueous environment when compared to the lab air environment. It was also observed that the crack growth rate increased at lower frequencies and at higher stress ratio. Dong-Hwan Kang et al. [4] investigated fatigue and corrosion fatigue crack propagation behaviors of high-strength steel, HSB800 in air and 3.5% NaCl aqueous environment using single-edge notched bending (SENB) specimens. The corrosion fatigue crack propagation rates in a seawater environment were higher than those in air environment. However, ΔK_{th} and K_{crit} values were not so much changed according to environmental change. Meanwhile, simultaneously increasing R and f lead especially increase of ΔK_{th} . Lin weng et al. [5] conducted CFCG experiments in dry air, distilled water and 3.5% NaCl aqueous solution using pre-cracked C(T) specimens. It was observed that the CFCG rate was effected by a pronounced R -ratio in 3.5% NaCl aqueous solution. The higher the R -ratio the greater the crack growth velocity. This behavior held until the curves merge together with fatigue crack growth curves in air.

In the present work, fatigue crack growth study was carried out on ESE(T) specimen made of IS 2062 steel in corrosion environment. The corrosion environment was 3.5% NaCl solution and corrosion process was accelerated by applying constant direct current (DC) of 0.2 A. The FCG test was carried out by using a computer controlled servo-hydraulic fatigue rated Universal Testing Machine (UTM) of ± 250 kN capacity under constant amplitude sinusoidal cyclic loading. The maximum and minimum load values were 15 kN and 1.5 kN. The test frequency was 0.375 Hz and the stress ratio was maintained as 0.1. Crack growth data were recorded at regular intervals of fatigue loading cycles. Data obtained during the

experiment have been discussed and crack growth curves were plotted. Using crack growth curves material constants C and m were found. Stress intensity factor range values were found and compared with analytical results.

2. MATERIAL PROPERTIES

The steel used in the present study is a high tensile structural steel suitable for general engineering purposes and suitable for all types of connections - welded, bolted and riveted conforming to IS 2062 - 2011 [8]. Chemical analysis was done to find the chemical composition of the material. Table 1 gives the chemical composition of the steel and the specified values of various constituents as per IS 2062. Mechanical properties of the material were determined by carrying out tension tests as per ASTM E 8M - 11 [9]. Table 2 gives the mechanical properties of the steel and it satisfies the requirements of Grade E300 (Fe 440) of IS 2062.

Composition	Tested values (%)	Specified (max) (as per IS 2062:2011) (%)
Carbon	0.13	0.20
Manganese	1.10	1.5
Phosphorus	0.034	0.045
Sulphur	0.038	0.045
Silicon	0.03	0.45

Table 1. Chemical Composition of Steel

Properties	Tested values (%)	Specified (min) (as per IS 2062:2011) (%)
Tensile strength, σ_u (MPa)	468	440
Yield strength, σ_y (MPa)	306	300
% Elongation	31.5	22
Young's modulus, E (GPa)	200	-

Table 2. Mechanical Properties of Steel



Figure 1. ESE(T) specimen configuration

3. SPECIMEN DETAILS

ASTM E 647 - 11 [10] recommends three types of specimens, viz., Compact Tension [C(T)], Middle Tension [M(T)] and Eccentrically-loaded Single Edge notch Tension [ESE(T)] specimens for carrying out FCG studies on materials. ESE(T) specimen was chosen due to its extended configuration. Figure. 1 shows a typical ESE(T) specimen configuration according to ASTM E 647 - 13a. Where, W is width of the specimen, B is thickness of the specimen, a_n is initial notch length and a is crack length. It is recommended that the thickness of the specimen be in the range of $(W/20) \leq B \leq (W/4)$. The length, width and thickness of the specimen were 277.5 mm, 75 mm and 8 mm respectively. The diameter of the holes were 15 mm (0.2W).

A notch of length 11.25 mm was cut at the mid height of the specimen using the EDM (electro-discharge machine) process. ASTM 1820 - 11 [12] specifies the different types of notches (chevron notch, straight through notch, notch ending in drilled hole and narrow notch) and their configurations. The maximum width of the notch is $W/16$ and maximum included angle of the notch is 60°. In this work straight through notch was provided. The width of the notch was kept as 4.5 mm and the included angle of the notch was kept as 60°. Figure. 2 shows the details of the test specimen.

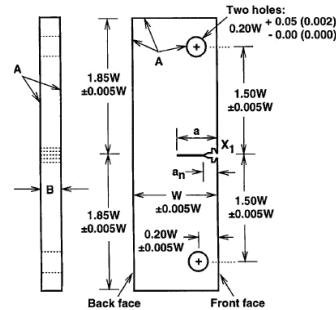


Figure 1. ESE(T) specimen configuration

Figure 2. Details of the specimen

4. CORROSION RATE CALCULATION

According to ASTM G102 - 2010 [11] the corrosion current density and corrosion rate were calculated and the corresponding values were 2500 $\mu\text{A}/\text{cm}^2$ and 28.669 mm/yr. Table 3 gives the corrosion rate.

Faraday's Law can be used to calculate the corrosion rate

$$CR = K_1 \frac{i_{cor}}{\rho} EW$$

where,

$$CR = \text{corrosion rate (mm/yr)},$$

$$i_{cor} = \text{corrosion density } (\mu\text{A}/\text{cm}^2),$$

$$K_1 = 3.27 \times 10^{-3}, \text{ mm g}/\mu\text{A cm yr},$$

$$\rho = \text{density (g}/\text{cm}^3)$$

Table 3. Corrosion rate

Specimen ID	Corrosion current (A)	Current density, i_{cor} ($\mu\text{A}/\text{cm}^2$)	EW	Corrosion Rate (mm/yr)
IS-CFCG8-4 AC	0.2	2500	27.53	28.669

5. EXPERIMENTAL STUDY

The fatigue crack growth experiment was conducted using a of ± 250 kN capacity computer controlled servo-hydraulic fatigue rated Universal Testing Machine (UTM). For carrying out CFCG tests it was required to provide a corrosion environment surrounding the notch. A chamber made of 'Perspex' sheet containing 3.5% sodium chloride solution, was fixed around the notch which acted as corrosion environment. The water level in the chamber was kept at 30 mm below the notch and 15 mm above the notch. The same level of 45 mm was maintained throughout the test because the exposed area of specimen in corrosion environment should not be varied. The corrosion process was accelerated by increasing the corrosion current which was supplied by a Regulated Power Supply (RPS). The test was conducted at corrosion current of 0.2 A and the test frequency was 0.375 Hz. The stress ratio was maintained as 0.1.

For the test, the maximum and minimum load values were 15.0 kN and 1.5 kN. The maximum load of the specimen was determined by following equation as per ASTM E 1820 - 11 [12].

$$P_m = \frac{0.4Bb_0^2\sigma_y}{(2W + a_0)}$$

Where,

$$B = \text{thickness of the specimen, mm}$$

$$W = \text{width of the specimen, mm}$$

$$a_0 = \text{initial notch length, mm}$$

$$b_0 = \text{uncracked ligament} = W - a_0, \text{ mm}$$

$$\sigma_y = \text{yield strength of the material, MPa}$$

Table 4 gives details of FCG tests. At regular intervals the corrosive medium was removed and crack growth data was recorded. Number of cycles for crack initiation and crack propagation were recorded for specimen. The experiment was continued till crack growth in the specimen became unstable.

Table 4. Details of FCG Tests

Specimen ID	Frequency (Hz)	Stress ratio, R	Corrosion Current (A)
IS-CFCG8-4 AC	0.375	0.1	0.2

Figure. 3 shows the experimental set-up. Figure. 4 shows the close-up view of the specimen and Fig. 5 shows the close-up view of the specimen after failure. For the FCG results to be valid, it is required that the specimen be predominantly elastic at all values of applied force. For the ESE(T) specimen the following has to be satisfied:

$$(W - a) \geq (4/\pi)(K_{max}/\sigma_{ys})^2$$

Where,

$$(W - a) = \text{uncracked ligament}$$

$$\sigma_{ys} = \text{yield strength}$$

$$K_{max} = \text{maximum SIF}$$

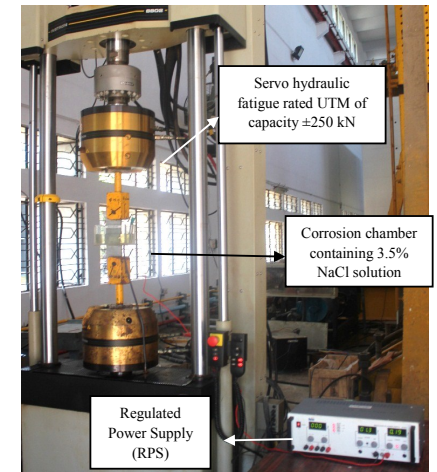


Figure 3. Experimental set-up

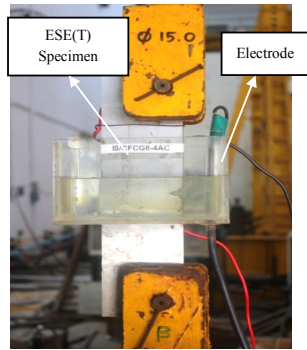


Figure 4. Close-up view of the specimen



Figure 5. Close-up view of the specimen after failure

6. COMPARISON OF ΔK VALUES

According to the specifications of ASTM - 647 the stress intensity factors range for ESE(T) specimen were calculated. Using Abaqus, a finite element software models were created

Table 6. Results of FCG Tests

for different crack lengths. For different crack lengths the stress intensity factor range values were found. The values obtained from experiment and Abaqus were compared. Table 5 gives the comparison of values of stress intensity factor range.

Table 5. Comparison of ΔK Values

7. RESULTS AND DISCUSSIONS

Table 6 gives the details of crack initiation and growth till elastic limit and failure of the tested specimen. It also gives number of cycles at the end of experiment and the corresponding crack length including initial notch length. The test was terminated when the crack growth in the specimen became unstable and the uncracked ligament was insufficient to take further cyclic load. Figure. 6 shows images

Crack length (mm)	Stress intensity factor range, ΔK (MPa \sqrt{m})	
	From experiment	From Abaqus*
11.25	13.273	8.97
13.191	14.610	10.166
15.566	16.295	11.460
18.615	18.610	13.119
20.595	20.245	14.287
32.431	33.726	23.714

* - Effect of corrosion is not considered.

at different stages of fatigue cycles for the specimen. The crack lengths were measured and plotted against the corresponding number of load cycles as shown in Fig. 7.

Figure. 8 shows the variation of fatigue crack growth rate with log stress intensity factor range. Based on this relation, the fatigue crack growth related material constants C and m were found.

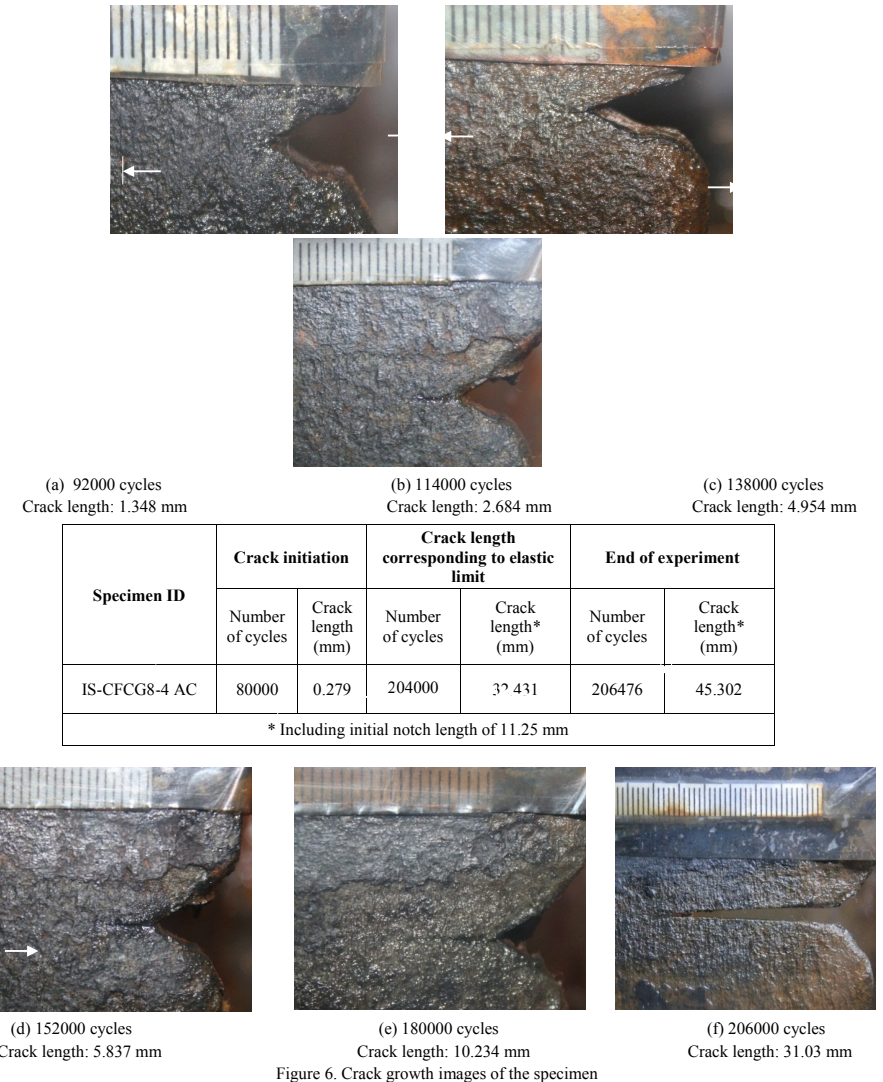


Figure 6. Crack growth images of the specimen

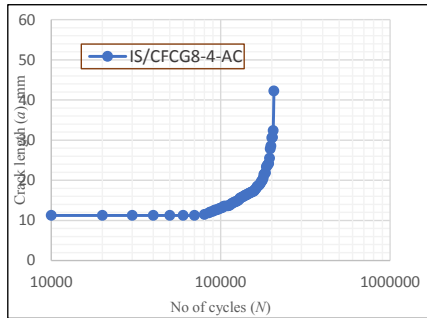


Figure 7. Crack length vs. number of cycles curves

Stress intensity factor range (ΔK) for different crack length values was computed using the expression given in ASTM E 647-11:

$$\Delta K = \left[\frac{\Delta P}{B\sqrt{W}} \right] F$$

and

$$\Delta P = P_{max} - P_{min}$$

$$F = \alpha^{1/2} [1.4 + \alpha] [1 - \alpha]^{-3/2} G$$

where,

$$G = 3.97 - 10.88\alpha + 26.25\alpha^2 - 38.9\alpha^3 + 30.15\alpha^4 - 9.27\alpha^5$$

$$\alpha = a/W$$

for $0 < \alpha < 1$

W - width of the specimen
 B - thickness of the specimen

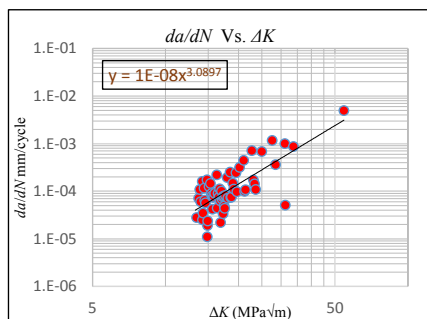


Figure 8. da/dN vs. ΔK curve

From the plot of da/dN vs. ΔK curve the following equation was obtained from which the corrosion crack growth constants were found. Table 7 gives the Paris constants.

$$y = 1 \times 10^{-8} x^{3.0897}$$

Table 7. Corrosion Fatigue Crack Growth Parameters

8. CONCLUSIONS

Corrosion fatigue crack growth study was carried out on ESE(T) specimen of IS 2062 steel in corrosion environment. The test was conducted under constant amplitude loading by using a ± 250 kN capacity fatigue rated UTM. The corrosion process was accelerated by applying a constant direct current of 0.2 A. The loading frequency was 0.375 Hz and the stress ratio was maintained as 0.1. Number of cycles to crack initiation was determined and corrosion fatigue crack growth rate was monitored. Based on the corrosion fatigue crack growth data, FCG parameters C and m were determined. The present experiment forms a part of the studies being carried out at CSIR-SERC to evolve an accelerated corrosion fatigue methodology to simulate real life corrosion fatigue damage.

9. ACKNOWLEDGEMENTS

The first author thanks the Director, CSIR-SERC for the opportunity provided to her to carry out her post-graduate project work at the Fatigue & Fracture Laboratory, CSIR-SERC. The assistance rendered by the technical staff of FFL, CSIR-SERC in conducting the experimental investigations is gratefully acknowledged. This paper is published with the kind

Specimen ID	C	m
IS-CFCG8-4-AC	1×10^{-8}	3.0897

permission of Director, CSIR-SERC.

10. REFERENCES

- [1] G. Raghava, "Fatigue and fracture investigations on structural components and materials", Advanced Course on Fatigue and Fracture Behaviour of Materials, Components and Structures, CSIR - SERC, Chennai (2009), Sigma Publications, Chennai, pp. 203-229
- [2] G. Raghava, P. Gandhi and A.G. Madhava Rao, "Corrosion fatigue in offshore structural steels - A review", International Symposium on Fatigue and Fracture in Steel and Concrete Structures, Madras, 1991, pp. 759-776
- [3] Chinniah Madduri, and Raghu V Prakash, "Corrosion Fatigue Crack Growth Studies in Ni-Cr-Mn Steel", International Journal of Mechanical and Materials Engineering 1 (2010) pp. 20-25
- [4] Dong Hwan Kang, Jong-Kwan Lee and Tae-Won Lee, "Corrosion fatigue crack propagation in a heat affected zone of high performance steel in an underwater sea environment", Engineering Failure Analysis, 18 (2011), pp. 557-563
- [5] Lin Weng, Jixi Zhang, Sergiy Kalnaus, Miaoling Feng and Yanyao Jiang "Corrosion fatigue crack growth of AISI 4340 steel", International Journal of Fatigue 48 (2013), pp. 156-164
- [6] S. Sivaprasad, S. Tarafder, V.R. Ranganath, M. Tarafder and K.K. Ray, "Corrosion fatigue crack growth behaviour of naval steels", Corrosion Science, 48 (2006), pp. 1996-2013.
- [7] Thierry Palin-Luc, Rubén Pérez-Mora, Claude Bathias, Gonzalo Domínguez, Paul C. Paris and Jose Luis Arana "Fatigue crack initiation and growth on a steel in the very high cycle regime with sea water

corrosion", Engineering Fracture Mechanics, 77 (2010) pp. 1953-1962

- [8] IS 2062: 2011, "Hot rolled low-, medium and high tensile structural steel", Bureau of Indian Standards, New Delhi.
- [9] ASTM E 8M - 2011, "Standard test methods for tension testing of metallic materials", ASTM International, USA.
- [10] ASTM E 647 - 2013, "Standard test method for measurement of fatigue crack growth rates, ASTM International, USA.
- [11] ASTM G 102 - 1989, "Standard practice for calculation of corrosion rates and related information from electrochemical measurements", ASTM International, USA.
- [12] ASTM E 1820 - 2011, "Standard test method for measurement of fracture toughness, ASTM International, USA.
- [13] M.A. Wahab and M. Sakano, "Experimental study of corrosion fatigue behaviour of welded steel structures", Journal of Materials Processing Technology, 118 (2001), pp. 117-122

FREQUENCY CONTOUR METHOD FOR DAMAGE DETECTION IN A STRUCTURAL COMPONENT

A.R. Sheri
M.E Student
Department of Civil
Engineering,
Mepco Schlenk
Engineering College,
Sivakasi-626005

S. Parivallal
Principal Scientist
CSIR-Structural
Engineering
Research Centre,
CSIR Campus,
Taramani
Chennai-600113

K. Ravisankar
Chief Scientist,
CSIR-Structural
Engineering
Research Centre,
CSIR Campus,
Taramani
Chennai-600113

R. Theenathayalan
Assistant Professor,
Department of Civil
Engineering,
Mepco Schlenk
Engineering college,
Sivakasi-626005

Abstract: Structural health monitoring (SHM) is the process of monitoring the performance and evaluating the state of health of structures based on measurements from on-structure sensing systems. This technique helps to detect the damages at the earlier stage before failure occurs. The occurrence of damage in a structure produces changes in its global dynamic characteristics such as its natural frequencies, mode shapes, modal damping, modal participation factors, impulse response and frequency response functions. Various methods are available to detect the damages based on the dynamic characteristics of the structures as damage alters the dynamic behaviour of the structure. Frequency Contour method is used in this paper, which is one of the less time consuming method, in which the damage location and size can be detected accurately.

In a steel beam of size 20 mm x 20 mm and of length 300 mm, Numerical study is undergone to validate the Frequency Contour method. The free vibration analysis is done in the beam in undamaged state and the first three natural frequencies is obtained using ABAQUS, FEA Software. The same is done in damaged beams. In damaged beams cracks were created at various locations along the length of the beam by varying the depths to 5 mm, 10 mm, 12 mm and 15 mm. The ratio of damaged to undamaged natural frequencies gave the Normalized natural frequencies. The intersection of the contours of Normalized natural frequencies for the first three modes plotted gives the crack location and depth. In order to plot the contours of Normalized natural frequencies code is written in MATLAB. The prediction of damage by using Frequency contour method gave good results.

Keywords: Structural Health Monitoring, Non-Destructive, Dynamic, Frequency Contour, Normalized natural frequencies, damage.

1. INTRODUCTION

SHM is concerned with performance monitoring of structures to ascertain the strength and performance states of critical members of the structures and determine the presence of damage, or evaluate its degradation and remaining service life. Damage changes the vibratory behaviour of a structure and, therefore, structural diagnostics based on dynamic methods has potentially great importance in engineering applications. The parameters such as natural frequencies, Mode shapes and Modal damping changes due to the presence of damages in a structure. This has lead to the detection of damage location, depth and its severity in the structure. The essential underlying principle here is to compare the structural behaviour in the damaged and undamaged states. In the field of Structural Health Monitoring, Such studies have become an active research.

Structural damage is often thought as a decay of the mechanical properties of a portion of the structure and it is represented by a localized decrease of stiffness. The presence of damage in a structure can be detected using various methods. In this study Frequency Contour method is used, which is based on the changes in natural frequencies of the structure. The study is carried out in a Simply supported steel beam. The frequency measurements can be done accurately and quickly which is the benefit of this method. In case of single crack, measurement of first three Natural frequencies will be sufficient to determine the crack location and depth. Numerical study is undergone in this paper to validate the Frequency Contour Method.

Conner Shane, et al [1] investigated three damage locations for three damage cases for each location. In this study, discrete packets of sensor data were analyzed using the Singular Value Decomposition (SVD) which is a discrete

realization of POD. To test the ability of the damage detection algorithm to predict and localize damage, a finite element (FE) model of a carbon-fiber epoxy plate was developed using ANSYS. The results have shown that the developed algorithm is capable of detecting both location and severity of damages even under changing loading conditions and with a high level of confidence. Jae-Hyung Park, et al [2] proposed an improved GA-based damage detection algorithm using a set of combined modal features that include natural frequency, mode shape, and modal strain energy. Experimental tests were performed on free-free beams; it was selected to reduce modelling uncertainty related to support boundary conditions. L. Pieczonka, W. J., et al [3] presented some preliminary results with respect to investigates related to the effect of low-frequency vibration on nonlinear vibro-acoustic wave modulations. Numerical simulations have been performed to investigate possible modal excitation frequencies for future nonlinear vibro-acoustic wave modulation test used to detect impact damage composites. T. Siebel, et al [4] studied the application of vibration-based damage detection methods to a wind turbine model. A numerical study has shown that the proposed algorithms were capable to locate damage correctly based on both strain and acceleration data. However, it was demonstrated that curvatures calculated from acceleration data have a high sensitivity to noise. Ahmed S. Noman, et al [5] examined the Structural Health Monitoring Using Vibration-Based Methods and Statistical Pattern Recognition Techniques. The methods have been applied to the Crowchild Bridge in Calgary to detect various damages. The Damage Index and Matrix Update algorithms have been chosen for the analysis. The method was found suitable for the study.

The main objective of this paper is to numerically study the crack location and depth in a simply supported Steel beam, using Frequency Contour Method.

2. THEORETICAL ASPECTS

The first three natural frequencies of a Uniform simply supported beam is derived as follows. The equation governing the transverse vibration of a straight beam subjected to external force is used for deriving the Natural vibration frequencies. The general solution obtained is

$$\Phi(x) = C_1 \sin \beta x + C_2 \cos \beta x + C_3 \sinh \beta x + C_4 \cosh \beta x \quad (1)$$

$$\text{and } \beta^4 = \frac{\omega^2 m}{EI} \quad (2)$$

At both ends of the beam displacement and bending moment are zero. Thus applying for $x=0$ and $x=L$ in the corresponding equations and substituting in equation (1) gives

$$\Phi(x) = C_1 \sin \beta x + C_3 \sinh \beta x \quad (3)$$

$$\beta L = n\pi \quad n = 1, 2, 3, \dots \quad (4)$$

By using equation (2) we get

$$\omega_n = n^2 \pi^2 (EI/mL^4)^{1/2} \quad n = 1, 2, 3, \dots \quad (5)$$

By substituting $n = 1, 2, 3, \dots$ the vibration frequencies for infinite series can be obtained. The first, Second and Third natural frequencies obtained are $\omega_1 = \pi^2 (EI/mL^4)^{1/2}$, $\omega_2 = 4\omega_1$, $\omega_3 = 9\omega_1$.

3. FREE VIBRATION ANALYSIS USING ABAQUS FEA SOFTWARE

3.1 Modelling

A decrease in natural frequencies, Stiffness and damping can be observed due to the presence of crack in structures. In Frequency Contour method, the changes in natural frequencies were taken as a basic criterion to detect the damages. Free vibration analysis is carried out in a simply supported steel beam using ABAQUS FEA Software. Table 1 shows the properties of the beam.

The first three natural frequencies for the beam in undamaged state has been obtained by free Vibration Analysis. In the beam a single crack has been modeled and the free vibration analysis was performed considering the geometric and material non linearity. Totally 116 damaged beams were used for the analysis, in which the cracks provided were modeled as Open cracks along the bottom of the beam with various depths (d) of 5mm 10mm, 12mm and 15mm at each location(x) of 8mm interval along the length of the beam as shown in Figure.2.

The first three natural frequencies were obtained for each damaged beam model. The damaged natural frequencies obtained were lesser than the undamaged natural frequencies, which confirmed the damage.

Table 1. Properties of the beam

Width of the beam	20 mm
Depth of the beam	20 mm
Length of the beam	300 mm
Poisson's ratio	0.35
Elastic modulus	2.06×10^5 MPa
Density	7850 kg/m^3
Element type	C3D8I, an eight noded brick element

The damaged and undamaged natural frequencies obtained were used for finding the Normalized natural frequencies, which is the ratio of damaged natural frequency (ω_d) to that of the undamaged natural frequency (ω_u).



Figure.1 Cracked beam model

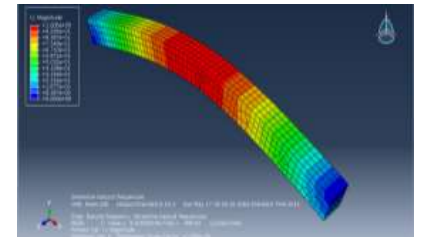


Figure.2 First Mode Shape of a damaged beam (d = 5 mm, x = 158 mm)

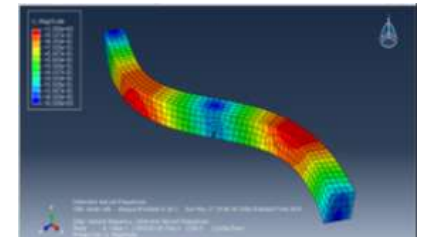


Figure.3 Second Mode Shape of a damaged beam (d = 5 mm, x = 158 mm)

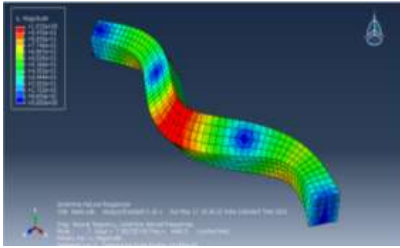


Figure.4 Third Mode Shape of a damaged beam
(d = 5 mm, x = 158 mm)

Figure.2, 3, 4 shows the first, second and third Mode shape of a damaged beam with damage located (x) at 158 mm and depth (d) 5 mm.

4 RESULTS AND DISCUSSIONS

Tables 2, 3 and 4 lists the first three Normalized natural frequencies of the damaged beams with single crack located at various locations with varying depths.

4.1 Comparison of Normalized natural frequencies

The comparison of the Normalized natural frequencies of the damaged beams is done using the surface plot. The effect of damages in beams varies depending upon the location and depth of the crack. The surface plot is plotted by writing coding in MATLAB Software. Figure.5 shows the surface plot of the first Normalized natural frequencies. The changes in natural frequency were found to be low at both the ends of the beam, and at the centre of the beam the variation is higher. Therefore, it may be concluded that, towards the centre of the beam there will be a greater change in natural frequency in the case of simply supported beams. The Bending Moment will be Maximum at the centre and zero at the supports for simply supported beams. Hence, there will be a decrease in Normalized natural frequency when there is an increase in Bending Moment and vice versa. From Figure.5 it may be noted that when the depth of crack is more, a greater variation in Normalized natural frequencies were observed. In some cases a particular natural frequency may correspond to the different crack locations.

Figure.5 Surface plot for first Normalized natural frequencies

Table 2. First Normalized natural frequencies

x	d = 5	d = 10	d = 12	d = 15
8	1	0.9951	0.9898	0.957
18	0.9997	0.9887	0.9776	0.9107
28	0.9977	0.9769	0.955	0.8524
38	0.9947	0.9614	0.9272	0.7934
48	0.9909	0.9453	0.8998	0.7399
58	0.9881	0.929	0.8711	0.6937
68	0.9824	0.9124	0.8494	0.6596
78	0.9792	0.8954	0.8268	0.6121
88	0.9765	0.8777	0.8034	0.6286
98	0.9725	0.8679	0.7839	0.5687
108	0.9696	0.8603	0.7711	0.5549
118	0.9678	0.8485	0.7598	0.5426
128	0.9668	0.8415	0.7523	0.5353
138	0.9640	0.8341	0.748	0.5314
148	0.9636	0.8349	0.7468	0.5311
158	0.9655	0.8357	0.7443	0.5428
168	0.9654	0.8412	0.7542	0.5426
178	0.9678	0.8458	0.7629	0.5481
188	0.9718	0.8599	0.7745	0.5739
198	0.9738	0.8701	0.7893	0.584
208	0.9777	0.8834	0.8084	0.6072
218	0.9799	0.8961	0.8297	0.6363
228	0.9854	0.9139	0.8543	0.6485
238	0.9893	0.9314	0.8811	0.726
248	0.9920	0.9487	0.9085	0.787
258	0.9956	0.9656	0.9369	0.8414
268	0.9978	0.9803	0.9611	0.8933
278	0.9999	0.9915	0.9817	0.9481
288	1	0.9987	0.9938	0.9819

x = Crack location, d = Crack depth

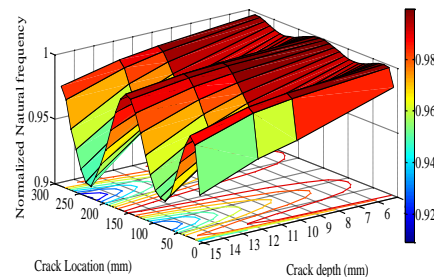
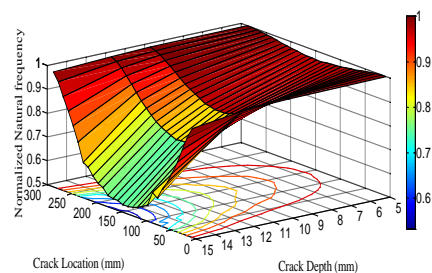


Figure.6 Surface plot for second Normalized natural frequencies

Table 3. Second Normalized natural frequencies

x	d = 5	d = 10	d = 12	d = 15
8	0.9841	0.9606	0.9531	0.9356
18	0.9981	0.9914	0.9874	0.9729
28	0.9990	0.9940	0.9902	0.9785
38	0.9980	0.9906	0.9854	0.9697
48	0.9965	0.9845	0.9768	0.9550
58	0.9947	0.9774	0.9665	0.9398
68	0.9931	0.9716	0.9584	0.9264
78	0.9922	0.9678	0.9534	0.9204
88	0.9917	0.9664	0.9526	0.9213
98	0.9922	0.9690	0.9556	0.9252
108	0.9932	0.9740	0.9625	0.9360
118	0.9951	0.9804	0.9713	0.9498
128	0.9968	0.9869	0.9808	0.9654
138	0.9983	0.9927	0.9892	0.9794
148	0.9994	0.9968	0.9948	0.9889
158	0.9996	0.9979	0.9964	0.9910
168	0.9990	0.9958	0.9933	0.9858
178	0.9977	0.9907	0.9864	0.9740
188	0.9960	0.9843	0.9769	0.9586
198	0.9941	0.9767	0.9668	0.9416
208	0.9923	0.9707	0.9579	0.9291
218	0.9913	0.9655	0.9512	0.9181
228	0.9905	0.9634	0.9479	0.9090
238	0.9909	0.9638	0.9487	0.9105
248	0.9921	0.9681	0.9525	0.9191
258	0.9938	0.9742	0.9613	0.9331
268	0.9957	0.9817	0.9719	0.9474
278	0.9974	0.9883	0.9827	0.9683
288	0.9976	0.9912	0.9874	0.9772

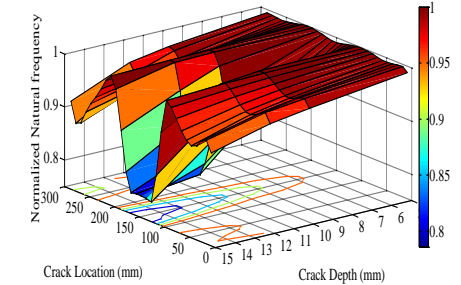


Figure.7 Surface plot for third Normalized natural frequencies

Table 4. Third Normalized natural frequencies

x	d = 5	d = 10	d = 12	d = 15
8	0.9888	0.9648	0.9531	0.9250
18	0.9959	0.9798	0.9705	0.9451
28	0.9953	0.9772	0.9650	0.9399
38	0.9935	0.9717	0.9584	0.9272
48	0.9929	0.9689	0.9552	0.9229
58	0.9930	0.9703	0.9577	0.9303
68	0.9942	0.9763	0.9661	0.9439
78	0.9971	0.9845	0.9775	0.9626
88	0.9987	0.9926	0.9887	0.9806
98	0.9999	0.9974	0.9949	0.9891
108	0.9999	0.9971	0.9899	0.9263
118	0.9979	0.9722	0.9295	0.8402
128	0.9954	0.9269	0.8722	0.7861
138	0.9928	0.8899	0.8289	0.7890
148	0.9914	0.8709	0.8043	0.7904
158	0.9912	0.8710	0.8042	0.7907
168	0.9930	0.8910	0.8346	0.7884
178	0.9955	0.9287	0.8871	0.8247
188	0.9982	0.9764	0.9472	0.8990
198	1	0.9986	0.9969	0.9726
208	1	0.9984	0.9970	0.9931
218	0.9988	0.9931	0.9894	0.9814
228	0.9963	0.9841	0.9771	0.9615
238	0.9938	0.9744	0.9641	0.9418
248	0.9919	0.9675	0.9526	0.9268
258	0.9913	0.9592	0.9340	0.9070
268	0.9921	0.9595	0.9268	0.8829
278	0.9936	0.9708	0.9459	0.8782

288	0.9946	0.9749	0.9620	0.9154
-----	--------	--------	--------	--------

The surface plot for the second Normalized natural frequencies is shown in Figure. 6. At the centre of the beam, the natural frequency variations were found to be greater. The natural frequency variations are found to be very low at one-third and two-third positions. Comparing to first mode the changes in natural frequencies are very low. From Figure.7 it may be observed that there is a slight change in natural frequency at the supports of the beam and then there is a rapid decrease in natural frequency.

Only a slight variation in natural frequencies is observed in third mode comparing to first mode. A very small variation in frequency is observed when the crack depth is small. To determine the crack location and depth, measuring the first three natural frequencies will be sufficient. It may be concluded that when the crack depth is increased to 75% of beam depth the natural frequency is decreased significantly. In addition to the above conclusion it may also be noted that at the location where the Bending Moment is maximum, decrease in frequencies is greatest.

4.2 Damage Identification

In frequency contour method, the identification of damage is based upon the changes in natural frequencies. In this method, the intersection of the contours of the first three Normalized natural frequencies gives the crack location and depth. A contour line, which has the same normalized frequency change resulting from a combination of different crack depths and crack locations, could be plotted in a curve with crack location and crack depth as its axes. The crack located at 88mm from the left support of the beam with a crack depth of 12mm is considered for the study of single damage detection in the beam. The Normalized natural frequencies at this location are 0.8034 for first mode, 0.9526 for the second mode and 0.9887 for the third mode from Tables 2,3 and 4. The contour plot of the three Normalized natural frequencies was plotted by writing coding in MATLAB Software.

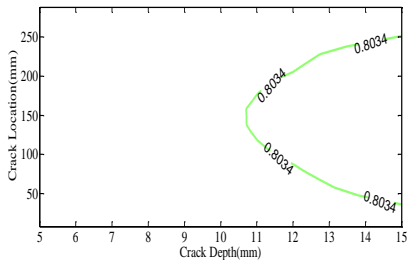


Figure.8 Frequency Contour plot for Normalized frequency of 0.8034 for the First Mode

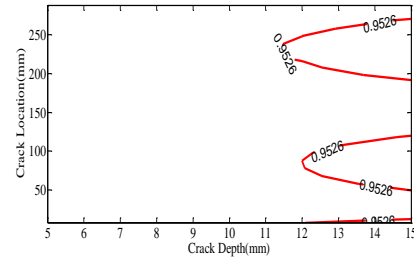


Figure.9 Frequency Contour plot for Normalized frequency of 0.9526 for the Second Mode

The contour plot of Normalized frequency for first, second and third modes were shown in Figure.8, Figure.9 and Figure.10 respectively. Since, the frequencies depend on the crack depth and location these values can be uniquely determined by the solution of a function having solutions one order higher than the number of unknowns to be determined. This is the reason for the requirement of three modes in order to detect a single crack location. If more parameters other than the crack depth and location are required, then one will require more number of modes to identify the unknown parameters.

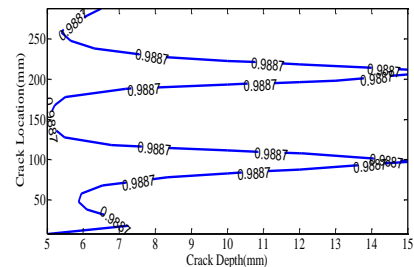


Figure.10 Frequency Contour plot for Normalized frequency of 0.9887 for the Third Mode

Figure. 8, 9, 10 shown above are then plotted on the same plot to detect the crack. The intersection of the three contours of Normalized natural frequencies gives the crack depth and location. Figure. 11 show the contour plot of the three Normalized frequencies. The three contours are found to intersect at the location (x) 88 mm and crack depth (d) 12 mm. This location detected is the actual location of the crack modelled in the beam.

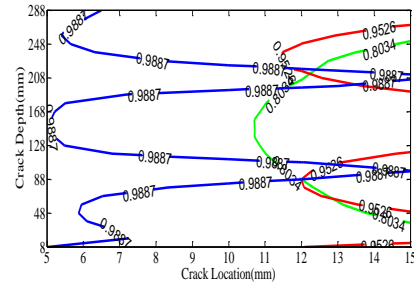


Figure.11 Frequency contour plot of first three modes of 0.8034, 0.9526, 0.9887 Normalized frequencies.

The location and depth of the crack is thus accurately and easily located using the Frequency contour method. Thus, the Frequency contour Method is validated.

5. CONCLUSION

Numerical study of damage detection using Frequency Contour Method in a steel beam is done in this paper. The basic assumption is that, due to damages in the structures the natural frequency, Stiffness gets decreased and the damping is increased. In this study it is found that when the crack depth is increased to 75% of the beam depth, greater decrease in natural frequencies were obtained this is due to the fact that as more materials gets removed the stiffness of the beam decreases and hence the natural frequency. The first three natural frequencies will be sufficient to determine the crack depth and crack location for a beam with a single crack. The method is found to be very simple and less time consuming. The location and depth of the cracks were accurately detected and matches with the damages created in the beam. Thus, this method can be used to detect the damage in actual structural elements.

6. ACKNOWLEDGEMENT

This paper is published with the permission of the Director, CSIR-Structural Engineering Research Centre.

7. REFERENCES

- [1] Anil K. Chopra, "Systems with Distributed Mass and Elasticity," in *Dynamics of Structures*, 2nd ed., vol. 1, USA, Prentice Hall, 1995, pp 585-595.
- [2] Carlos Alberto Riveros, Edwin Fabian García, Manuel Alonso Builes, "A Numerical Approach for fault detection in beam-like structures using Modal strain energy", *Journal of Revista EIA*, pp. 171-184. 2010.
- [3] Cawley, P and Adams, R. D, "The Location of Defects in Structures from Measurements of Natural Frequencies." *Journal of Strain Analysis*, pp. 49-57, 1979.
- [4] Mohamed Abdel-Basset Abdo, "Damage detection in plate-like structures using High-Order mode shape

derivatives", *International Journal of civil and structural engineering*, Volume 2, No 3, 2012.

- [5] Luna Majumder, C.S. Manohar, "A time-domain approach for damage detection in beam structures using vibration data with a moving oscillator as an excitation source", *Journal of Sound and Vibration*, pp. 691-716, 21 November 2002.
- [6] Lakshmanan, N, et al, "Detection of Contiguous and Distributed Damage through Contours of Equal Frequency Change." *Journal of Sound and Vibration*, 329, pp. 1310-1331, 2010.
- [7] Mehdi Salehi, et al, "A Structural Damage Detection Technique Based on Measured Frequency Response Functions", *Journal of Contemporary Engineering Sciences*, Vol. 3, no. 5, pp. 215 – 226, 2010.
- [8] Ratcliffe, C. P, "Damage Detection Using a Modified Laplacian Operator on Mode Shape Data", *Journal of Sound and Vibration*, 204 (3), pp. 505-517, 1997.
- [9] A. V. Deokar and V. D. Wakchaure, "Experimental Investigation of Crack Detection in Cantilever Beam Using Natural Frequency as Basic Criterion", *Nirma University, Ahmedabad*, pp. 08-10 December, 2011.
- [10] Pandey, A.K, et al, "Damage detection from changes in curvature mode shapes", *Journal of Sound and Vibration* 145 (2), pp. 321-332, 1991.

Analytical Study Of Explosion Resistance Scaling On Reinforced Concrete Slab Under Free Air-Burst Blast Load

M.Gowtham
Department of Civil Engineering,
Mepco Schlenk Engineering College,
Sivakasi-626005

N.Chellakavitha
Department of Civil Engineering,
Mepco Schlenk Engineering college,
Sivakasi-626005

Abstract: In real condition the experimental study of scale on explosion resistance of reinforced concrete slab has highly expenses in conduction experiments. This analytical result of the work are overly desirable and close to the real time condition. This work indicates the obvious effect of scale on dynamic response resistance, stress strain behaviour, deflection of unilateral slab of reinforced concrete which are exposed to blast loading due to sudden explosion. To achieve this study reinforced concrete slab which were exposed to blast loading. Explosion test on this reinforced concrete slab which has different standoff distance. The slab are supported at its two ends using a suitable support condition. This work is analyze using the finite element software ABAQUS. The result of this experimental work is compared with the result obtained from the analytical result. From result the detachment in two slab of reinforced concrete both big and small is similar. The analytical behaviour of the slab is moreover same as that of the experimental behaviour.

Keywords: Blast load, dynamic response resistance, deflection, damage mode, scaling.

1. INTRODUCTION

About 70 per cent of India's production of fireworks and matches accounts from Sivakasi, town in Virudhunagar district in Tamilnadu. With around 480 firework factories employing about 40000 direct labourers and 100000 indirect labourers, an equal proportion of unauthorized sector is also controlling the manufacturing of firework products. These units manufacture about 300 unique varieties of fireworks. The market for fireworks is likely to grow at the rate of 10 per cent per annum. So, in a desperate attempt to improvise and meet the demand for light over sound, the industries have been experimenting dangerously, trying new processes and chemical combinations, which the workers are not used to. For the employers the business becomes a highly profitable one but the workers suffer a lot, which mostly goes unnoticed. Sometimes, child labourers are compelled to experiment with high-risk chemicals such as potassium chlorate, which emphasizes mainly on glittering aerial display but, which might also cause a catastrophic effect that may affect not only them but the whole neighborhood. Accidental explosions during the manufacturing process can cause loss of men, material, money and infrastructure. On the other hand, some of the unregistered units operate in the night hours, violating the rules as even an electric spark can trigger major accidents. A random survey conducted in 77 authorized industries and 16 unauthorized industries, recommended for construction of a blast resistant structure with necessary infrastructure facilities to minimize the effects of an explosion. An explosion is a sudden increase in volume and release of energy in a violent manner, usually with the generation of high temperature and release of gas. It is a chemical reaction when initiated, undergoes a very rapid decomposition releasing large volume of highly heated gas that exert pressure

on the surroundings. Thus, the sudden conversion of chemical energy into kinetic energy with the release of heat, light and

mechanical shock causes abrupt destruction. The Explosives Act, 1884 is a comprehensive law regulating the manufacture, possession, sale, transportation, exportation and importation of explosives in India. Based on this act, Explosives Rules 1983, Gas Cylinders Rules 1981 and Static and Mobile Pressure Vessels Rules 1981 were framed to prevent accidents at various points of handling of explosives in India.

Behavioral analysis and calculations of resistant construction which is used for protecting against dynamic loading such as aerial blast must be noticed both in military and civil and buildings with different uses. Herein blast tests on reinforced concrete symbols and in complete scale are necessary. However, these tests are somehow limited due to safety and economic issues. This research includes evaluation of scale on RC one-sided reinforced concrete under blast loading.

2. FREE AIR BURST LOADING

When a blast is occurred next to or over a construction that there is not any kind of reinforcement of first shock between the source of explosives and construction, in that case the load of blast on construction pressure is called open space blast.

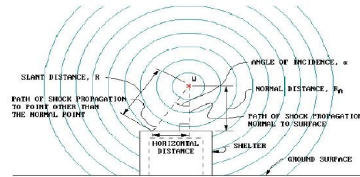


Figure 1.blast due to explosion in open space(TM5-1300, 1969).

2.1 SCALING RULE OF WOVE BLAST

Hopkinson-Komez scaling rule which is usually known as cube root has the most usage in scaling blast (Mays and Smith, 1995; Bangash, 1993). Consider two bombs with W1 and W2 weights that have d1 and d2 diameter respectively and are made from the same explosive.W1 and W2 are related to the.

$$d_1/d_2 = (w_1/w_2)^{1/3}$$

3. FREE AIR-BURST LOADING USING ABAQUS FEA SOFTWARE

The slab is modelled using the finite element modeling software ABAQUS. The specimen tested using the software are of size 1000x1000x40mm.

The analytical work of the experimental work is done using the ABAQUS software. The blast load is applied using the explicit dynamics in the ABAQUS. The TNT value used in the analytical work for 0.31kg and the standoff distance is 0.4m.

After feeding the necessary data's in the software for the slab is loaded and the result is checked is compared using the result obtained from the experimental work.

Table 1. Properties of materials

MATERIAL	DENSITY (kg/m ³)	YOUNG'S MODULUS (Gpa)	POISSON'S RATIO
Concrete	2500	28.3	0.2
Re-bars	7850	200	0.3

Table 2. Specification of blast loading

SCALE FACTOR	DIMENSION (mm)	EXPLOSION MASS(kg)	STANDOFF DISTANCE(m)	SCALE DISTANCE E(m/kg ^{1/3})
1.25	1000X1000X40	0.31	0.4	0.591

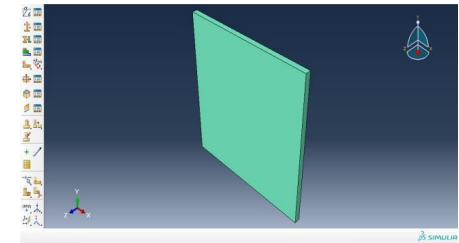


Fig 1. Property assigned specimen.

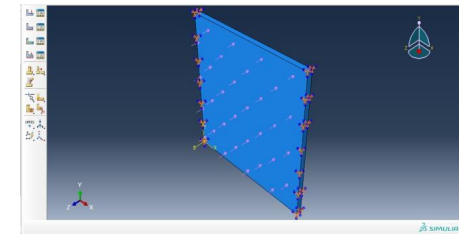


Fig 2. Load and boundary conditions applied specimen.

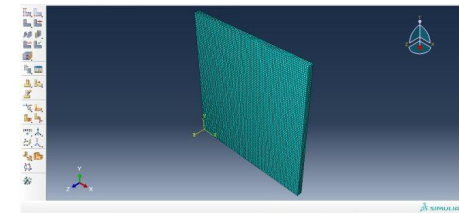


Fig 3. Meshed model of the specimen.

4. RESULT AND DISCUSSION

The deflection value obtained in the analytical study of the reinforced concrete slab slightly varies when compared to the experimental value. The variation in the deflection is due to the application of the load in open environment which alter the load effect on the test specimen. The deflection of the first slab is about 9mm where as in the analytical study the deflection is about 14.54 mm which is slightly higher. More over the deflection obtained for the analytical study is about plus or minus 5-10%

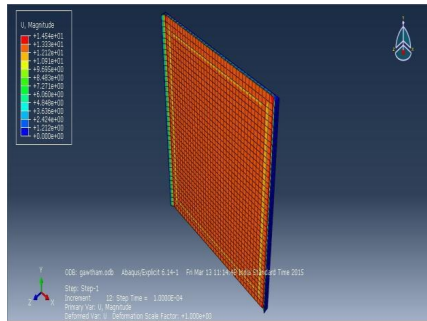


Fig 4. Deflection of the slab.

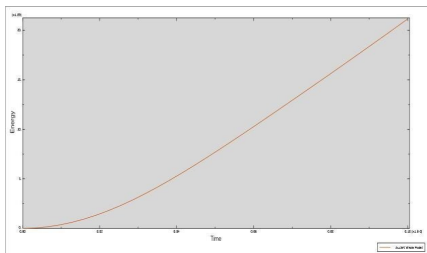


Fig 5. External work graph.

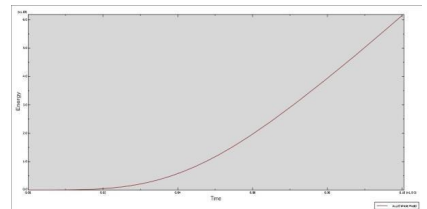


Fig 6. Internal work graph.

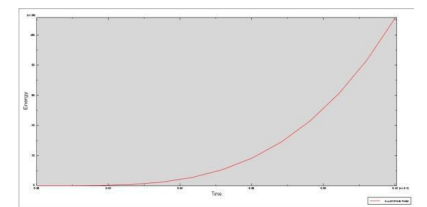


Fig 7. Strain energy graph.

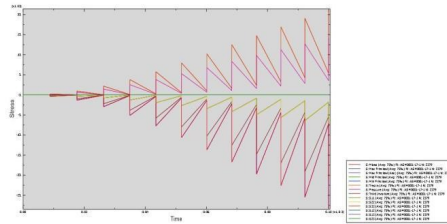


Fig 8. Stress vs Time graph.

Table 3. Comparison of experimental and analytical deflection.

SCALE FACTOR	DIMENSION (MM)	EXPLOSIVE MASS (KG)	CENTRAL DEFLECTION (MM)	ANALYTICAL DEFLECTION (MM)
1.25	1000X1000X40	0.31	15	14.54

Table 4. Comparison of experimental and analytical δ/h .

SCALE FACTOR	DIMENSION (MM)	EXPLOSIVE MASS (KG)	EXPERIMENTAL Δ/H	ANALYTICAL Δ/H
1.25	1000X1000X40	0.31	0.375	0.388

5. CONCLUSION

The considered scaling principals for this experiment were like similitude geometric while scaling for blast load was based on Hopkinson rule.

The crack develop more at the place where the blast effect hits.

The damage level of the slab is mainly due to the strain which caused by the blast load. The damage level of the slab will be more when amount of explosion amount is more.

From the result the failure pattern are the same for almost all of cases. Bigger samples face with more damages and smaller one face less damages.

The surface which expose to the blast loading are damaged severely which causes more damage. The standoff distance, explosion mass has the major influence over the damage of the slab.

The spacing and the size of the reinforcement plays a major role. Less spacing and bigger size reinforcement sample will encounter a less amount of damage.

The locally damages on concrete slabs with bigger scale compared to concrete slabs with smaller scale factor indicate that by increasing the number of scale, this amount decreases.

6. ACKNOWLEDGMENTS

This paper is published with the permission of the guide, department of civil engineering, Mepco Schlenk engineering college.

7. REFERENCES

- [1] Lok, T.S, Xiao J.R.; 1999. Steel-fibre-reinforced concrete panels exposed to air blast loading; Proc Inst Civil Eng Struct Build; 134:319e31.
- [2] Mays, G.C; Hetherington, J.G; Rose, T.A.; 1999. Response to blast loading of concrete wall panels with openings; ASCE J StructEng; 125(12):1448e50. Tavel, P. 2007 Modeling and Simulation Design. AK Peters Ltd.
- [3] Mosalam, K.M; Mosallam, A.S.; 2001. Nonlinear transient analysis of reinforced concrete slabs subjected to blast loading and retrofitted with CFRP composites; Compos Part B-Eng; 32:623e36.
- [4] Mosallam, A; Haroun, M; Mosalam, K.M.; 2001. Repair and rehabilitation of reinforced and unreinforced concrete slabs with polymer composites. In: Forde MC, editor. Proceedings of the structural faults Repair-2001. London, UK. Edinburgh UK: Engineering Technics Press; 2001, July 4e6. A keynote paper, CD-ROM.
- [5] Lawver, D; Daddazio, R; Jin Oh, G; Lee, C.K.B; Pifko, A.B; Stanley, M.; 2003. Simulating the response of composite reinforced floor slabs subjected to blast loading; ASME Int Mech Eng Cong Wash DC; 15e22.
- [6] Ngo, T.; 2005. Behaviour of high strength concrete subject to impulsive loading; Ph.D. thesis, Univ. of Melbourne, Australia.
- [7] Luccioni, B.M; Luege, M.; 2006. Concrete pavement slab under blast loads, Int J Impact Eng; 32:1248e66.
- [8] Lu, B; Silva, P.F.; 2007. Improving the blast resistance capacity of RC slabs with innovative composite materials; Compos Part B-Eng; 38:523e34.
- [9] Silva PF, Lu B. Blast resistance capacity of reinforced concrete slabs. (2009); J StructEng-ASCE; 135:708e16.
- [10] Mcvay, M.K.; 1998. Spall damage of concrete structures. Technical Report SL 88e22; US Army Corps of Engineers Waterways Experiment Station. al study on the effectiveness of fiber sheet reinforcement on the explosive-resistant performance of concrete plates. Int Impact Eng; 35:1702e8.
- [11] Wu, C; Oehlers, D.J; Rebentrost, M; Burman, N; Whittaker, A.S.; 2009. Blast testing of ultrahigh performance fiber concrete slabs and FRP retrofitted RC slabs; EngStruct; 31:2060e9.
- [12] Nash, P.T; Vallabhan, C.V.G; Knight, T.C.; 1995. Spall damage to concrete walls from close in cased and uncased explosions in air; ACI Struct J; 92(6):680e8.
- [13] Rabczuk, T; Eibl, J; Stempniewski, L.; 2004. Numerical analysis of high speed concrete fragmentation using a mesh free Lagrangian method; EngFractMech; 71(4e6):547e56.
- [14] Wu, C; Nurwidayati, R; Oehlers, D.J.; 2009. Fragmentation from spallation of RC slabs due to airblast loads; Int J Impact Eng; 36:1371e6.
- [15] Rabczuk T, Eibl J.; 2003. Simulation of high velocity concrete fragmentation using SPH/MLSPH. Int J Numer Meth Eng; 56(10):1421e44.
- [16] Xu, K; Lu, Y.; 2006. Numerical simulation study of spallation in reinforced concrete plates subjected to blast loading; Comput Struct; 84:431e8.
- [17] Zhou, X.Q; Hao, H; Deeks, A.J.; 2005. Modeling dynamic damage of concrete slab under blast loading; In: Hao H, Lok TS, Lu GX, editors. Proceeding of the 6th Asia-Pacific conference on shock and impact loads on structures, December, Perth, WA, Australia; p. 703e10. ISBN: 981-05-3550-3.
- [18] Ngo, T; Mendis, P; Krauthammer, T.; 2007. Behavior of ultrahigh-strength pre-stressed concrete panels subjected to blast loading; J StructEng-ASCE; 133: 1582e90.

Experimental Study on Seismic Performance in Beam-Column Joint Using Hybrid Fibers

Ganesh Kumar.D
Mepco Schlenk Engineering College, Sivakasi-
626005,
Tamilnadu, India

Dr. S.Prabavathy
Mepco Schlenk Engineering College, Sivakasi-
626005,
Tamilnadu, India

Abstract: An experimental investigation was carried out to study the effect of hybrid fibers on the strength and behavior of High performance concrete beam column joints subjected to cyclic load. A total of 12 reinforced concrete beams column joints were casted and tested. Design mix of M25 is chosen which is widely used in residential. Crimped steel fibers and Glass fibers were used in hybrid form. From cube tests, the volume fraction of (i) crimped steel fibers 0.75% (ii) glass fibers viz. 0.33% gives best results. Addition of fibers in hybrid form improved many of the engineering properties such as the crack pattern, ultimate load and ductility factor of the composite. The combination of 0.75% volume fraction of steel fibers and 0.33% volume fraction of Glass fibers gave better performance with respect to energy dissipation capacity and stiffness degradation than the other combinations. This project proposed that beam column joint is the weak zone where failure occurs and crack pattern is linear form. To resist the cracks, different types of fibers in linear form are introduced in the joint and also to improve the ductility property in the weak zone of the Beam-Column joint.

Keywords: energy dissipation, stiffness degradation, hybrid fibers, beam-column joint, ductility factor

1. INTRODUCTION

Concrete made from ordinary Portland cement is strong in compression but weak in tension and tends to be brittle. Recent Earthquakes Failures majorly happen by improper design of reinforced concrete structures with low ductility. This study is to increase Strength and ductility of structures depend mainly on proper detailing in beam column joints. The forces acting at the junction interrupt the shear strength of the member. Seismic force is a type of force in which horizontal and vertical forces whose magnitudes are very much higher in the adjacent beam columns. Ordinary Portland cement loses its tensile resistance after the formation of multiple cracks at the zone. To resist these types of cracks and to improve the strength and to make the structure more ductile in nature Hybrid mix of Fibers are added to resist Tensile resistance of cyclic loading. Beam column joint is the crucial zone in structural component. To transfers the loads from beam to column adequate stiffness and strength is provided. Formation of Plastic hinge is prevented in column which makes the entire structure collapse within fraction of time. To make the Beam column joint more ductile in nature closed hoop stirrups are provided in Transverse reinforcement for the entire Development length Reinforcing Bars was recommended in IS 13920:1993 with maximum of 150mm spacing. Diagonal reinforcement is provided in joint zone which transfer the compression loads to tensile zone.

This Study aims to provide information on the properties and applications of the more commonly available fibers and their uses to produce concrete with certain characteristics. A fiber is a small reinforcing material produced from various materials like steel, glass. A numerical parameter describing a fiber as its aspect ratio is defined as the fiber length, divided by fiber diameter [l/d]. Typical aspect ratio [l/d] range from 30 to 150. Fibers of diameters are 0.25 to 0.76 mm for steel and 0.02 to 0.5 mm for other fibers. In this Study selection of Steel fiber of aspect ratio 60 and Glass fiber of aspect Ratio 100 is chosen. The plain concrete fails suddenly when the deflection corresponding to the ultimate flexural strength is increased, on the other hand fiber-reinforced concrete

continue to sustain considerable loads even at deflections considerably in excess of the fracture deflection of the plain concrete.

N.Ganesan et. al has carried out an experimental programme to compare the behavior of high performance concrete (HPC) and steel fiber reinforced concrete (SFRHPC) beam –Column joints under cyclic loading. Liu, Cong et. al has investigated the seismic behaviour and failure modes of beam-column joint sub-assemblies reinforced with steel fibers to compare the performance of steel fiber reinforced Beam – Column joints were compared with that of conventional joints. Tang Jiuru et. al has studied about the behavior of beam-column joints that employ steel-fiber reinforced concrete (SFRC), under reversed cyclic loading. K.R.Bindhu et. al has investigated the effect of cross-inclined bars at the joint as confining reinforcement on the behaviour of exterior reinforced concrete beam-column connections subjected to earthquake loading.

2. RESEARCH SIGNIFICANCE

Reinforcement detailing is very difficult in the Beam-column Joint because of providing transverse reinforcement is getting congested compaction is not possible at that zones. This study is to increase tensile resistance of the exterior beam-column joints and to increase the strength of the joints.it is possible to achieve the high ductile behavior in the beam column joints by providing hybrid combination mix of steel and glass fibers. By providing hybrid fibers at these joints, it reduces the transverse reinforcement and prevents the congestion in reinforcement at the joints.

3. EXPERIMENTAL PROGRAMME

3.1 Materials

3.1.1 Steel Fiber reinforced concrete

Steel fiber reinforced concrete is a composite material which is made up from cement concrete mix and steel fibers as a reinforcing. The steel fibers, which are uniformly distributed in the cementations mix. This mix, have various volume fractions, geometries, orientations and material properties. It has been shown in the research that fibers with low volume

fractions (<1%), in fiber reinforced concrete, have an insignificant effect on both the compressive and tensile strength.

Steel Fiber of size (30mm with 0.5 Diameter) which have a Aspect ratio of 60.

Generally SFRC is very ductile and particularly well suited for structures which are required to exhibit:-

- High fatigue strength resistance to impact, blast and shock loads
- Shrinkage control of concrete
- Tensile strength, very high flexural, shear
- Erosion and abrasion resistance to splitting
- Temperature resistance, high thermal
- Earth quake resistance

The degree of improvement gained in any specific property exhibited by SFRC is dependent on a number of factors that include:-

- Concrete mix and its age
- Steel fiber content, volume fraction
- Fiber geometry, its aspect ratio (length to diameter ratio) and bond characteristics volume fraction.

3.1.2 Glass Fiber reinforced concrete

Glass fiber-reinforced concrete is (GFRC) basically a concrete composition which is composed of material like cement, sand, water, and admixtures, in which short length discrete glass fibers are dispersed. Glass Fiber of size (50mm with 0.2 Diameter) which have an aspect ratio of 100. Including fibers in the concrete can improve the tensile strength and impact strength of the material. GFRC has been used for a period of 30 years in several construction elements but at that time it was not so popular, mainly in non-structural ones, like facing panels (about 80% of the GRC production), used in piping for sanitation network systems, decorative non-recoverable formwork, and other products. At the beginning age of the GFRC development, one of the most considerable problems was the durability of the glass fiber, which becomes more brittle with time, due to the alkalinity of the cement mortar. After some research, significant improvement have been made, and presently, the problem is practically solved with the new types of alkali-resistant (AR resistance) glass fibers and with mortar additives that prevent the processes that lead to the embrittlement of GFRC.

3.2 Mix Proportion

Normal Concrete Design of M25 is chosen with reference to IS 13920 which is normally used for Residential buildings. The Code prefers a Minimum grade of M20. Workability of the Concrete mix is kept constant at the compaction factor of 0.9. Mix proportions were maintained constant for all the mixes. However the Steel and Glass Fibers were added to the reinforced concrete to increase the tensile resistance in the beam column joint.

Table 1 Mix Proportions (kg/m³)

Cement	Fine Aggregate	Coarse Aggregate	Water
412	419.25	1349	0.43

3.3 Specimen Details

In this paper, twelve exterior beam column joints were cast and tested under cyclic loading. The dimensions and details of the reinforcement of the beam column joints are given in Figure 1. The column was reinforced with four numbers of 12 mm diameter high yield strength deformed (HYSD) bars, and the beam was provided with 12 mm diameter HYSD bars at

the top and bottom to entire length of the Beam. HYSD bars of 6 mm diameter were used as ties in columns and stirrups in the beams. Different Mix proportions of Steel Fibers of 0.25, 0.50, 0.75 and 1.00 and glass Fibers of 0.33, 0.67 and 1 is mixed along with all the proportions with steel and glass together into a hybrid form. From the results obtained from the different volume fractions of Fibers, Steel of 0.75% and glass of 0.33% gives the best values in both compression and tension.

Experimental study of casting and testing of 12 numbers of exterior beam column joints tested with reverse cyclic loading. Mix proportions of crimped steel fibers 0.75% (58. kg/m³) and glass fibers of 0.33% (24.2 kg/m³). The Cross sections of Beam-column joint is 150 x 200mm. Column is Reinforced with Four numbers of 12mm diameter, and 10mm diameter of diagonal reinforcement with development length of 280mm from both the joints along top and bottom directions in column. Beam is reinforced with 2Nos of 12mm diameter of HYSD bars at top and bottom. 6mm diameter bar is used as ties in columns and stirrups in beams. The dimensions and detailed reinforcement is shown in figure 1.

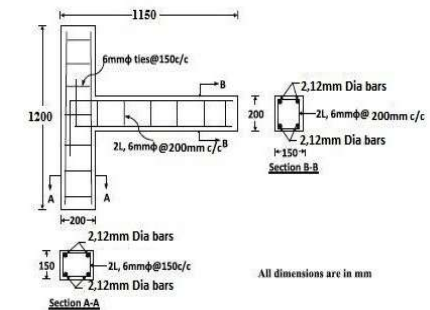


Figure 1 Details of Reinforcement

3.4 Testing

The Test Frame Setup of 20tonnes is arranged in order to apply cyclic load on the exterior beam column joint as Cantilever action. Specimens were tested after 28days of curing. Column is arrested at both top and bottom to provide lateral movements while applying loads. Top portion of column is arrested like hinges support by use of Load cell, bottom portion is arrested by steel casing arranged for the specimen size.

Axial Compressive load of 20% of axial capacity of the column is applied over the column to make stable. Beam is loaded with reverse cyclic loading through 200kN hydraulic jack connected to loading was increased; the loading was continued till the failure obtains at the joint. For every intervals of loading, the deflection at the beam is noted down by use of dial gauge having a least count of 0.01mm and 50mm travel.



Figure 2 Experimental Test Setup

3.5 Behavior of the specimens:

The failure is first observed in beam column junction. Continuous increasing in load additional cracks on beam portion and propagation of some of the initial cracks. Failure of the cracks widened leading to the failure of the joint. Most of the cracks developed at the beam near the column. Hybrid mix concretes have more number of finer cracks was formed the hybrid combination of glass and steel fiber is used to control the cracks both micro and macro level. Glass fiber arrest the macro cracks and it control the formation of macro cracks, Steel fiber plays a role in restrict the widening of macro cracks and increase the energy absorption capacity of the member.

3.6 Finite Element Analysis using Abaqus

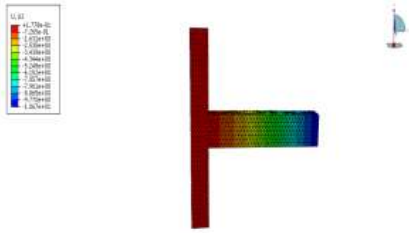


Figure 3 Plotting of Deflection contour in specimen

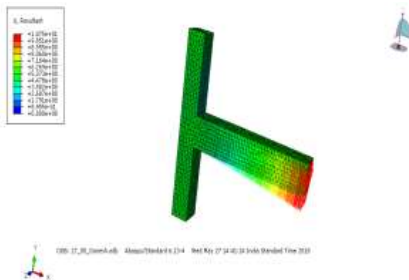


Figure 4 Resultant deflection (deformed+undeformed Shape)

4. RESULTS AND DISCUSSION

4.1 Load-Deflection behavior

It shows the typical load deflection plots of HFRC specimen tested under reversed cyclic loading. The load-deflection obtained for the joints was similar to that obtained for steel fiber reinforced concrete. The load deflection is drawn in graph for graphical representation by use of the load applied to the specimen to its deflection value. Using these envelopes the first crack load, energy absorption capacity and ductility factor for the specimens were obtained and listed. It can be observed from Fig. that in HFRC, the ultimate load and the corresponding deflection of specimens were increased as the hybrid fibre content increases. This could be attributed to the ability of these fibres in arresting the micro cracks as well as macro cracks. As and when micro cracks develop in the matrix, the glass fibres in the vicinity of such micro cracks will try to arrest these cracks and prevent further propagation. After the formation of cracks steel fibres intercept them and the bridging action of fibres reduces the widening of cracks. Also the cracks have to take a meandering path due to the interception of fibres which results in the demand of more energy for further propagation of cracks; this in turn increases the ultimate load. However, at higher percentages of glass fibre content, in fact, a reduction in strength has been found.

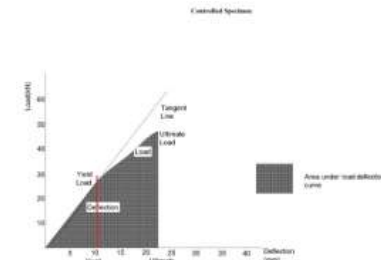


Figure 5 Energy Absorption Graph

Table 2 Energy Absorption

Designation of the Specimen	Area Under load (mm ²)	Deflection curve	Energy Absorption
GS 0	11.5	10	1.15
GS 1	19	7.4	2.57
GS 2	20	7.4	2.70
GS 3	19.5	7.4	2.63

Table 3 Ductility Factor

Specimen	Ultimate Deflection (mm)	Yield Deflection (mm)	Ductility Factor
GS 0	20	11	1.82
GS 1	19.8	6.45	3.07
GS 2	19.4	6.35	3.06
GS 3	19.2	6.4	3

4.2 First Crack and Ultimate Load

First crack load and ultimate load of the specimens are given in Table. First crack load was determined from the envelop curve of the load deflection plot corresponding to the point at which the curve deviated from linearity. From the calculated values it can be observed that first crack load increased with increase in fiber content, which may be due to the increase in tensile strain carrying capacity of concrete in the neighborhood of fibers. The first crack load increased by 18% for GFRC and 31% for SFRC specimens. It has been found that addition of hybrid fibres increases first crack load by 37% and ultimate load by 62% for HFROC specimen with 0.75% (55.5 kg/m³) steel fibres and 0.33% (24.4 kg/m³) glass fibres when compared to specimen without. Energy absorption capacity and displacement ductility The area under the load deflection curve indicates the energy absorption capacity. Energy absorption capacity was calculated and the values obtained are given in Table 2. From the Table it can be seen that energy absorption capacity consistently increases and maximum for HFRC specimen with 0.75% (55.5 kg/m³) steel fibres and 0.33% (24.4 kg/m³) glass fibres, which is approximately 3 times higher than that of HPC joints. It is required that an earthquake resistant structure should be capable of deforming in a ductile manner when subjected to lateral loads in several cycles in the elastic range. Ductility of a structure is its ability to undergo deformation beyond the initial yield deformation, while still sustaining load. The ductility factor which is a measure of ductility of a structure is defined as the ratio of maximum deflection (d_u) to the deflection at yield (d_y). The ductility factors were calculated and the results obtained are given in Table. The details of the procedure adopted are described elsewhere [22]. The values in Table 2 and 3 shows that the fibers present in the mixtures influence the energy absorption capacity and ductility. Compared to HPC specimen the ductility factor is increased by 2.5 times.

5. CONCLUSION

The main aim of this paper is to determine load deflection characteristics, energy dissipation, ductility and stiffness degradation of hybrid fiber reinforced beam column joints subjected to reverse cyclic loading were investigated.

- 1) Hybrid mix Fiber shows the increase the first- crack Strength as well as better ductile in nature. Glass Fiber reduces the micro Cracks, where Metallic fiber of steel Reduce the macro cracks.
- 2) Expecting results of more than 3times the strength of Controlled mix specimen with 0.75% of steel fiber and 0.33% of glass fiber mixed with hybrid type in the junction.
- 3) This study deals possible to reduce the reinforcement in the beam-column joints for construction difficulties.
- 4) The comparison between the analytical with the experimental values there is no much difference between this deflection and loading values more or less same in both.

6. ACKNOWLEDGMENTS

The authors would like to thank to all the members who have contributed towards development and success of this research work.

7. REFERENCES

[1] S. Rajagopal, S. Prabavathy (2013), "Investigation on the seismic behavior of exterior beam-column joint using T-type

mechanical anchorage with hair-clip bar"1-11,Journal of King Saud University – Engineering Sciences.

[2] N. Ganesan et al(2014)"Behaviour of hybrid fibre reinforced concrete beam-column joints under reverse cyclic loads"686-693, Materials and Design 54.

[3] R. Kiran et al(2014),"A case study on pre 1970s constructed concrete exterior beam-column joints" 20–25,Case Studies in Structural Engineering 1.

[4] Akanshu Sharma et al(2011),"A new model to simulate joint shear behavior of poorly detailed beam-column connections in RC structures under seismic loads" 1034–1051, Engineering Structures 33.

[5] Gerson Moacyr Sisniegas Alva et al (2013), "Moment-rotation relationship of RC beam-column connections: Experimental tests and analytical model" 1427–1438, Engineering Structures 56.

[6] Roberto Realfonzo (2014), "Cyclic behavior of RC beam-column joints strengthened with FRP systems", 282-297, Construction and Building Materials 54.

[7] C.E. Sofias et al(2014), "Experimental and FEM analysis of reduced beam section moment endplate connections under cyclic loading" 320-329, Engineering Structures 59.

[8] K.R. Bindhu et al(2009), "Performance of Exterior Beam-Column Joints Under Seismic Type Loading" 47–64, ISET Journal of Earthquake Technology, Paper No. 503, Vol. 46, No. 2.

[9] Gustavo J. et al(2005),"Highly Damage-Tolerant Beam-Column Joints Through Use of High-Performance Fiber-Reinforced Cement Composites"487-495, ACI Structural Journal.

[10] S. S. Patil et al(2013), "Analysis of Reinforced Beam-Column Joint Subjected to Monotonic Loading"149-158,International Journal of Engineering and Innovative Technology (IJEIT).

[11] Bo Yang et al(2014),"Behavior of Composite Beam-Column Joints in a Middle-Column-Removal Scenario: Experimental Tests" 04013045-1-04013045-20.

[12] Mohamed Mady (2011), "Seismic Behavior of Beam-Column Joints Reinforced with GFRP Bars and Stirrups", Journal of Composites for Construction, 875-886.

[13] S M Kularni (2013), "A Novel Reinforcement Pattern for Exterior Reinforced Concrete Beam-Column Joint" Procedia Engineering 51, 184 – 193.

[14] M. Kazem Sharbatdar et al(2012)"Cyclic performance of retrofitted reinforced concrete beam-column joints using steel prop"287-294,Construction and Building Materials 36.

[15] J.G. Ruiz-Pinilla et al(2014),"Experimental tests on retrofitted RC beam-column joints under designed to seismic loads - General approach", 702-714, Engineering Structures, 59.

[16] Gee-Joo Ha (2013), "Seismic improvement of RC beam-column joints using hexagonal CFRP bar combined with CFRP sheets"464-470, Composite structures 95

Experimental and analytical study on flexural behaviour of concrete filled GFRP Box Beams

K. Vinayaki
Department of civil engineering
Mepco Schlenk Engineering college
Sivakasi – 626005

R.Theenathayalan
Department of civil engineering
Mepco Schlenk Engineering college
Sivakasi – 626005

Abstract: This paper deals with the experimental study on the variation in the load carrying capacity between concrete filled GFRP box beams of size 1200x150x200 mm is predicted by varying thickness of GFRP box beams as 4mm, 6mm and the concrete strength as M40. The material properties of cement, fine aggregate and coarse aggregate would be found out. The compressive strength of concrete cube would be found out to confirm the strength – grade 40. Study results showed that in addition to many advantages due to its formation, the Box Beam showed superior physical and mechanical properties. It was found that the flexural strength and fracture toughness values of Composite beams significantly increased stiffness when compared to reference values. Flexural two point load would be applied on the box beams filled with plain concrete. The experimental test was performed to find the flexural strength, load carrying capacity, deflection, load deflection relationship, load strain relationship and stiffness ratio for various thickness of box beams. The analytical Study was performed by using ANSYS to evaluate the deformation of the specimen. The experimental study of beams showed that the box beam having higher thickness will increase the load carrying capacity and stiffness and also decrease the deflection. In ANSYS by varying both thickness of GFRP box as well as grade of concrete is analysed. The proposed finite element model shows increased resistance to deformation when concrete is used as infill material and the deformation decreases when the grade of concrete and thickness of box beam increases.

Keywords: Glass Fiber Reinforced Polymer (GFRP), Box Beams, Flexural Strength, Stiffness.

1. INTRODUCTION

The needs and demands of humans in the field of material technologies increase each day in parallel to the problems experienced in materials. Researchers investigate new material types and applications and try to produce new designs to decrease these problems and to satisfy these demands. In recent years, many researchers have concentrated on composite materials, which can be considered as a derivative of these materials. Composite materials have required properties and are preferred in a wide variety of fields including the construction sector. In addition to their high resistance and good performance towards environmental factors, these materials are preferred since they have all the properties desired by the researchers and they can be produced in different combinations. In addition to their superior mechanical resistance, these new generation composite materials draw the attention of researchers due to the properties such as their lightweight structure, corrosion resistance and high resistance to chemicals, electric insulation, low density and high resistance/density ratio.

Concrete-filled glass fiber-reinforced polymer (GFRP) box beams represent an efficient structural building element having several advantages over conventional reinforced concrete elements. The GFRP Box acts as stay-in-place formwork, greatly reducing construction cost and time as well as serving as external reinforcement eliminating the need for internal steel reinforcement. In addition, the GFRP Box provides concrete confinement as well as increased resistance to degradation in corrosive environments. Although many studies have been performed for circular concrete-filled GFRP members in both axial and flexural applications, much less attention has been given to rectangular sections. The studies show that a closed hollow rectangular GFRP section with webs extending above the compression flange providing formwork for a concrete compression flange. The

investigated rectangular filament wound concrete filled tubes with combined axial and flexural loading, studied T-beams constructed of concrete filled rectangular GFRP pultruded beams with concrete slabs attached with shear studs.

GFRP composites are generally used in curtain wall systems, pedestrian and vehicle bridges, soil improvements, pipes, repair and reinforcement works in the construction industry. The construction sector constitutes a significant part of the GFRP composite market, followed by the automotive sector. However, since these materials are not yet well recognized by users and designers, they are not considered as a replacement for other materials. It is estimated that GFRP composites can be a good solution in a significant part of available applications. Recently, the use of composite materials has rapidly increased and it is gradually developing in many technical fields including the construction sector. In this development process, the construction industry is constantly working to develop new construction technology to design and obtain more economical solutions. These new generation composites, which are generally preferred in secondary constructions, which are not considered as bearing elements in the construction sector, are today also used as bearing elements, as main construction elements. Particularly after the increase of the serial production of GFRP composites, they began to be used more effectively in buildings for different purposes. The use of Glass fiber reinforced composites, which are lightweight and have a high resistance, in corrosion, repair and improvement works has increased.

Reinforcement and improvement works involving the wrapping of GFRP laminates on the bottom surfaces of beams and GFRP fabrics on all surfaces of columns are the most widely known applications of these types of composites with concrete. Like in various study units, the most recent

research and development studies have concentrated on hybrid systems where conventional construction materials particularly such as concrete and composite materials are used in combination. Recently much of the research has focused on hybrid GFRP columns formed by concrete-filled or hollow GFRP pipes. The tendency in scientific studies clearly shows that in the near future, the use of GFRP composites in new buildings will mainly concentrate on the use of box structure. Many studies have shown that the use of GFRP composites with conventional materials like concrete were one of the solutions to eliminate certain deficiencies and disadvantages in construction elements. The first studies on hybrid designs, where GFRP profiles and concrete were used in combination, began. In the first studies, positive results were obtained by using concrete to increase rigidity and compressive strength inside GFRP profile.

The idea of using GFRP - Concrete box system as a flexural element it were reported that the GFRP profile used in the formed system offered advantages in formwork, lightweight structure and resistance and could yield more than 50% lightweight structure when compared to conventional plate systems. They formed permanent formwork by using concrete in a T-section GFRP profile and increased material resistance. In previous studies on hybrid systems which were formed by filling concrete inside the GFRP profile; the behavior of a box beam system under uniaxial load flexural behavior were again analyzed. Various studies were conducted on the long term creep and shrinkage effects of box beams, on behaviors under repetitive loads, on the effects on impact loads, on shear behavior and material fatigue and on frost-thaw effects.

2. MATERIAL USED

Cement: Ordinary Portland cement of 53 grade conforming to IS 8112 – 1989 and specific gravity of 3.15 is used.

Sl.No	Tests	Results
1	Specific gravity	3.15
2	Initial setting time	80 minutes
3	Final setting time	453 minutes
4	28days compressive strength	45.33/mm ²

Table 1 Properties of cement

Fine aggregate: Locally available Natural River sand of specific gravity 2.6 and size below 4.75 mm conforming to zone II of IS 383 – 1970 is used. Its fineness modulus and bulk density are 2.67 and 1415 kg/m³

Sl.No	Tests	Results
1	Specific gravity	2.67
2	Fineness modulus	2.67
3	Water absorption	0.6%

Table 2 Properties of fine aggregate

Coarse aggregate: Crushed stone of size less than 20mm with specific gravity of 2.66 and bulk density of 1415 kg/m³ is used

Sl.No	Tests	Results
1	Specific gravity	2.72
2	Fineness modulus	2.67
3	Bulk density	1806 kg/m ³
4	Water absorption	1.1%

Table 3 Properties of coarse aggregate

Super plasticizer : Conplast SP 430 is based on sulphonated Naphthalene Polymer and supplied as brown liquid instantly dispersible in water, having specific gravity of 1.220 to 1.225 @ 30⁰C

MIX PROPORTION

Design of concrete mixes involves determination of the proportions of the given constituents namely, cement, Water, Coarse aggregate and fine aggregate with admixtures if any. Workability is specified as the important property of concrete in the fresh state. For hardened state compressive strength and durability will be considered. According to IS 1343 – 2009 mix ratio for M40 grade is 1 : 2.56 : 3.26 : 0.4

GFRP BOX

In this paper GFRP BOX of various thickness such as 4mm and 6mm is used for concrete filling. The GFRP BOX acts as stay in-place formwork, greatly reducing construction cost and time as well as serving as external reinforcement eliminating the need for internal steel reinforcement. GFRP BOX provides concrete confinement as well as increased resistance to degradation in corrosive environments. The box-beams made of the fiber-reinforced composite materials are used extensively in many engineering applications because of their good mechanical properties, such as high strength.

Density, Kg/m ³	1960
E _a Gpa	505
E _b Gpa	9.9
Pr _{ba}	0.063
G _{ab} Gpa	3.7
G _{bc} Gpa	1.4
G _{ca} Gpa	1.4
X _c Gpa	2.277
X _i Gpa	1.265
Y _c Gpa	0.065
Y _i Gpa	0.05

Table 4 Material properties of GFRP

3. SPECIMEN DETAILS

A box beam of length 1200mm and width 150 mm having depth 200 mm is casted for varying thickness of GFRP Box as 4mm and 6mm respectively. The concrete of grade M40 is filled inside the box beam. The Box itself acts as a external reinforcement so there is no need for any internal reinforcement. Four specimens are casted for various thickness.

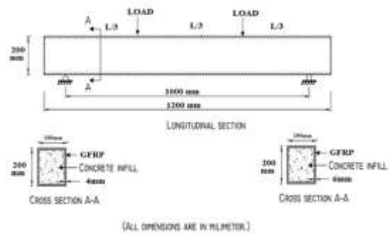


Fig 1 Beam specification details

4. EXPERIMENTAL STUDY

The beam were simply supported over an effective span of 1000mm and the loads were applied vertically as two point static loading ,at the middle third position of the beam, vertical displacement and strains were monitored throughout the test. The displacements were measured at mid-span using LVDT and strain was measured by a DEMEC (detachable mechanical gauge) with gauge points. The beams were loaded using hydraulic jack. The load was measured by means of load cell. The load was applied at an increment of 10 KN, for each load interval the deflections were measured. The 50T capacity testing frame was used for testing of beams.



FIG 2 EXPERIMENTAL TEST SETUP

5. EXPERIMENTAL TEST RESULT

The following are the result obtained during experiment. The result are as follows :

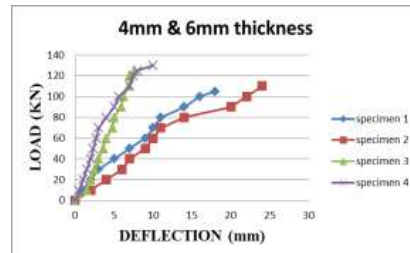
Specimen details	Ultimate load (KN)	Flexural strength (N/mm ²)	Ultimate deflection (mm)	Ultimate Strain	Stiffness (KN/mm)	Stiffness ratio
Specimen 1 (4mm thickness)	105.3	3.31	17	0.0085	6.19	1.00
Specimen 2 (4mm thickness)	110	3.67	16.2	0.008	6.79	1.10
Specimen 3 (6mm thickness)	123.1	4.17	10	0.015	12.31	2.00
Specimen 4 (6mm thickness)	130	4.33	9.5	0.018	13.68	2.21

Table 5 Test results

Load –Deflection relationship

The deformation and load carrying capacity of GFRP box for

Fig 3 Load Vs Deflection curve

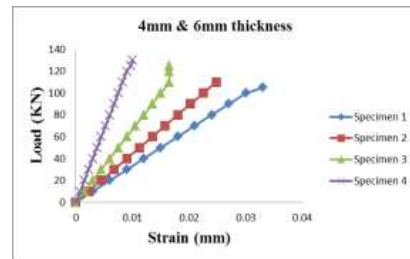


various thickness is found experimentally. The load carrying capacity increases with increase in thickness of GFRP box and the deflection gets decreases with increase in thickness. So the deflection level considerably less for higher thickness and the load carrying capacity will be higher for increased thickness.

LOAD –STRAIN BEHAVIOUR

Fig 4 compares the load – strain relationships for various beam specimen. It is seen that the GFRP box having higher thickness withstand more strain compared to box beam having minimum thickness with increasing load.

Fig 4 Load vs Strain Curve



LOAD – STIFFNESS RELATIONSHIP

As the thickness increases the stiffness also increases. The specimen 4 showed high stiffness compared to specimen 1

Fig 5 Load vs Stiffness curve

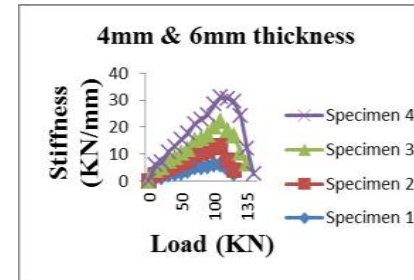
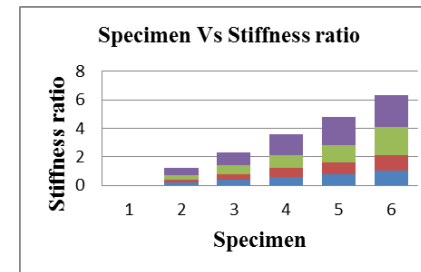


Fig 6 STIFFNESS RATIO



FAILURE PATTERN

Fig 7 Deformed Shape of box beam



Fig 8 Crushed infilled concrete at ultimate load



5. ANALYTICAL STUDY

ANSYS is a general purpose finite element analysis (FEA) Software Package. Finite element analysis is a numerical method of deconstructing a complex system into very small pieces (of user-designated size) called elements. The software implements equations that govern the behavior of these elements and solves them all; creating a comprehensive explanation of how the system acts as a whole. These results then can be presented in tabulated or graphical forms. This type of analysis is typically used for the design and optimization of a system far too complex to analyze by hand. Systems that may fit into this category are too complex due to their geometry, scale or governing equations.

FINITE ELEMENT MODELLING

The ultimate purpose of this finite element modelling is to recreate mathematically the behaviour of structures and components. It is also used for obtaining the deflections occurred in any structure under any loading conditions. The results obtained can then be compared with the Experimental values.

PRE-PROCESSING

Define the element type, Real constants, Material models of the concrete model.

Element type

SOLID 65 allows the presence of four different materials within each element, one matrix material (e.g concrete). Concrete material is capable of directional integration point cracking and crushing besides incorporating plastic and creep behaviour. Shell 181 is used for concrete filled box beam. Concrete material is assumed to be initially isotropic. GFRP material having orthotropic nature. Element is defined by eight nodes having three degrees of freedom at each node: translations in the nodal x-,y-,and z- directions. Special features of SOLID 65 are : Plasticity, Creep, Cracking, Crushing, Large deflection and Large Strain.

Real constants

Real Constant Set 1 is used for the Solid 65 element. Real constant set 2 is used for the shell element for that the thickness of box such as 3mm,4mm,5mm and 6mm.

Material model

Two material models were given : material 1 for concrete and material 2 for box element, under linear isotropic and orthotropic material definition.

Table 6 Details of specimen

Dimension of concrete filled GFRP Box Member (mm)	Thickness (mm)	Dr Ratio	Concrete Strength (Mpa)
200 X 150	3	66.67	20
	4		30
			40
200 X 150	5	40	30
			40
	6		33.33
200 X 150	6	33.33	20
			40

Modelling

The model was created using key points, lines. Then it is extruded to get the volume. The length of the beam is taken as 1200 mm. No additional reinforcement is used in the sections.

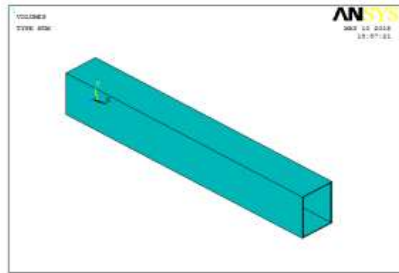


Fig 9 Box Beam model

Meshing

For Solid 65 element the mesh was set up such that square or rectangular elements were created. The beam was meshed by both line and volume mesh.

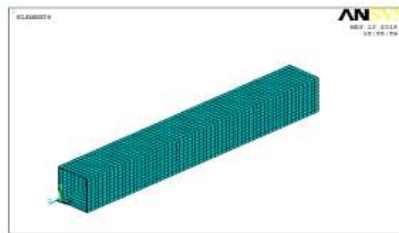


Fig 10 Box Beam after meshing

Boundary conditions and loads

Displacement boundary conditions are needed to constrain the model to get a unique solution. To ensure that the model acts the same way as the experimental beam, boundary conditions need to be applied at points of symmetry and where the supports and loadings exist.

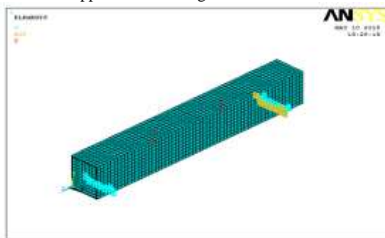


Fig 11 Two point loading acting in Beam

Post – Processing

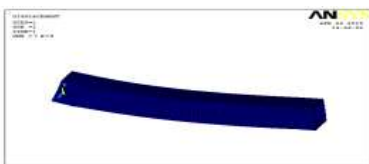


Fig 12 Displacement of beam

Fig 13 Deformed + Undeformed Solution

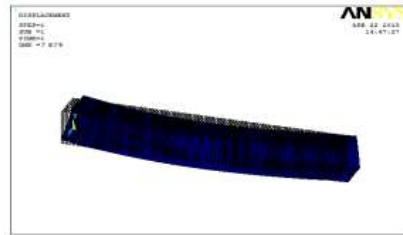


Fig 14 Nodal Solution

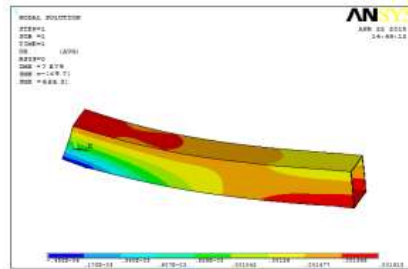


Fig 15 Vector Solution

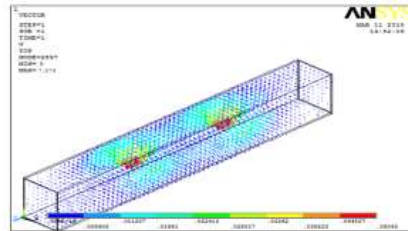


Fig 16 Von Mises Stresses

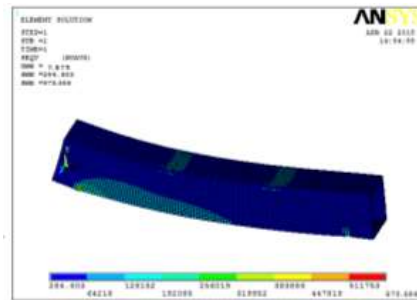


Fig 17 Nodal Solution of the beam

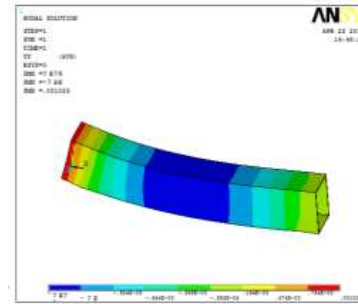


Fig 18 Element Solution of the beam

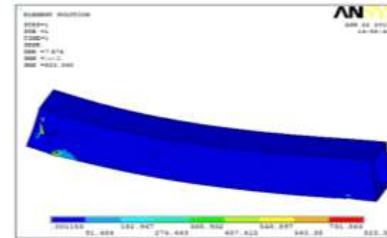


Fig 19 Shear stress of the beam

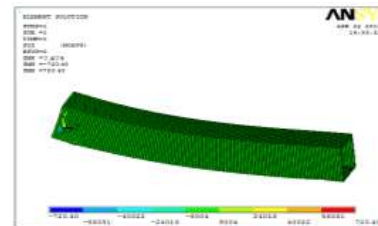
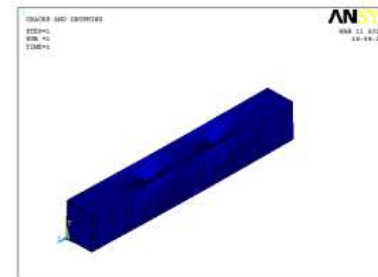


Fig 20 Cracks & Crushing



6. RESULTS & DISCUSSION

The load versus deflection behavior of typical concrete filled GFRP Box beam sections is given in Figures 21 and 22, respectively. It can be seen that the total deformation at any given load for all concrete filled sections is lesser because of the increase in stiffness due to the infill. In all cases as the grade of concrete increases, more improved performance against deformation is seen. The deformation capacity of the analyzed specimens was significantly plotted. The load carrying capacity of the specimen having increased grade having increased thickness is significantly increased. The deflection is higher for beam having minimum thickness similarly beam with high grade will having minimum deflection level than beam having less grade of concrete will deflect more.

Fig 21 Load Vs Deflection Curve For 3mm thickness

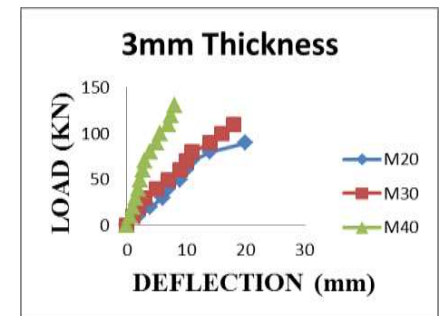


Fig 22 Load Vs Deflection Curve For 4mm thickness

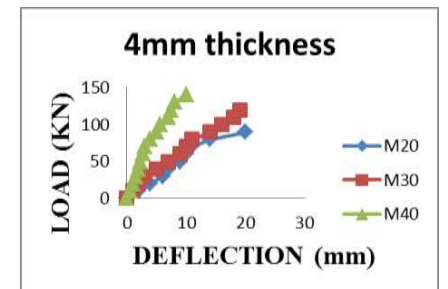


Fig 23 Load Vs Deflection Curve For 5mm Thickness

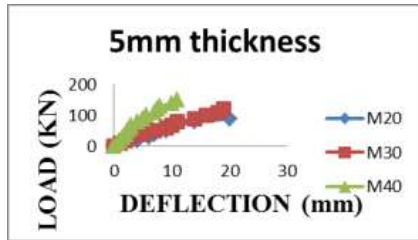


Fig 24 Load Vs Deflection Curve For 6mm Thickness

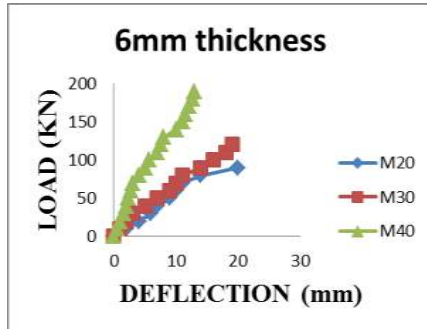
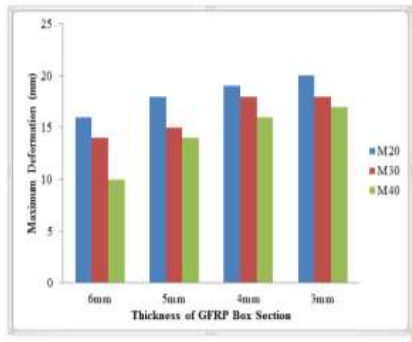


Fig 25 Maximum Deformation of beams



The load versus total deformation capacity of the concrete filled GFRP box beam sections for different thickness is shown in Figure 21,22,23 & 24. It can be seen that concrete filled box beam exhibit less deformation irrespective of the thickness. It is also observed that the deformation decreases when the grade of infill increases. The stiffness of the concrete filled GFRP box is nearly 4 to 7.5 times of conventional beam. From the Figure 25 it is observed that the deformation of beam with 6mm thickness shows higher resistance to deformation than other beams. The reduction in deflection of 6mm thick concrete filled GFRP box section is about 58% when compared to conventional beam.

7. CONCLUSION

Based on the experimental and analytical study, following conclusions were made:

The proposed finite element model shows the resistance to deformation when concrete is used as infill material and the deformation decreases when the grade of concrete and thickness of box beam increases. The Concrete filled GFRP box beam with 6mm thickness shows good response against deformation. The load carrying capacity of box beam is increased 3 times when compared to normal conventional concrete. Increasing the grade of concrete will increase the moment carrying capacity as well as having increased stiffness up to 70%. The stiffness of the concrete filled GFRP box is nearly 4 to 7.5 times of conventional beam. The beam having 6mm thickness showed higher stiffness ratio of 2.21%. The reduction in deflection of 6mm thick concrete filled GFRP box section is about 58% when compared to conventional beam. Deflections and stresses at the two point of the beam along with initial and progressive cracking of the finite element model compare well to experimental data obtained from concrete filled GFRP box beams. The failure mechanism of Concrete filled GFRP box beam is modelled quite well using FEA, and the failure load is very close to the failure load measured during experimental testing.

8. ACKNOWLEDGEMENT

I sincerely express my deepest sense of my thanks and gratitude to my guide for his valuable suggestions, excellent guidance and constant support I would like to express my gratitude and sincere thanks to our Head of the Department for providing all the facilities. I thank teaching and non-teaching staff members of Civil Engineering Department, all my friends and parents who give constant support and encouragement

9. REFERENCES

1. FerhatAydn, MehmetSaribiyik, "Investigation of flexural behaviors of hybrid beams formed with GFRP box section and concrete" Journal of Construction and Building Materials 41 (2013) 563–569
2. B. E. Belzer, M. J. Robinson, D. R. Fick, "Composite Action of Concrete -Filled Rectangular GFRP Tubes" Journal of Composites for Construction 32 (2013) 175 – 189
3. Huu-Tai Thai a, Brian Uya, Mahbub Khana, Zhong Tao , Fidelis Mashiri, "Numerical modelling of concrete-filled steel box columns incorporating high strength materials" Journal of Constructional Steel Research 102 (2014) 256–265
4. Bishnu Prasad Gautam and Takashi Matsumoto, "Shear deformation and interface behaviour of concrete-filled CFRP box beams" Journal of Composite Structures 89 (2009) 20–27
5. Kyungsik Kima, Chai H. Yoob, "Ultimate strengths of steel rectangular box beams subjected to combined action of bending and torsion" Journal of Engineering Structures 30 (2008) 1677–1687

6. Thuc Phuong Vo, Jaehong Lee, "Flexural–torsional behavior of thin-walled closed-section composite box beams" Journal of Engineering Structures 29 (2007) 1774–1782

7. B. Uy, "Strength of short concrete filled high strength steel box columns" Journal of Constructional Steel Research 57 (2001) 113–134

8. Thuc Phuong Vo, Jaehong Lee, "Interaction curves for vibration and buckling of thin-walled composite box beams under axial loads and end moments" Journal of Applied Mathematical Modelling 34 (2010) 3142–3157

9. Bishnu Prasad Gautam and Takashi Matsumoto, "Failure Mechanism of Empty and Concrete-Filled CFRP Box Beams" Journal of Composite material and Construction 14 (2010) 336-345

10. Yunita Idris and Togay Ozbakkaloglu, "Seismic Behavior of High-Strength Concrete-Filled FRP Tube Columns" Journal of Composite material and Construction 17 (2013) 183-196

11. M. Gokhan Gunay and Taner Timarci, "Free Vibration of Composite Box-beams by ANSYS" , Journal of Constructional Steel Research 60 (2004) 313–337

12. Arivalagan.S, Kandasamy.S, "Flexural and Cyclic Behaviour of Hollow and Concrete- Filled Steel Tubes" Journal of Constructional Steel Research 60 (2004) 313-337

13. Wassim Naguib and Amir Mirmiran, "Flexural Creep Tests and Modeling of Concrete-Filled Fiber Reinforced Polymer Tubes" Journal of composite material and Construction 6 (2002) 272-279

14. Bishnu Prasad Gautam, "Damage and failure mechanism of concrete filled CFRP box beams" Journal of Structural Engineer 38 (2008) 356-369

15. Libo Yan , Nawawi Chouw, "Experimental study of flax FRP tube encased coir fibre reinforced concrete composite column" Journal of Construction and Building Materials 40 (2013) 1118–1127

Experimental and Analytical Study on Flexural Behavior Of Curved Beams

D.K.Kayathri
Mepco Schlenk Engineering College
Sivakasi – 626 005,
Tamil Nadu, India

C.D.R.Balaji
Mepco Schlenk Engineering College
Sivakasi – 626 005
Tamil Nadu, India

Abstract: This paper involves an experimental investigation on the flexural behaviour of curved beams and comparison of its results with conventional beams. Curved beams of size 1200 x 150 x 100 mm with varying initial curvature as 4000mm, 2000mm and the concrete strength as M40 is considered. Various reinforcement are provided in the curved beams to predict which reinforcement detail would give more resistant over maximum loading. The material properties of cement, fine aggregate, coarse aggregate and the compressive strength of concrete cube were found out. A total of 12 specimens of curved beams were casted with various combination of reinforcement along with three control specimens. The beams are tested under two point loading both horizontally and vertically. The deflection and maximum moment carrying capacity are investigated to understand its strength. Also analytical modelling is done to determine the ultimate moment carrying capacity using Finite Element Software ABAQUS to compare with the experimental model.

Keywords: Curved beams, ABAQUS.

1. INTRODUCTION

A beam in which the neutral axis in the unloaded condition is curved instead of straight or if the beam is originally curved before applying the bending moment, are termed as "Curved Beams". The beam theory can also be applied to curved beams allowing the stress to be determined for shapes including crane hooks and rings. When the cross section are small compared to the radius of curvature of the longitudinal axis the bending theory can be relatively accurate. When this is not the case even using the modified BernoulliEuler only provides approximate solutions.

One of the assumptions of the development of the beam bending relations is that all longitudinal elements of the beam have the same length, thus restricting the theory to initially straight beams of constant cross section. Although considerable deviations from this restriction can be tolerated in real problems, when the initial curvature of the beams becomes significant, the linear variations of strain over the cross section is no longer valid, even though the assumption of plane cross sections remaining plane is valid. Horizontally curved beams are frequently used in construction of bridges, Interchange facilities and balconies, because of the constraints in existing land use. The curved beam is a unique problem, which has drawn the attention of various investigators who have tried to solve it by different techniques including finite element. As a result, a number of curved beam elements have been developed. (1)

2. EXPERIMENTAL PROGRAM

This paper deals with the flexural behaviour of curved beams of various reinforcement details. To study the behaviour, 12 curved beams of length 1200 mm, width 150mm and depth 100mm having various initial curvature as 4000mm and 2000mm was casted using M40 grade of concrete. Concrete cube specimen of size 150mmx 150mm was casted to study the compressive strength of concrete. After 28 days curing,

flexural two point load would be applied on the curved beams with suitable support condition. The experimental results of beams would predict the deflection, ultimate moment capacity, and gives the result that which reinforcement detail would give more resistant over torsional moment and control the diagonal tension cracks due to torsion

2.1.MATERIALS USED

2.1.1 Cement: Ordinary Portland cement of (53 grade cement) conforming to IS: 81121989 is used. The properties of cement are given in the below Table 1.

2.1.2 Fine Aggregate: Natural river sand of size below 4.75mm conforming to zone II of IS 383-1970 is used as fine aggregate. Laboratory tests were conducted for fine aggregate to determine the physical properties as per IS: 2368 (part III). The test results are shown in Table 1.

Table 1.Test Results

Sl. No	Tests	Results
1	Specific gravity	3.15
2	Initial setting time	80 minutes
3	Final setting time	453 minutes
4	28days compressive strength	45.33/mm ²

Table 2 . Properties of Cement

Sl. No	Tests	Results
1	Specific gravity	2.72
2	Fineness modulus	2.67
3	Bulk density	1806 kg/m ³
4	Water absorption	1.1%

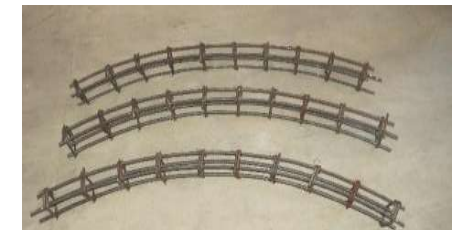


Fig .1 Reinforcement details

According to IS 10262 –2009 mix ratio for M40 grade is 1 : 2.56 : 3.26 : 0.4

2.1.3. Course Aggregate: Course aggregate used in this study consist of crushed stone of size 20mm. Laboratory tests were conducted on course aggregate to determine the different physical properties as per IS: 383-1970. The test results are shown in the table 3.

Table 3: Course aggregate Properties

Sl. No	Tests	Results
1	Specific gravity	2.67
2	Fineness modulus	2.67
3	Water absorption	0.6%

2.1.4 Superplasticizers: Conplast SP430 is based on Sulphonated Naphthalene Polymer and supplied as brown liquid instantly dispersible in water, having specific gravity of 1.220 to 1.225@ 30°C

2.1.5 Reinforcements: High Yield Strength Deformed Steel Bars of 6mm, 8mm, 10mm, 12mm Diameter was used for the study. 8mm, 10mm, 12mm were used as longitudinal reinforcement and 6mm bars were used for lateral ties.

2.3 MIX PROPORTION

Design of concrete mixes involves determination of the proportions of the given constituents namely, Cement, Water, Coarse aggregate and Fine aggregate with admixtures if any. Workability is specified as the important property of concrete in the fresh state. For hardened state compressive strength and durability will be considered.

2.4 REINFORCEMENT

The diameter of main reinforcement are 8mm, 10mm, 12mm and the lateral ties are 6mm. The lateral ties are spaced at a distance of 125 mm.

2.5 CASTING OF SPECIMENS

A total of 12 curved beams and 3 conventional beams of various reinforcement are casted. The concrete is poured inside the curved beam mould and by proper compaction the beam is casted. The cube was casted for finding the compressive strength of concrete



Fig .2 Curved Beam Mould



Fig 3: Superplasticizers



Fig.4 Casting of specimens

2.6 Testing Of Specimens

The cubes were tested in hydraulic compression testing machine. The cubes were tested on the same date of testing of their corresponding beams. The experimental values of cubes tested after 7days, 14days and 28 days.



Fig. 5 Testing of concrete cubes

Table. 4 Compressive strength of cubes

Grade of concrete	Tested days	Average Compressive Strength(N/mm ²)
40	7days	27
40	14days	36
40	28days	45.90

2.7 Test for Curved Beams

For the purpose of investigating the flexural behaviour of curved beams, a two point loading beam test was carried out for each specimen. This beam test provided a pure flexural zone in the presence of shear. The specimen was placed in the Universal Testing Machine in such a manner that the load was applied to the uppermost surface of the specimen. The load was applied without shock and increased continuously and the corresponding deflection was taken until the specimen reaches the ultimate load. The compression tests were conducted on companion concrete cubes on the same day and the average compressive strength was recorded

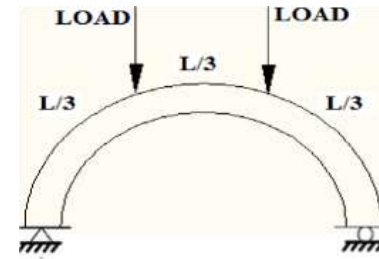


Fig .6 Diagrammatic Loading setup



Fig .7 Dial Gauges setup



Fig .8 Beam after Loading

2.8 Experimental Results

1. Compressive Strength

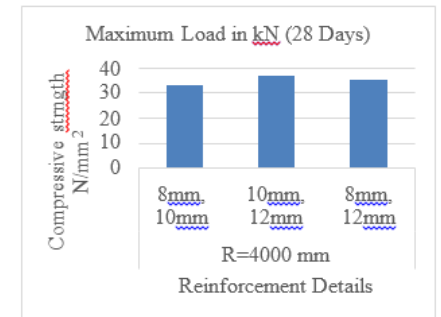


Fig. 9 Compressive strength of curved beams of initial curvature R=4000mm

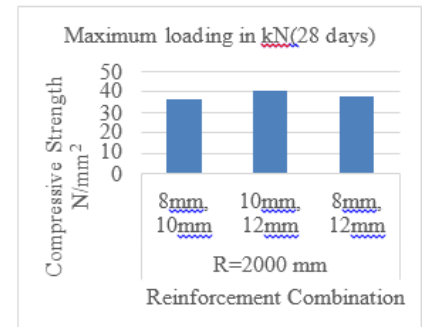


Fig .10 Compressive strength of curved beams of initial curvature R=2000mm

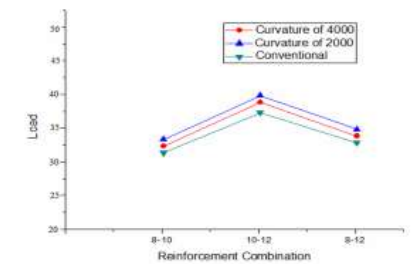


Fig. 11 Comparison of curved and conventional beams

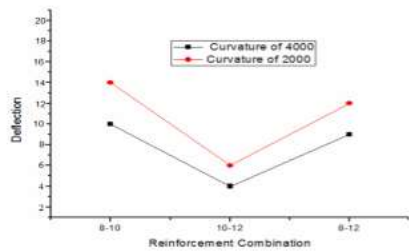
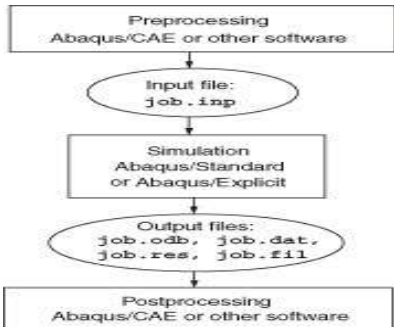


Fig. 12 Maximum deflection of curved beams

3.FINITE ELEMENT MODELLING

FEM ABAQUS/standard software was used in this study. ABAQUS is highly sophisticated, general purpose finite element program designed primarily to model the behaviour of solids and structures under externally applied loading. A complete Abaqus analysis usually consists of three distinct stages: preprossing, simulation and post processing. These three stages are linked together by files as shown below:



The model's details (geometry and properties of materials) were same as experimental specimen. Solid element types (C3DR8) were adopted to represent the concrete material, whereas the steel bars were represented by using three-dimensional truss elements (T3D2). All the beams were simply supported, and the load was applied automatically with the values that are obtained from experimental results. The bonding between the steel and concrete was assumed to be perfect and represented in ABAQUS using an interaction element.

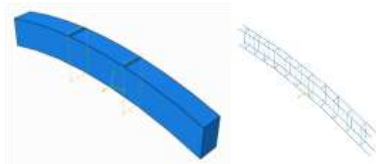


Fig. 13 Modelling of beam& Reinforcement steel

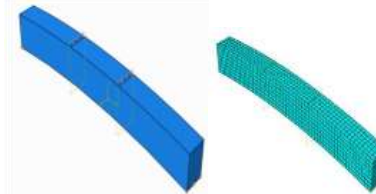


Fig 14. Loading of beam& Meshing of beam

Two types of loading conditions were analysed in the analytical study to determine under which loading the beam is more resistant. They are vertical and horizontal loading. They were described in the figure below.

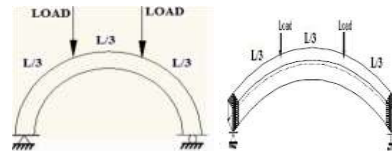
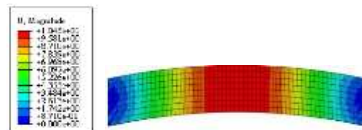


Fig 15. Horizontal and Vertical

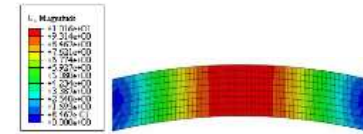
Analytical results

A) Curved beams (R=4000 mm) for vertical loading

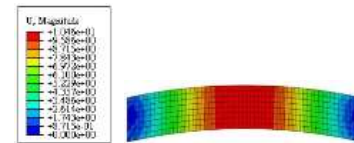
1. Deflection for R=4000 mm (8mm, 10mm)



2. Deflection for R=4000mm (10mm, 12mm)

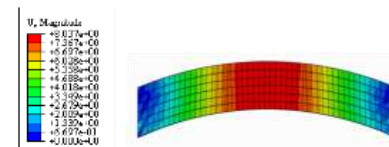


3. Deflection for R=4000mm (8mm, 12mm)

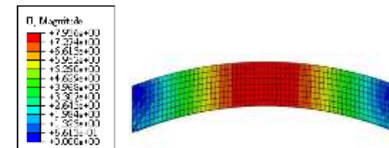


B) Curved beams (R=2000 mm) for vertical loading

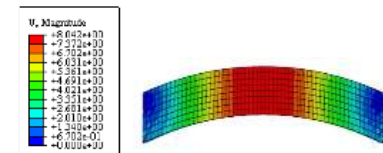
1. Deflection for R=2000 mm (8mm, 10mm)



2. Deflection for R=2000mm (10mm, 12mm)

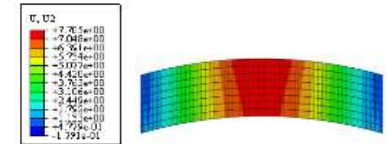


3. Deflection for R=2000mm (8mm, 12mm)

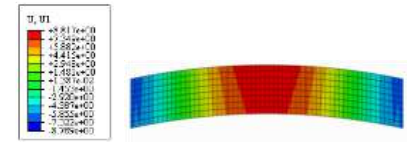


C) Curved beams (R=4000 mm) for Horizontal loading

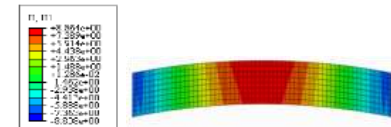
1. Deflection for R=4000 mm (8mm, 10mm)



2. Deflection for R=4000mm (10mm, 12mm)

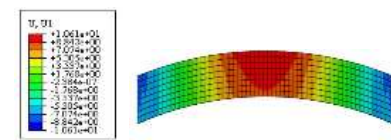


3. Deflection for R=4000mm (8mm, 12mm)

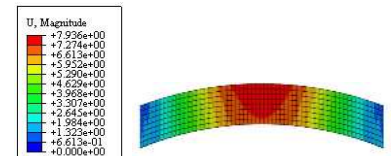


D) Curved beams (R=2000 mm) for Horizontal loading

1. Deflection for R=2000 mm (8mm, 10mm)



2. Deflection for R=2000mm (10mm, 12mm)



3. Deflection for R=2000mm (8mm, 12mm)

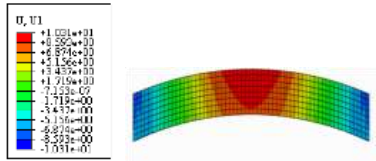


Figure .16 Deflection of the Curved Beam

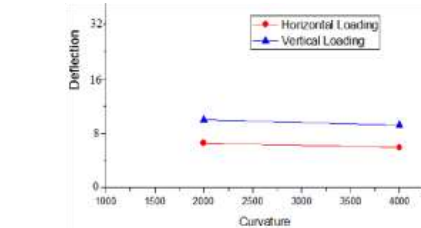


Figure .17 Deflection of the Curved beams in Different Loading Condition

Among the two loading condition, the horizontal loading condition gives out minimum deflection compared to vertical loading condition in various reinforcement combinations. So horizontal condition is recommended in curved beams.

4. CONCLUSION

- The ultimate strength of the curved beam is suspected to increase by 10-15% over the conventional rectangular straight beam.
- The sectional area can be reduced by using the curved beams with improved capacity.
- In a curved beam with a small curvature, the ultimate strength becomes large and for the curved beam with large curvature, the ultimate strength becomes small.

- In curved beams, the horizontal loading condition is recommended rather than vertical due to minimum deflection.

5. REFERENCES

1. T. Subramani, M. Subramani, K.Prasath, "Analysis of Three Dimensional Horizontal Reinforced Concrete Curved Beam Using Ansys", T. Subramani et al Int. Journal of Engineering Research and Applications ISSN 2248-9622, Vol. 4, Issue 6(Version 6), June 2014, pp.156-161
2. Kadonaga T, Shigematu T, Tamura T, and Hara T, 2004 "Study on R/C Member Subjected to Torsion, Bending and Axial Tension", Third International Conferen on Advances in Structural Engineering and Mechanics, Seoul, Korea, CDROM.
3. Bauchau A, Hong CH. "Large displacement analysis of naturally curved and twisted composite beams", AIAA J 1987;25(11):1469-75.
4. Petrov E, Geradin M., "Finite element theory for curved and twisted beams based on exact solutions for three-dimensional solids, Part 2: Anisotropic and Advanced Beam Models", Comput Methods Appl Mech Eng 1998;165(1):93-127.
5. Tasaka, T., Shigematsu, T., Tamura, T., and Hara, T., 2002 "Study on shear strength of the R/C curved beam", The second international conference on advances in structural engineering and mechanics, CDROM.

Implementation methodology of Biogeography Based Optimization algorithm for dependent task scheduling

S.Selvi,
Associate Professor
Department of Electronics and
Communication Engineering,
Dr.Sivanthi Aditanar College of
Engineering, Tiruchendur -
628215, Tamilnadu, India.

Abstract: Biogeography Based Optimization (BBO) is a new evolutionary algorithm for global optimization that was introduced in 2008. BBO is an application of biogeography to evolutionary algorithms. Biogeography is the study of the distribution of biodiversity over space and time. It aims to analyze where organisms live, and in what abundance. BBO has certain features in common with other population-based optimization methods. Like GA and PSO, BBO can share information between solutions. This makes BBO applicable to many of the same types of problems that GA and PSO are used for, including unimodal, multimodal and deceptive functions. This paper explains the methodology of application of BBO algorithm for the constrained task scheduling problems.

Keywords: Biogeography Based Optimization, Constrained Task Scheduling, DAG, Makespan, Ranking,

1. INTRODUCTION

A task scheduling is the mapping of tasks to a selected group of resources which may be distributed in multiple administrative domains. A scheduling problem is specified by a set of machines, a set of jobs/operations, optimality criteria, environmental specifications, and by other constraints[1]. Given an application modeled by the Directed Acyclic Graph (DAG), the scheduling problem deals with mapping each task of the application onto the available heterogeneous systems in order to minimize makespan [2]. DAG includes the characteristics of an application program such as the execution time of tasks, the data size to communicate between tasks and task dependencies. The task scheduling problem has been solved several years ago and is known to be NP-complete [3,4]. In general, task scheduling algorithm for heterogeneous systems is classified into two classes: static and dynamic [5]. In static scheduling algorithms, all information needed for scheduling must be known in advance [6]. Static task scheduling takes place during compile time before running the parallel application. In contrast, scheduling decisions in dynamic scheduling algorithms are made at run time.

2. PROBLEM DEFINITION

The task scheduling problem is the process of assigning a set of v tasks in a DAG to a set of q computing nodes, which have diverse characteristics, without violating the precedence constraints. Before scheduling, the priority of execution of tasks is calculated based on the upward ranking methodology [4]. The tasks are sorted in the decreasing order of the upward rank value. The highest priority task (with high rank value), has the highest scheduling priority. If more than one task has equal upward rank value, the scheduling priority of the task is decided randomly.

In this paper, the schedule length of the given DAG application, namely makespan, is the largest finish time among all tasks, which is the actual finish time of the exit task, n_{exit} . The objective of the task scheduling problem is to minimize the makespan (fitness), without violating the

precedence constraints of the tasks. The objective function is defined in Equation (1) [4].

$$fitness = Makespan = f(x) = \begin{cases} EFT(n_{exit}), & \text{for single } n_{exit} \\ \max\{EFT(n_{exit})\}, & \text{for multiple } n_{exit} \end{cases} \quad (1)$$

where EFT is the Earliest Finish Time of the task n_i on the computing node p_j , defined in the Equation (2) [4].

$$EFT(n_i, p_j) = w_{i,j} + EST(n_i, p_j) \quad (2)$$

where $EST(n_i, p_j)$ is the Earliest Start Time of the task n_i on the computing node p_j , defined in the Equation (3) ([4].

$$EST(n_i, p_j) = \begin{cases} \max\{avail_time(p_j), ready_time(n_i)\}, & \text{if } n_i \neq n_{entry} \\ 0, & \text{if } n_i = n_{entry} \end{cases} \quad (3)$$

where $avail_time(p_j)$ is the earliest time at which the computing node p_j is ready for the task execution and $ready_time(n_i)$ is the time when all data needed by n_i has arrived at the computing node p_j , defined in the Equation (4) [4]. $ready_time(n_i) = \max_{n_m \in pred(n_i)} (EFT(n_m) + c_{m,i})$ (4)

where $pred(n_i)$ is the set of predecessor tasks of the task n_i .

3. BIOGEOGRAPHY BASED OPTIMIZATION ALGORITHM

Biogeography describes how species migrate from one island to another, how new species arise and how species become extinct. An island is any habitat that is geographically isolated from other habitats. Geographical areas that are well suited as residences for biological species are said to have a high Habitat Suitability Index (HSI). The variables that characterize habitability are

called Suitability Index Variables (SIVs). SIVs can be considered as the independent variables of the habitat, and HSI can be calculated using these variables. Habitats with a high HSI tend to have large number of species, while those with a low HSI have a small number of species. Habitats with a high HSI have many species that migrate to nearby habitats, simply by virtue of the large number of species that they host. Migration of some species from one habitat to other habitat is known as emigration process. When some species enter into one habitat from any other outside habitat, it is known as immigration process[7]. The pseudo code for BBO algorithm is illustrated in Algorithm 1.

Algorithm 1. Biogeography Based Optimization Algorithm

```

Initialize the BBO parameters
Create a random set of habitats (population)
H1,H2,.....Hp
Compute HSI values;
While the halting criterion is not satisfied do
    Compute immigration rate λ and emigration rate μ
    for each habitat based on HSI;
    For each habitat (solution)
        For each SIV (solution feature)
            Select habitat Hi with probability αλi
            If Hi is selected then
                Select Hj with probability αμj
            If Hj is selected then
                Hi(SIV) ← Hj(SIV)
            End if
            End if
            Select Hi(SIV) based on mutation
            probability mi;
            If Hi(SIV) is selected then
                Replace Hi(SIV) with a randomly
                generated SIV;
            End if
            Next for
                Recompute HSI values;
            Next for
                End while
    
```

4. IMPLEMENTATION OF BBO ALGORITHM FOR SCHEDULING DEPENDENT TASKS

The following subsections deal with the representation of solution, and the generation of initial solution.

4.1 Solution representation

The solution is represented as an array of length equal to the number of jobs [8]. The value corresponding to each position *i* in the array represent the node to which task *i* was allocated. The representation of the solution for the problem of scheduling 13 tasks to 3 computing nodes is illustrated in Figure 1. The first element of the array denotes the first task (*n*₁) in a batch which is allocated to the computing node 2; the

second element of the array denotes the second job (*n*₂) which is assigned to the computing node 1, and so on.

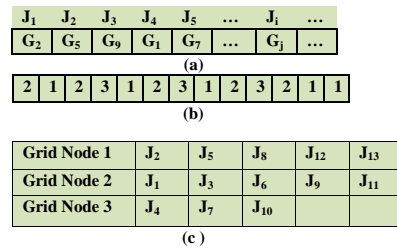


Fig. 1. (a) Solution Representation (b) Solution for the problem of 13 tasks and 3 computing nodes (c) Mapping of tasks with computing nodes for the solution given in (b)

4.2 Initial solution generation

Numerous methods have been proposed to generate the initial solution when applying meta heuristics to the scheduling problem in the heterogeneous environment[9,10]. Random solution may also be generated to initiate the process.

4.3 Computational experiments

To illustrate, a small scale DAG scheduling problem involving 3 nodes and 10 tasks is considered (Fig 2) with the computation cost matrix given in Table 1. The upward rank and the order of the tasks for execution are given in Table 2 and 3 respectively. BBO algorithm was executed with the following parameters. Habitat size-15, Habitat Modification Probability-1,Immigration probability bounds per gene-[0-1],Step size for numerical Integration-0.2,Maximum immigration and emigration rate for each island-1,Mutation probability-0.005, Number of iterations- 50. The makespan value obtained for the example problem is found to be 73.

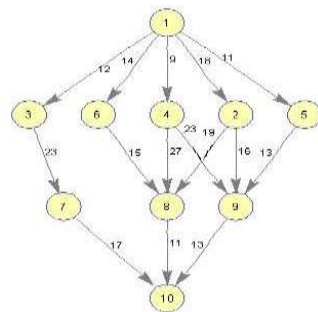


Figure 2. An example DAG

Table 1
Computation cost matrix for random DAG

Task id	P1	P2	P3
1	14	16	9
2	13	19	18
3	11	13	19
4	13	8	17
5	12	13	10
6	13	16	9
7	7	15	11
8	5	11	14
9	18	12	20
10	21	7	16

Table 2
Upward rank of the tasks

Task id	Upward Rank
1	108.00000
2	77.00000
3	80.00000
4	80.00000
5	69.00000
6	63.33333
7	42.66667
8	35.66667
9	44.33333
10	14.66667

Table 3
Execution Order of tasks

Order of Task id
1
4
3
2
5
6
9
7
8
10

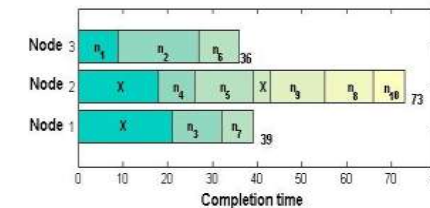


Figure 3. A schedule produced by the BBO algorithm for the example DAG

5. CONCLUSION

The methodology of implementation of BBO algorithm for the constrained dependent task scheduling problem had been discussed. The methodology adopted for this algorithm gives

rise to the development of scheduling algorithms using other meta heuristic methods.

6. REFERENCES

- [1] Selvi, S,Manimegalai, D.Research Journal of Applied Sciences, Engineering and Technology 8(8): 964-975, 2014
- [2] P. Chitra, R. Rajaram, P. Venkatesh, Application and comparison of hybrid evolutionary multiobjective optimization algorithms for solving task scheduling problem on heterogeneous systems, Applied Soft Computing 11 (2011) 2725–2734
- [3] E. Ilavarasan, P. Thambidurai, R. Mahilmanan, Performance effective task scheduling algorithm for heterogeneous computing system, in: Proc. 4th International Symposium on Parallel and Distributed Computing, France, 2005, pp. 28–38.
- [4] Topcuoglu, H., Hariri, S., Wu, M.Y.: Performance-Effective and Low-Complexity Task Scheduling for Heterogeneous Computing. IEEE Trans. Parallel and Distributed Systems 13(3), 260–274 (2002)
- [5] B.Hamidzadeh, L.Y.Kit, D.J.Lija, Dynamic task scheduling using online optimization, IEEE Trans. Parallel Distributed systems 11(11)(2000) 1151-1163.
- [6] Mohammad I. Daouda, Nawwaf Kharmia ,A hybrid heuristic–genetic algorithm for task scheduling in heterogeneous processor networks, J. Parallel Distrib. Comput. 71 (2011) 1518–1531
- [7] Simon, D., (2008). Biogeography-based optimization. IEEE Transactions on Evolutionary Computation.12(6): 702–713.
- [8] Selvi, S,Manimegalai, D. Task Scheduling using Two Phase Variable Neighborhood Search Algorithm on heterogeneous computing and grid environments, Arabian journal for science and engineering March 2015, 40(3):817-844.
- [9]Abraham A, Liu H, Zhao M. Particle swarm scheduling for work-flow applications in distributed computing environments. Studies in Computational Intelligence 2008; 128: 327–342.
- [10] Xhafa F, Duran B, Parallel memetic algorithms for independent job scheduling in computational grids, in: Recent Advances in Evolutionary Computation for Combinatorial Optimization, vol. 153 of Studies in Computational Intelligence, Springer, 2008, pp. 219–239.

Agile Manufacturing - An Overview

Manivelmuralidaran. V

Department of Mechanical Engineering, Kumaraguru College of Technology,
Coimbatore-641049, India

Abstract: Smaller lot sizes, shorter times to market, and lower manufacturing costs are typical requirements of a modern manufacturing facility. Under such constraints, agile manufacturing systems are desirable. Agile manufacturing uses technology, organizational approaches, systems and people in a manufacturing concept which truly belongs to the 21st century and which transcends existing methodology to facilitate ability of the organization to react to rapid change and respond to an increasingly unpredictable marketplace. Agile manufacturing can produce what customers want, when and exactly how they want it, at a cost-effective price. The main aim of this paper is to present the various possible research domains in the development of agile manufacturing era. The objective of this paper is to brief an overall idea and research needs of agile manufacturing with the focus of current fluctuations in the market scenario.

Keywords Agile Manufacturing, Lean manufacturing, Manufacturing Engineering, Production planning and control

1. INTRODUCTION

World-class performance is a moving target that requires constant attention, effort and the process is a never ending journey. In the past, economies of scale ruled the manufacturing world and everybody knew that mass production and full utilization of plant capacity was the way to make money. This style of manufacturing resulted in inflexible plants that could not be easily reconfigured, and were associated with swollen raw materials, work-in-process and finished goods inventories. For the elimination of excess inventory, shortened lead-times, requirement of flexibility in the flow lines and to enhance the advanced levels of quality in both products and customer service, industry analysts have popularized the terms 'world-class manufacturing' and agile manufacturing.

2. AGILE MANUFACTURING

Facing the competitive market, industrial manufacturers are hard pressed to adopt novel strategies and technologies to enhance product quality, to cut manufacturing cost and to reduce product lead time. Agile Manufacturing is primarily a business concept. Its aim is quite simple - to put our enterprises way out in front of our primary competitors. In Agile Manufacturing, our aim is to combine our organization, people and technology into an integrated and coordinated whole. Agile manufacturing can be defined as the capability to survive and prosper in a competitive environment of continuous and unpredictable change by reacting quickly and effectively to changing markets, driven by customer-designed products and services.

The concept of agility refers to a business model which makes an organization immune to damage caused by unpredictable events and changing circumstances. This is achieved by the organization being able to react and adapt rapidly [5]. The coming surprises of the future will not make an agile enterprise vulnerable because that enterprise will have already put in place a set of business practices, organization-wide culture changes and technology which will allow it to be prepared for any change in circumstances,

market forces or customer needs. Agile Manufacturing is a combination of speed and flexibility that is difficult to achieve because it requires radical changes to traditional thinking.

The concept of Agile Manufacturing is built around the synthesis of a number of enterprises that each have some core skills or competencies which they bring to a joint venturing operation, which is based on using each partner's facilities and resources [7]. Central to the ability to form these joint ventures is the deployment of advanced information technologies and the development of highly nimble organizational structures to support highly skilled, knowledgeable and empowered people. Agile Manufacturing builds on what is good in lean manufacturing and uses what can be adapted to western cultures, but it also adds the power of the individual and the opportunities afforded by new technologies.

Agile Manufacturing enterprises will be capable of rapidly responding to changes in customer demand. They will be able to take advantage of the windows of opportunities that, from time to time, appear in the market place. With Agile Manufacturing it is possible to develop new ways of interacting with customers and suppliers. The customers will not only be able to gain access to the products and services, but will also be able to easily assess and exploit the competencies, so enabling them to use these competencies to achieve the things that they are seeking.

The goal of this paper is to review several different aspects of agile manufacturing (AM) and to identify key aspects of agile manufacturing and outlook for the future of agile manufacturing technologies.

2.1 Comparison of Agile manufacturing and other manufacturing methods:

In traditional manufacturing system the long cycle time is with the high inventory which causes delay in the goods delivery. The problem here is the lack of strategy and no employee involvement and financial secrecy and record inaccuracy. In the context of world class manufacturing the advantages are long term profitability, productivity

improvement and less time to market in contrast to the traditional manufacturing system. The agile manufacturing system focusing in the integration of design and manufacturing and every aspect of manufacturing under one roof.

In Contrast to the traditional manufacturing strategy, the agile manufacturing concentrates on the customer enrichment, competitiveness through co-operation and this could be achieved by integration of the people, information and technology on a same roof. This could also be achieved by highly educated and trained workforce. Enhancing the competitiveness among the competitors and built the cooperation from all the enterprises and thus influence the knowledge sharing and sharing the technological innovations.

2.2 Needs of agile manufacturing system

The key to agility however, lies in several places. An agile enterprise needs highly skilled and knowledgeable people who are flexible, motivated and responsive to change. An agile enterprise also needs new forms of organizational structures which engender non-hierarchical management styles and also stimulate and support individuals as well as cooperation and team working. Agile manufacturing enterprises also need advanced computer based technologies to integrate information and to share the knowledge base [2].

To achieve Agile Manufacturing, enterprises will have to bring together a wide range of knowledge in the design of a manufacturing system that encompass suppliers, customers. It should also address all dimensions of the system including organisation, people, technology, management accounting practices, etc. Most importantly the inter-related nature of all these areas needs to be recognised and an interdisciplinary manufacturing systems design method adopted as standard practice[3]. This means going beyond the multidisciplinary approaches that are currently being adopted and looking at areas between professions.

2.3 Challenges of Agile manufacturing

Interdisciplinary design will form the basis of designing Agile Manufacturing systems in the new knowledge intensive era. Interdisciplinary design however, means more than just applying knowledge from other domains, such as psychology and organisational science, to the design of Agile Manufacturing systems. It also implies looking into the unexplored areas between these disciplines and the areas where they overlap, to find a new insights, new knowledge, new and original solutions. This is one of the most important challenges that managers and system designers and integrators will face in the years ahead. The interdisciplinary design leads us to new approaches and new ways of working and of thinking [4]. However, to successfully adopt an interdisciplinary design method, we also need to:

- Challenge the present design strategies and develop new and better approaches;
- Question the established and cherished beliefs and theories, and develop new ones to replace those that no longer have any validity;
- Consider how to address organisation, people and technology, and other issues in the design of manufacturing systems, so that the systems can achieve the better performance for the agile manufacturing environment and for the people who form a part of this system.

- Make use of the innovative technology in a way that makes human skill, knowledge, and intelligence more effective and productive which allows industries to tap into the creativity and talent of all people in an enterprise.

The challenges that face with respect to all these issues are enormous. In the world of manufacturing the challenges and problems are very complex. There are a massive number of interconnections between the various components and elements. A manufacturing enterprise is so complex that, in the past, it has been impossible to cope with it as a whole, and it has been necessary to reduce it into manageable areas which have tended to be examined separately.

2.4 Agile Manufacturing world wide scenario

The Agile Manufacturing Enterprise Forum (AMEF) at the Iacocca Institute of Lehigh University was created to disseminate the ideas of agile manufacturing and to increase the pace and scope of the transition to an agile manufacturing industry. The Agile Manufacturing Initiative aims to develop, demonstrate, and evaluate the advanced design, manufacturing and business transaction processes in the agile environment. The Concurrent Technologies Corp. (CTC) is developing an agile manufacturing testbed to provide Department of Defense (DoD) with increased weapon system readiness and added system mobility. The Agile Aerospace Manufacturing Research Center (AAMRC) at the University of Texas at Arlington is conducting research on agile business practices, business process identification and characterization, and enabling technologies. The Manufacturing Research, Education and Outreach Program at the University of Illinois at Urbana-Champaign is developing computer integrated manufacturing and machine tool systems. The Electronic Agile Manufacturing Research Institute (EAMRI) at Rensselaer Polytechnic Institute (RPI) is focusing on electronics product realization in distributed manufacturing environments using improved information infrastructures and architectures.

Agile manufacturing makes use of modern information technology to form virtual enterprises, which agilely respond to the changing market demands. A virtual enterprise, different from a traditional enterprise, is constructed by partners from different companies, who collaborate with each other to design and manufacture high quality and customized products. It is product-oriented, team-collaboration styled, and featured as fast and flexible. Frequent and dynamic interactions among partners in agile manufacturing enterprises entail the crucial role of an Agile Manufacturing Information System (AMIS). It is up to the AMIS to provide partners with integrated and consistent information, as well as to manage partner transactions accessing the information.

2.5 Transition to Agile Manufacturing

All the relevant dimensions of Agile Manufacturing, such as organisation, people, technology, management accounting, etc. are however, all written in different books and taught by different people. To make the transition to Agile Manufacturing we need to:

- Examine and define the underlying conceptual framework on which Agile Manufacturing enterprises will be built.
- Explore and understand the nature of the mass production paradigm and the nature of the cultural

and methodological difficulties involved in the transition to Agile Manufacturing.

- Define a methodology for designing a 21st century manufacturing enterprise.

The agile manufacturing is based on a systems perspective of technology, organisation and people, tied to clear business vision and goals. This will help the researchers to understand the full complexity of designing a 21st century manufacturing enterprise that is agile manufacturing system.

2.6 Characteristics of Agile Manufacturing

The characteristics of agile manufacturing are at the strategic level where strategic dimensions of agile manufacturing are identified as follows: 1. Enriching the customer - an agile company is one that is perceived by its customers as enriching them in a significant way, not only itself

2. Cooperating to enhance competitiveness - cooperation internally and with other companies in an agile competitor's operational strategy of first choice 3. Organizing to master change and uncertainty - an agile company is organized in such a way as to allow it to thrive on change and uncertainty, its structure is flexible enough to allow rapid configuration of human and physical resources; 4. Leveraging the impact of people and information - an agile company's management nurtures an entrepreneurial company culture that leverages the impact of people and information on operations. From these strategic dimensions of agility, one can move to consider the tactical and technological dimensions. In this effort, the AMRIs are concerned with research and development efforts to better understand the enabling technologies for agile manufacturing.

The benefits of Agile Manufacturing are Short time-to-market, fast new product development, Short/fast order processing, Low volumes, Low quantities, High product mix, Configurable components, Fast supplier deliveries, Short lead times, Short cycle times, Highly flexible and responsive processes, Highly flexible machines and equipment, Use of advanced CAD/CAM, Quick changeover, Empowered employees.

3. POTENTIAL RESEARCH PROSPECTS IN AGILE MANUFACTURING

There are lot of issues are related with the manufacturing and production in agile manufacturing environment. Some of the potential area are Product and manufacturing systems design, Process planning [5], Production planning scheduling and control, Facilities design, Facilities location, Material handling and storage systems, Integrated information systems, Information systems designed for supporting specific areas of Information exchange, Supply chain Strategies, Partner selection [4,6], Human factors.

3.1 Human Factors in Agile Manufacturing

In manufacturing we have tended to treat organisation, people and technology issues independently, and for the most part this division of knowledge has worked well in the past. In a report of Human Factors in Agile Manufacturing by Chris Forsythe at Sandia National Laboratories pointed out that Agile manufacturing will precede, by raising human factors issues and applying the knowledge and skills gained from other domains [1]. There is an opportunity for human factors to assume an important role positively influencing the future

of agile manufacturing. Still Agile manufacturing poses many questions best answered by human factors. Our willingness, as a researcher is to address these questions and enhance the agile manufacturing environment.

3.2 Production planning, scheduling and control

Production planning, scheduling and control is concerned with manufacturing the right product types, in the right quantities, at the right time, at minimum cost and meeting quality standards. Production planning, scheduling and control are the heart of manufacturing firms [7]. He and Kusiak (1996) developed two models for production planning and scheduling in a virtual corporation[7]. This paper considers that every virtual corporation is formed by a number of manufacturing companies (manufacturing centres) and assembly companies (assembly centres). The first model allocates products to the assembly centres so that the total average set-up and inventory cost is minimized. The model is solved with an efficient heuristic algorithm. The second model deals with scheduling the manufacturing centres. In this paper, the authors assume that each firm has a direct production capability (each one can produce different products). Additionally, they assume that partners are manufacturing centres or assembly centres, but not both.

Don-Taylor (1996) introduces the Design for Global Manufacturing and Assembly (DFGMA) as a tool to assist designers in making optimal sourcing, capital procurement, and market timing decisions in a multi-facility, global environment. More specifically, DFGMA is a mathematical tool that enables production planners optimally to introduce a new product into a suitable production line. The first of the new product with the existing mix is considered and the dynamic nature of the product mix is also considered [2]. DFGMA can also be used as a tool for performing sensitivity analysis for various costs, productivity levels, product configuration, mix assumptions at each facility, or analysis of parameters of interest to design, marketing and manufacturing. The mathematical model was formulated as a mixed-integer linear program (MILP) where the objective function specifies the minimization of all costs associated with the design, manufacture, inventory, transportation, logistics, set-up, tooling and capital procurement, to support the introduction of a new product. Six different types of constraints were included in the model. The LINDO software package was used to solve the model. Further work can be done in evaluating the use of the DFGMA model for concurrent sourcing decisions of multiple new products to sites characterized by various existing mixes. In addition DFGMA should be tested in situations with more explicit model market timing issues. Another area of research interest is the applicability and evaluation in a real system.

Sarmiento et al. (1999) reviewed recent work in the area of integrated analysis on systems that explicitly consider logistics (transportation systems) integrated into other functions in production, and also they identified areas where further research is needed. In addition, the authors were interested in identifying work done at the strategic or tactical level [8]. Among the conclusions, the authors' state that the integration of the logistics function into the analysis of previously isolated production is also an important criteria.

L. M. Sanchez et al. work has the potential of providing significant benefits to companies, in the form of cost savings and efficiency improvement. One problem encountered in forming a virtual corporation is to assign tasks to each partner

and to schedule the production based on the capabilities of each one of them [8]. They remark that it is important to have an integrated production planning, scheduling and control system. Still lot more areas are to be research for the agile manufacturing environment.

Another important aspect of agile manufacturing is the focus towards the customer feedback and replies. Though less amount of paper work has been done in this aspect and lot more have to be explored to enhance the quick response to the customer feedback. So it is essential to plot a road map to the processes and to speed up the procedure to quickly response to the customer needs. The research in this direction is very limited and this could be taken as a starting point for the exploration of agile manufacturing environment.

The key points to understand in the agile manufacturing are it is a strategy aimed at developing capabilities (the enterprise platform) to prosper in the 21st century. In this respect it is similar to a manufacturing strategy in that it should support business and marketing strategies. However, these strategies also need to be modified to take advantage of agile manufacturing capabilities. As a strategy, agile manufacturing is concerned with objectives, structures, processes and resources and not with individual point solutions, particular technologies, methods, etc. considered in isolation [9]. The emphasis is on designing the enterprise as a whole so that certain characteristics are achieved and not on the piecemeal adoption of quick fixes, prescriptions and panaceas. Agile manufacturing may require some current best practices, lean production concepts, technologies and taken-for-granted assumptions to be re-evaluated, modified or even abandoned. In the same way that mass-production marginalised many craft-based firms, agile manufacturing is likely to marginalise many mass production firms, even those with lean production enhancements. One of the biggest problems to overcome is the misunderstandings that lean and agile are synonymous. They are not, although most of what is portrayed as agile is in fact lean.

There is a need to view the agile manufacturing concept into the service industries and a quality management system should be formulated for assurance of quality in agile manufacturing enterprise and a well cost accounting method is to be established and designed to measure the cost of a product and decide about the product mix in the agile manufacturing environment[3].

4. CONCLUSION

Agility as a subject is still a developing area. Companies are starting to move towards agile behavior, often not in a planned way, more usually they "fall into it" and as a result it tends to be operational and lacks strategic direction. As a first step, companies need to understand the basic ideas and become intelligent respondents to the concepts. Agility is a long term issue for businesses and achieving agility is a

journey, not an objective to be attained before moving on to something else. The implementation of agility is still very much a frontier activity, involving radically new concepts concerning strategies, organisation, people and technologies. It takes businesses into a domain where fundamental and taken for granted assumptions are challenged. Agility is a paradigm shift and before one can move forwards one has to understand the existing paradigm and to face up to the often painful task of accepting that current practices and beliefs are no longer appropriate or relevant.

REFERENCES

- [1] Chris Forsythe., Ashby.M.R., Human factors in agile manufacturing, Journal of Ergonomics in Design, 4(1), pp. 15-21 Cho.H., Jung.M., Kim.M., Enabling Technologies of the agile manufacturing and its related activities in Korea, Computers and Industrial Engineering Journal, 30(3),pp. 323-324
- [2] Don-Taylor.G. and Nagi.R., Agile manufacturing in material handling and logistics:Implications and a research agenda. Progress in Material Handling Research, 1996, pp. 9±13.
- [3] Gunasekaran.A, Agile manufacturing :enablers and an implementation frame work, International Journal of Production Research, Vol 36, No.5,1223-1247.
- [4] Gupta.P., Nagi.R, Flexible optimization framework for partner selection in agile manufacturing, IERC Proceedings 1995, 4th Annual Industrial Engineering Research Conference, Norcross, GA, USA, pp 691-700
- [5] Gupta.S, Herrmann.J.W., Lam.G, Minis.I, Automated high level process planning to aid design for agile manufacturing, IERC Proceedings 1997, 6th Annual Industrial Engineering Research Conference, Norcross, GA, USA, pp1-19
- [6] Gupta.P.,Nagi.R., Process partner selection in agile manufacturing using linguistic decision making. Department of Industrial Engineering, State University of Newyork
- [7] He.D, Kusiak.A., Design for Agility: A Scheduling Perspective, Robotics and Computer-Integrated Manufacturing Systems, Vol. 14, No. 4, 1998, pp. 415-427.
- [8] Luis M. Sanchez :Rakesh Nagi, A review of agile manufacturing systems, International Journal of Production Research, 39(16), November 2001 , pp 3561 - 3600
- [9] Wang.Z.Y.,Rajkumar.K.P., Kapoor.A., Architecture for agile manufacturing and its interface with computer integrated manufacturing, Journal of Materials Processing and Technology, 61(1), 1996, pp. 99-103